AD-A194 167 AN ENDOCHRONIC RATE-SENSITIVE CONSTITUTIVE EQUATION FOR METALS APPLICATIO..(U) CINCINNATI UNIV OH R C VALANIS 01 MAR 88 ARO-21663.2-EG DAAG29-85-K-0017 1/3

UNCLASSIFIED F/G 11/6.1 NL

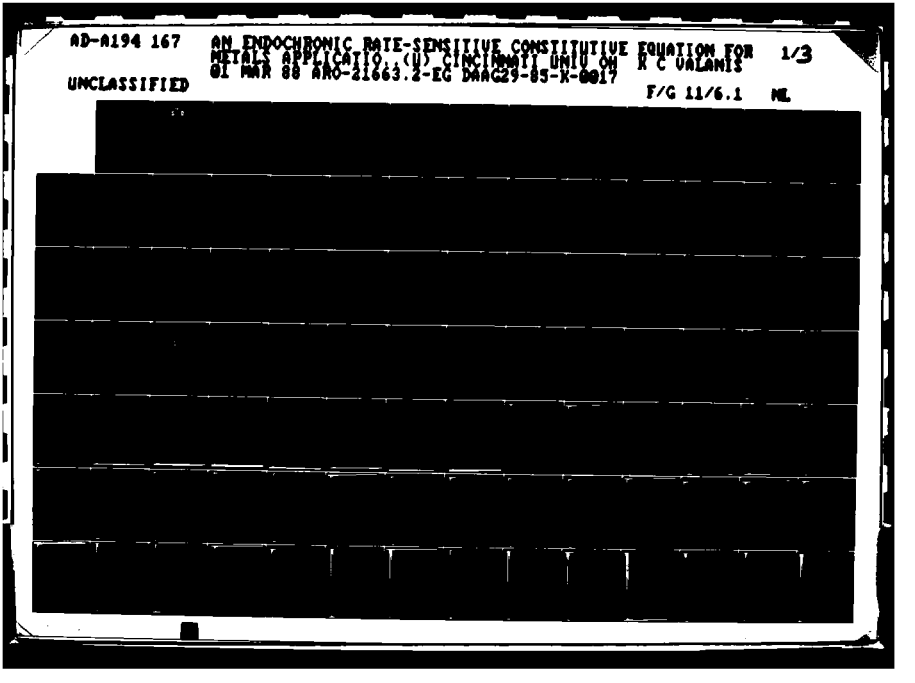

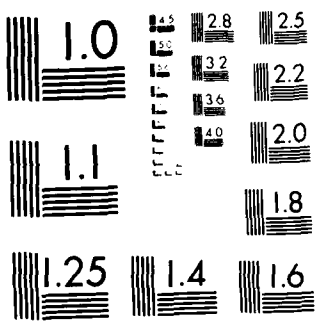

UNCLASSIFIED
SECURITY CLASSIFICATION OF THIS PAGE

AD-A194 167

REPORT DOCUMENTATION PAGE

1a REPORT SECURITY CLASSIFICATION: Unclassified	1b RESTRICTIVE MARKINGS
2a SECURITY CLASSIFICATION AUTHORITY	3 DISTRIBUTION / AVAILABILITY OF REPORT: Approved for public release; distribution unlimited.
2b DECLASSIFICATION / DOWNGRADING SCHEDULE	
4 PERFORMING ORGANIZATION REPORT NUMBER(S)	5 MONITORING ORGANIZATION REPORT NUMBER(S): ARO 21663.2-EG
6a NAME OF PERFORMING ORGANIZATION: University of Cincinnati / 6b OFFICE SYMBOL (If applicable)	7a NAME OF MONITORING ORGANIZATION: U. S. Army Research Office
6c ADDRESS (City, State, and ZIP Code): Cincinnati, OHIO 45221	7b ADDRESS (City, State, and ZIP Code): P. O. Box 12211, Research Triangle Park, NC 27709-22
8a NAME OF FUNDING / SPONSORING ORGANIZATION: U. S. Army Research Office / 8b OFFICE SYMBOL (If applicable)	9 PROCUREMENT INSTRUMENT IDENTIFICATION NUMBER: DAAG 29-85-K0017
8c ADDRESS (City, State, and ZIP Code): P. O. Box 12211, Research Triangle Park, NC 27709-2211	10 SOURCE OF FUNDING NUMBERS: PROGRAM ELEMENT NO / PROJECT NO / TASK NO / WORK UN ACCESSIO

11 TITLE (Include Security Classification): An Endochronic Rate-Sensitive Constitutive Equation for Metals. Application to Generalised Creep and Large Deformations.

12 PERSONAL AUTHOR(S): K.C.Valanis

13a TYPE OF REPORT	13b TIME COVERED	14 DATE OF REPORT (Year, Month, Day)	15 PAGE COUNT
FINAL	FROM 2-1-84 TO 9/1/87	March 1, 1988	144

16 SUPPLEMENTARY NOTATION: The view, opinions and/or findings contained in this report are tho of the author(s) and should not be construed as an official Department of the Army posit policy, or decision, unless so designated by other documentation.

17 COSATI CODES		
FIELD	GROUP	SUB-GROUP

18 SUBJECT TERMS (Continue on reverse if necessary and identify by block number): Endochronic, plastic, viscoplastic, rate-sensitive constitutive equation, generalised creep, large deformation.

19 ABSTRACT (Continue on reverse if necessary and identify by block number)

A constitutive equation is proposed with a view to describing the rate dependent mechanical response of metals at high temperatures. The equation is of the endochronic type and derives its physical foundations from deformation kinetics. Of importance is the fact that hardening is associated with a change in the energy barriers brought about by the inelastic deformation of a metal. The equation is used to describe the results, by Ohno and his associates, of experiments on the creep response

20 DISTRIBUTION / AVAILABILITY OF ABSTRACT	21 ABSTRACT SECURITY CLASSIFICATION
☐ UNCLASSIFIED/UNLIMITED ☐ SAME AS RPT. ☐ DTIC USERS	Unclassified
22a NAME OF RESPONSIBLE INDIVIDUAL	22b TELEPHONE (Include Area Code) / 22c OFFICE SYMBOL

DD FORM 1473, 84 MAR — 83 APR edition may be used until exhausted. All other editions are obsolete.

SECURITY CLASSIFICATION OF THIS PA
UNCLASSIFIED

of metals to piece-wise constant hostories. The metal in the present case is 304 stainless steel at 600 degrees C. It is shown that the theory gives analytical results that are in agreement with experiment.

Note should be made of the fact that the constitutive equation applies to general three-dimentional histories and is thus not limited to histories associated with creep.

The theory is also extended to finite deformations. A constitutive equation is derived, using internal variable theory, to the effect that the Cauchy stress is quadratic functional of the relative Finger tensor and in terms of a time scale which is intrinsic. The precise definition of the time scale is given in the text. A number of important proplems are solved in closed form under conditions of constant strain rate. The industrially important problem of the axial compression of a block is solved numerically.

AN ENDOCHRONIC RATE-SENSITIVE CONSTITUTIVE EQUATION FOR METALS. APPLICATION TO GENERALIZED CREEP AND LARGE DEFORMATIONS

FINAL REPORT

by

K.C.Valanis
Research Professor
Applied Research Center
University of Portland
Portland, OREGON
and
President of ENDOCHRONICS Inc
An Engineering Research and Consulting Co.
8605 Lakecrest Court NW
Vancouver, WA 98665

March 1988

Research Funded by the Army Research Office
Research Triangle Park, NC
Grant No DAAG 29-85-K001

Table of Contents

List of Figures

Abstract

A constitutive equation is proposed with a view to describing the rate dependent mechanical response of metals at high temperatures. The equation is of the endochronic type and derives its physical foundations from deformation kinetics. Of importance is the fact that hardening is associated with a change in the energy barriers brought about by the inelastic deformation of a metal. The equation is used to describe the results, by Ohno and his associates, of experiments on the creep response of metals to piece-wise constant stress histories. The metal in the present case is 304 stainless steel at 600^{o} C. It is shown that the theory gives analytical results that are in agreement with experiment.

Of consequence is the fact that the constitutive equation applies to three-dimensional stress or strain histories and is thus not limited to those stress histories associated with creep.

The theory is also extended to large deformations. This is done by using the internal variable theory. The resulting constitutive equation is a statement to the fact that the Cauchy stress is a quadratic functional of the relative Finger Tensor in terms of an intrinsic time wich is defined in the text.

1. Introduction

In the present paper we develop an endochronic theory of viscoplasticity which accounts for the history of strain and strain rate on the stress response of metals at high temperatures. The theory is based on the concepts of endochronic plasticity (see typically Ref.'s [1], [2], and [3]), however, the increment of intrinsic time scale is no longer proportional to the plastic strain path but depends also on the rate at which the path is traversed. The development of the theory is dealt with at length in the subsequent sections.

The resulting constitutive equation is used to analyze the creep response of 304 stainless steel to piece-wise constant shear stress histroies at 600°C and to compare the results with the experimentally determined creep response of the same material at this temperature as reported by Ohno et als. in Ref [4],

The constitutive behavior of metals at high temperature where the strain rate sensitivity of the mechanical response cannot be ignored, has been the subject of extensive research in recent years. We do not wish to give in this paper an exhaustive review of the literature on this subject but merely cite references which are typical of the enormous amount of work which is being done in this field. In this context, the works of Chaboche [5], Krieg [6], Malvern [7], Haisler [8], Bradley [9], Leckie [10], Krempl [11], Walker [12], Miller [13], and Hart [14], among others are mentioned. We also wish to cite the works of Ohashi et als. [15], and Murakami and Ohno [16], and Ohno et als. [4] who have been enjoying a measure of success in using a creep hardening surface theory in describing the creep response of metals to piece-wise constant stress histories, a subject with which we will be dealing in this paper. This aspect of the mechanical response of metals has given rise to greater difficulties than say, the stress response to piece-wise constant strain rate histories.

The work of Krausz [17] and his co-workers also occupies a significant position in the literature because of its more fundamental nature in that a microscopic theory of deformation kinetics is used to gain understanding of the mechanical response of metals at the bulk level.

In our initial approach to the subject, with specific attention to the strain (creep) response to piece-wise constant, pure shear stress histories, we used a strictly phenomenological approach, in the context of an endochronic theory. Specifically in one dimension we probed the data with the constitutive equation

$$e^p = \int_{0-}^{z} J(z-z') \frac{ds}{dz'} dz' \tag{1.1}$$

Henceforth convolution integrals such as the one appearing on the right hand side of eq. (1.1) will be given in symbolic form according to eq. (1.1a):

$$\int_{0-}^{z} J(z - z') \frac{ds}{dz'} dz' \overset{\text{def}}{=} J(z)*ds \tag{1.1a}$$

In equation (1.1) e^p has the same connotation as e^c, i.e., it is the inelastic shear strain where

$$\dot{e}^p = \dot{e}^c = \dot{e} - \frac{\dot{s}}{2\mu_0} \tag{1.2}$$

and μ_0 is the elastic shear modulus. We caution, however, that other definitions of e^c have been used in the literature. The intrinsic time z was defined by equation (1.3) where

$$dz = \frac{d\zeta}{f(\zeta,\dot{\zeta})} \tag{1.3}$$

and $\dot{\zeta} = |\dot{e}^c|$ is the usual fashion. The dependence of f on $\dot{\zeta}$ lends "strain rate sensitivity" to the equation, which otherwise would be strain rate insensitive.

While equations of the type (1.1), (1.2) and (1.3) were shown to give satisfactory results in the case of constant strian rate histories as demonstrated by Wu and Yip [18,19] and Lin and Wu [20,21], we found that these equations did not prove satisfactory in the case of piece-wise constant stress histories. With specific reference to the data of Ref. [4], it was found that f had to be essentially independent of z, to account for the periodic creep response to piecewise constant cyclic histories. Thus, limiting f to a dependence on $\dot{\zeta}$ only resulted in a gross overestimate of the creep strain under cyclic conditions. Correcting f so as to match the data gave rise to oscillations in f which could not be accounted for by means of equation (1.3). Furthermore, the phenomenological approach did not give any hint as to the physical mechanism(s) responsible for such fluctuations in f. To overcome the difficulties we appealed to the theory of deformation kinetics in the context of the internal variable theory. The latter is treated briefly in Section 2 while the former is represented in detail in Section 3.

2. Internal Variable Theory

Irreversible thermodynamics of internal variables is now a well established field so we proceed to give a very breif outline of the theory for the sake of completeness. We limit ourselves to small strain fields. In the Helmholtz formulation the thermodynamic state is described by the free energy density ψ which is a function of the strain tensor $\underset{\sim}{\epsilon}$ the temperature T and n interval variables $\underset{\sim}{q}^r$ which, for thermomechanical processes, are tensors of the second order. The stress $\underset{\sim}{\sigma}$ and the entrpy density η are then given by equations (2.1) and (2.2)

$$\underset{\sim}{\sigma} = \frac{\partial \psi}{\partial \underset{\sim}{\epsilon}} \tag{2.1}$$

$$\eta = - \frac{\partial \psi}{\partial T} \tag{2.2}$$

In the case of a spatially uniform thermal field the condition of positive rate of irreversible entropy gives rise to the inequality

$$- \frac{\partial \psi}{\partial \underset{\sim}{q}^r} \cdot \dot{\underset{\sim}{q}}^r > 0 \ , \ \| \dot{\underset{\sim}{q}}^r \| \neq 0 \tag{2.3}$$

r, not summed.

In the linear version of the endochronic theory ψ is a quadratic function of its arguments and the evolution equations for $\underset{\sim}{q}^r$ have the form

$$\frac{\partial \psi}{\partial \underset{\sim}{q}^r} + \underset{\sim}{b}_r \cdot \frac{d\underset{\sim}{q}^r}{dz} = 0 \tag{2.4}$$

r not summed, where n such equations exist, one for each variable $\underset{\sim}{q}^r$, and $\underset{\sim}{b}_r$ are positive definite tensors of the fourth order.

When isothermal conditions prevail and the solid is initially isotropic and the tensors $\underset{\sim}{b}_r$ are constant, then equations (2.1) and (2.4) combive to give rise the integral constitutive equations

$$\underset{\sim}{s} = 2\mu(z)*d\underset{\sim}{e} \tag{2.5}$$

$$\sigma = 3K(z)*d\varepsilon \tag{2.6}$$

where $\underset{\sim}{s}$ is the stress deviator, $\underset{\sim}{e}$ the strain deviator and σ and ε the hydrostatic stress and strain respectively. The kernels $\mu(z)$ and $K(z)$ are sums of positive decaying exponential functions, i.e.,

$$\mu(z) = \sum_r \mu_r e^{-\alpha_r z}, \quad K(z) = \sum_r K_r e^{-\lambda_r z} \tag{2.7a,b}$$

where μ_r, α_r, K_r and λ_r are all non-negative.

In the generalized endochronic internal variable theory the evolution equations are expressed in terms of the intrinsic times of the mechanisms of internal motion. See Ref [22]. Specifically to each $\underset{\sim}{q}^r$ the theory ascribes an intrinsic time z_r such that the equations of evolution become

$$\frac{\partial \psi}{\partial \underset{\sim}{q}^r} + \underset{\sim}{b}_r \cdot \frac{d\underset{\sim}{q}^r}{dz_r} = 0 \text{ (r not summed)} \tag{2.8}$$

r = 1, 2 ... n.

In the endochronic theory of plasticity of metals as it has been used in the past

$$z_1 = z_2 = \ldots = z_n = z \tag{2.9}$$

and the elastic bulk modulus K in constant, i.e, the material is plastically incompressible. Also,

$$dz = \frac{d\zeta}{f(\zeta)}, \quad d\zeta = \|d\underset{\sim}{e}^p\| \tag{2.10a,b}$$

and

$$\underset{\sim}{de}^{p} = \underset{\sim}{de} - \frac{\underset{\sim}{ds}}{2\mu_0} \tag{2.11}$$

where μ_0 is the elastic shear modulus. The function f is positive and non decreasing. Thus in the case of plasticity, and in the context of the above assumptions, equations (2.5) and (2.6) have the form

$$\underset{\sim}{s} = 2\mu_0(z) * \underset{\sim}{de} \tag{2.12}$$

$$G = 3K\epsilon \tag{2.13}$$

Substitution of equation (2.11) in equation (2.12) gives an equivalent constitutive equation which relates $\underset{\sim}{s}$ directly to the history of $\underset{\sim}{e}^{p}$. Thus

$$\underset{\sim}{s} = 2\rho(z) * \underset{\sim}{de}^{p} \tag{2.14}$$

See Valanis, Ref. [23]. The relation between ρ and μ is given in terms of their Laplace transforms in equation (2.15).

$$\bar{\rho}\left(1 - \frac{p\bar{\mu}}{\mu_0}\right) = \bar{\mu} \tag{2.15}$$

It has been found that in the case of metals at room temperature p and f are well represented by the relations

$$\rho = \rho_0 \frac{1}{z^{\alpha}} e^{-kz}, \quad f = 1 - ae^{-bz} \tag{2.16a,b}$$

where ρ_0, α, a, b are positive and k is non-negative.

In the Gibbs formulation the thermodynamic state is described by the free energy density ϕ, which is a function of the stress tensor $\underset{\sim}{\sigma}$ the temperature T and n internal variables $\underset{\sim}{q}^{r}$ which, again, are second order tensors. The function ϕ is related to ψ by the equation

$$\phi = \psi - \sigma_{ij}\,\varepsilon_{ij} \tag{2.16}$$

The counterparts of equations (2.1) and (2.2) are

$$\underset{\sim}{\varepsilon} = -\frac{\partial \phi}{\partial \underset{\sim}{\sigma}} \tag{2.17}$$

and

$$\eta = -\frac{\partial \phi}{\partial T} \tag{2.18}$$

whereas the positive rate of irreversible entropy gives rise to the inequality

$$-\frac{\partial \phi}{\partial \underset{\sim}{q}^r} \cdot \dot{\underset{\sim}{q}}^r > 0, \quad \|\dot{q}^r\| \neq 0 \tag{2.19}$$

for each r, where $-\frac{\partial \phi}{\partial \underset{\sim}{q}^r}$ is the internal microforce for the internal mechanism r while the evolution equations for $\underset{\sim}{q}^r$ are, in the case of the generalized endochronic formulation

$$\frac{\partial \phi}{\partial \underset{\sim}{q}^r} + \underset{\approx}{b}_r \cdot \frac{d\underset{\sim}{q}^r}{dz_r} = 0 \tag{2.20}$$

If we now stipulate that ϕ is quadratic in its variables and $dz_r = dz$ for all r, and $\underset{\approx}{b}_r$ are constant then in the case of isotropic materials and isothermal conditions, equations (2.17) and (2.20) combine to give the constitutive equations

$$\underset{\sim}{e} = \frac{1}{2} L(z) * d\underset{\sim}{s} \tag{2.21}$$

$$\varepsilon = \frac{1}{3} N(z) * d\sigma \tag{2.22}$$

When plastic incompressibility applies N is a constant and equal to $\frac{1}{K}$ (see equation (2.13). Also μ and L are related by equation (2.23).

$$\mu(z)*dL = H(z) \tag{2.23}$$

where H(z) is the unit step function.

In view of equation (2.11)

$$\underset{\sim}{e}^p = \underset{\sim}{e} - \frac{1}{2}\frac{\underset{\sim}{s}}{\mu_0} \tag{2.24}$$

Thus

$$\underset{\sim}{e}^p = \frac{1}{2} J(z)*d\underset{\sim}{s} \tag{2.25}$$

where

$$J(z) = -\frac{1}{2\mu_0} H(z) + L(z) \tag{2.26}$$

The functions J(z) and $\rho(z)$ are also related as shown in equation (2.27)

$$J(z)*d\rho = H(z) \tag{2.27}$$

Spectrum of Intrinsic Times

Of the n internal mechanisms let group r have an intrinsic time z_r. Then to the group r of internal variables n_r in number, there will correspond an intrinsic time z_r. Evidently $\sum_{r=1}^{m} n_r = n$ where m is the number of groups.

A straightforward analysis using equations (2.16) (2.17) and (2.20) when ϕ is a quadratic isotropic function of e_{ij} and $q_{ij}^{(r)}$ and $\underset{\sim}{b}_r$ are constant isotropic tensors leads to the equations

$$\underset{\sim}{e}^p = \sum_{r=1}^{n} J_r(z_r)*d\underset{\sim}{s} \tag{2.28}$$

$$\varepsilon^p = 0, \quad \varepsilon = \frac{1}{3} N\sigma \tag{2.29a,b}$$

where plastic incompressibility has been observed. They physical interpretation of equation (2.28) is that each of the m groups of mechanisms, say r, contributes to the total strain a partial strain $\underset{\sim}{e}^p_r$ such that

$$\sum_{r=1}^{m} \underset{\sim}{e}^p_r = \underset{\sim}{e}^p \tag{2.30}$$

where

$$\underset{\sim}{e}^p_r = J_r(z_r) * d\underset{\sim}{s} \tag{2.31}$$

The intrinsic time z_r is related to ζ by the equation

$$dz_r = \frac{d\zeta}{f_r}$$

where f_r is the hardening function of graph r.

The need for this more general approach which was presented in a previous reference [22], has been discussed in the introduction and has to do with the fact that one intrinsic time is just not sufficient to describe the creep response of metals to piece-wise constant stress histories. The physical justification for this possibility is discussed in the section on deformation kinetics, but simply put, it means that the hardening function f is not the same for all mechanisms at high temperatures, though the assumption of an f common to all $\underset{\sim}{q}^r$ suffices at room temperatures as demonstrated in our work on endochronic plasticity. The appeal to deformation kinetics is necessitated by the desire to determine how f is influenced by the micro-mechanical process which accompanies the inelastic deformation.

3. Deformation Kinetics

The theory of deformation kinetics was founded by Eyring [24] and its application to rate processes has been pursued by Eyring, Krausz [24] and their co-workers with a great deal of success.

In keeping with the ideas of deformation kinetics we attribute macromotion to additive effects of micromotions brought about by local distortion of atomic "energy barriers". At this point it is essential that we distinguish between diffusion of particles and diffusion of dislocations or vacancies. The distinction may be stated most simply in terms of the mean free path ℓ of a particle. In the case of particle diffusion ℓ is large compared to its counterpart in the case of dislocation or flaw diffusion. If a particle travels n units of distance "a" before coming to rest, then $\ell = na$. However, if a flaw travels n units of distance a, the mean free path of a particle is still a, because a different particle partakes each time in the motion of the flaw. Thus in the case of particle diffusion $n >> a$. Most important, however, is the fact that, in either case, each unit of motion consists of an atom moving across an energy barrier.

In addition we would expect that in the case of flaw or dislocation diffusion the energy barriers would be lower than those of particle diffusion. In fact, the activation energy of self diffusion is lower at low homologous temperatures (where dislocation motion is dominant) than at higher temperatures where particle diffusion dominates the process.

To apply the ideas of deformation kinetics to the viscoplastic deformation and flow of solids we appeal to a simple atomic model whereby prior to the application of stress each atom of the solid is situated at the bottom of a symmetric potential well. A typical potential well with the accompanying local potential surface is shown in Figure 1 by a solid line. The forward and backward barriers are equal and both have a height ε_0^r. When stress is applied,

the atoms will be displaced from their initial positions and the local potential surface of an atom will distort. The distorted potential surface is also shown. The effect of the distortion is to reduce the forward barrier by an amount w_f^r and increase the backward barrier by an amount w_b^r. It will be shown that this type of barrier distortion will give rise to an average forward motion of the atoms occupying potential wells with barriers ϵ_0^r.

Boltzmann Statistics. To determine quantitatively the effect of barrier distortion on the mean atomic motion we appeal to Boltzmann statistics. Accordingly the probability of finding an atom in an energy state ϵ_i is given by equation (3.1):

$$p_i = \alpha e^{-\beta\epsilon_i} \tag{3.1}$$

where

$$\alpha = 1/\sum_i e^{-\beta\epsilon_i}, \quad \beta = \frac{1}{kT} \tag{3.2a,b}$$

in the usual notation.

Let N_r be the number of atoms occupying potential wells with initial energy barriers ϵ_0^r. The probability that an atom is in an energy state greater than ϵ_0^r is p_0^r where

$$p_0^r = \sum_{\substack{r \\ \epsilon_i > \epsilon_0^r}} \alpha \exp(-\beta\epsilon_0^r) \tag{3.3}$$

States ϵ_i^r such that $\epsilon_i^r > \epsilon_0^r$ we have called activated states [25] differing from Eyring. Thus, the number of atoms in an activated state is $N_r p_0^r$. As the barriers are symmetric the probability that an atom will move forward is equal to the probability that it will move backwards so that the net motion (average displacement) of the atoms N_r is zero.

When the potential energy surface is distorted the number of atoms A_r partaking in a forward motion is now changed to

$$A_r = N_r \sum_{\substack{r \\ \varepsilon_i^r > \varepsilon_0^r - w_f^r}} \alpha \exp(-\beta \varepsilon_i^r) \tag{3.4}$$

while the number B_r of atoms partaking in as backward motion is

$$B_r = N_r \sum_{\substack{r \\ \varepsilon_i^r > \varepsilon_0^r + w_b^r}} \alpha \exp(-\beta \varepsilon_i^r) \tag{3.5}$$

The net number of atoms that partake in a forward motion is, thus, $A_r - B_r$ where

$$A_r - B_r = N_r \sum_{\substack{r \\ \varepsilon_b^r - w_f^r < \varepsilon_i^r < \varepsilon_0^r + w_b^r}} \alpha \exp(-\beta \varepsilon_i^r) \tag{3.6}$$

To evaluate the sum on the right had side of equation (3.6) we shall assume that w_f^r and w_b^r are both small. In this case we represent the distribution of energies ε_i^r in the vicinity of ε_0^r in terms of the local tangent to the distribution at ε_0^r by writing

$$\varepsilon_i^r = \varepsilon_0^r + k^r (i - i_0) \tag{3.7}$$

where i_0 is the value of i at $\varepsilon_i^r = \varepsilon_0^r$ and k^r is the slope of the distribution which is a function (in general) of ε_0^r. See Figure 2.

Substitution of the relation (3.7) in the sum on the right hand side of equation (3.6) leads to the simple expression

$$A_r - B_r = 2N_r \alpha \frac{e^{-\beta \varepsilon_0^r} \sin \beta_r w_r}{1 - e^{\beta k^r}} \tag{3.8}$$

where

$$w^r = \frac{w_f^r - w_b^r}{2} \quad , \quad \Delta\varepsilon_0^r = \frac{w_b + w_f^r}{2} . \tag{3.9,10}$$

We note that the terms $e^{-\beta\varepsilon_0^r}$ and $1 - e^{-\beta k^r}$ are related to the initial state, i.e., the barrier height and the energy distribution, while the terms $\sin \beta w_r$ and $\exp(-\beta\Delta\varepsilon_0^r)$ are brought about by barrier distortion.

The mean velocity v_r^p relative to the lattice of the atoms in group r may now be calculated in terms of the barrier distortion parameters N_r and $\Delta\varepsilon_0^r$. If λ is the mean lattice distance and τ_r is the average time taken by the atoms of group r to traverse that distance across the barrier ε_0^r then

$$v_r^p = (\lambda/\tau_r)(A_r - B_r)/N_r \tag{3.11}$$

We now define an internal variable q_r by the relation

$$\dot{q}_r = v_r^p/\lambda \tag{3.12}$$

Evidently in view of equation (3.11)

$$\dot{q}_r = (A_r - B_r)/N_r \tau_r \tag{3.13}$$

In view of equations (3.8) and (3.13)

$$\dot{q}_r = \frac{2\alpha e^{-\beta\varepsilon_0^r}}{1 - e^{-\beta k^r}} \left(\frac{1}{\tau_r}\right) e^{-\beta\Delta\varepsilon_0^r} \sinh \beta w_r \tag{3.14}$$

In so far as steady creep is concerned the assumption is usually made that of all the operating mechanisms only one survives in the steady state, i.e., $r = 1$ and w_1 is proportional to the stress (in one-dimensional stress fields). However, in the case of transient creep it is the local microforce, i.e., $-\frac{\partial\phi}{\partial q_r}$ on the group r that will determine the barrier distortion. Thus, following Ref. [25], we let w_r be proportional to $-\frac{\partial\phi}{\partial q_r}$ according to equation (3.15)

$$W_r = -C_r \frac{\partial \phi}{\partial q_r} \tag{3.15}$$

where C_r may depend on temperature.

Thus if we let

$$b_{00}^r = (1 - e^{-\beta k^r}) e^{\beta \varepsilon_0^r}/2\alpha \tag{3.16}$$

then in view of equations (3.14 - 3.16)

$$b_{00}^r \dot{q}_r + \frac{1}{\tau_r} e^{-\beta \Delta \varepsilon_0^r} \sinh (\beta C_r \frac{\partial \phi}{\partial q_r}) = 0 \tag{3.17}$$

<u>This is an "internal variable" form of the equation for the mean irreversible motion of the group r of paricles facing a potential barrier ε_0^r .</u>

<u>Discussion of equation (3.17)</u>. As we pointed out equation (3.17) establishes a physical meaning for the internal variables in that q_r is the mean displacement relative to the lattice of a group r of particles facing a potential barrier of magnitude ε_0^r . The above equation was published by Valanis and Lalwani in Ref. [25], with $\Delta \varepsilon_0^r = 0$. The appearance of the term $\Delta \varepsilon_0^r$ in equation (3.1) was inferred as a result of our effort to describe analytically the creep response of 306 stainless steel to piece-wise constant stress histories. This will be discussed in Section 4.

The time to traverse the barrier, i.e., τ_r is also of central importance in equation (3.17). Eyring used simplifying assumptions to arrive at the conclusion that τ_r is proportional to the square root of the ambient temperature. However, one can show that it depends at least in part on the barrier shape and height (Ref. [25]). In this work we have found that is also sensitive to the plastic strain rate. This is to be expected sind τ_r depends on the barrier conformation, which in turn depends on the plastic strain. The rate of plastic strain affects the rate of barrier distortion which must affect the traversal time τ_r.

Consider now two processes (a) and (b) the first of which is proceeding at a faster plastic strain rate than the second. With regard to the forward motion of a particle, the height of the barrier will be diminishing faster in case (a) than in (b), so that the forward moving particle will be encountering a consistently lower barrier in case (a) than in (b). It follows that the time to cross the barrier in case (a) will be shorter than in case (b). Thus

$$\tau_a < \tau_b \text{ whenever } \dot{\zeta}_a > \dot{\zeta}_b$$

The above inequality will be satisfied if

$$\tau = \frac{\tau_0}{g(\dot{\zeta})} \tag{3.18}$$

where τ_0 is a constant and g is a monotonically increasing function of $\dot{\zeta}$. In this work we have set

$$g(\dot{\zeta}) = \frac{1}{\dot{\zeta}^{1-m}} \tag{3.18a}$$

where m is a material constant.

Deformation kinetics is brought into accord with linear irreversible thermodynamics if in equation (3.17) the argument of the hyperbolic sine is sufficiently small for the approximation

$$\sinh\left(\beta C_r \frac{\partial \phi}{\partial q_r}\right) \sim \beta C_r \frac{\partial \phi}{\partial q_r} \tag{3.19}$$

to be appropriate. In this event equation (3.17) becomes a standard linear evolution equation, i.e.,

$$b^r \dot{q}_r + \frac{\partial \phi}{\partial q_r} = 0 \tag{3.20}$$

where

$$b^r = b_{00}^r \frac{\tau_r}{\beta C_r} e^{\beta \Delta \varepsilon_0^r} \tag{3.21}$$

In view of equations (3.18a), (3.20) and (3.21) one finds that the "endochronic" form of equation (3.20) is

$$b_0^r \frac{dq^r}{dz_r} + \frac{\partial \phi}{\partial q_r} = 0 \tag{3.22}$$

where

$$b_0^r = b_{00}^r \frac{\tau_0}{\beta C_r} \tag{3.23}$$

and

$$dz_r = \frac{dz}{\dot{\zeta}^m f_r} \tag{3.24}$$

$$f_r = e^{\beta \Delta \varepsilon_0^r} \tag{3.25}$$

Thus in deformation kinetics terms the rate sensitivity is attributable to the time to cross the barrier while the hardening (softening) is related to the change in the mean height of the barrier as a result of the stress history. Thus if $\Delta \varepsilon_0^r$ increases the material hardens while if it decreases the material softens in accord with our physical intuition regarding such processes.

4. Analysis of Piece-wise Constant Stress Histories in Pure Shear.

We begin with the integral

$$e^p = J(z)*ds \tag{4.1}$$

where e^p represents a shear creep strain component, s is the corresponding shear stress component and J the appropriate creep function. As usual

$$dz = \frac{d\zeta}{g(\dot{\zeta})f} \tag{4.2}$$

where g is the rate sensitivity function and f the hardening function. Also

$$d\zeta = k|de^p| \tag{4.3}$$

where k is an appropriate scalar constant. Typically, it e^p denotes a creep shear strain component and

$$d\zeta = \|d\underline{e}^p\| \tag{4.4}$$

then $k = \sqrt{2}$ and J is the creep function in pure shear.

For our purposes it is more convenient to write equation (4.1) in the explicit form

$$e^p = \int_0^t J(z(t) - z(t')) \frac{ds}{dt'} dt' \tag{4.5}$$

for reasons that will become apparent.

4.1. Monotonic Creep in the Presence of a Constant Stress History

In this specific case

$$s(t) = s_0 H(t) \tag{4.6}$$

where H(t) is the unit step function whose "derivative" is the Dirac delta function. In this instance substitution of equation (4.6) in equation (4.5) gives the creep response in the simple form

$$e^p = s_0 J(z) \tag{4.7}$$

where s_0 is the amplitude of the step function of applied stress. It is apparent from equation (4.7) that if the form of $J(z)$ is known then knowledge of $z(t)$ determines creep strain in terms of the stress amplitude s_0. We caution that e^p is not necessarily linear in s since $z(t)$ depends on s_0 as we shall demonstrate.

To this end differentiate equation (4.7) with respect to t and use equations (4.2) and (4.3) to find that under monotonic conditions

$$g(\dot{\zeta}) = k s_0 J'(z) \dot{z}^{-1} \tag{4.8}$$

where $J'(z)$ is the derivative of J with respect to z. Thus

$$\dot{\zeta} = g^{-1} \{ k\, s_0\, J'(z)\, \dot{z}^{-1} \} \tag{4.9}$$

But from equations (4.7) and (4.3)

$$\dot{\zeta} = k\, s_0\, J'(z)\, \dot{z} \tag{4.10}$$

Thus from equations (4.9) and (4.10)

$$\dot{z} = \frac{g^{-1}\{k s_0 J'(z) \dot{z}^{-1}\}}{k\, s_0 J'(z)} \tag{4.11}$$

Equation (4.11) gives $z(t)$ by numerical integration if f is known.

To assign analytical forms to the functions $J(z)$ and $g(\dot{\zeta})$ we appeal to experiment and the underlying assumptions of endochronic plasticity. It is common experience that metals become more strain rate sensitive as the temperature rises. However, the spirit of the endochronic theory is that this change is brought about not by a change in the form of $J(z)$ but by virtue of $g(\dot{\zeta})$ which is evidently dependent on temperature even though this dependence is suppressed in equation (4.2).

At room temperature where rate effects are not significant J(z) is represented very closely by the analytical impression

$$J(z) = J_0 z^{\alpha} \tag{4.12}$$

where α is the vicinity of 0.85 for a number of metals. This form is retained by virtue of the above argument, at higher temperatures.

Experiments also indicate that under monotonic creep conditions

$$e^p = F(s_0)\, t^{\beta} \tag{4.13}$$

i.e., that the stress and time dependence of creep strain are factorable and that the time dependence is represented very closely by a power law. If during monotone creep f is a constant - which was found to be so for one component of the creep - then for equation (4.13) to hold $g(\dot{\zeta})$ must also be a power function. Thus we have set

$$g(\dot{\zeta}) = \dot{\zeta}^m \tag{4.14}$$

In view of these stipulations equation (4.11) now becomes

$$f^{\frac{1}{m}} \dot{z} = (k\, \alpha\, s_0\, J_0)^{\frac{1-m}{m}} z^{\frac{(\alpha-1)(1-m)}{m}} \tag{4.15}$$

Special solutions to equation (4.15). We proceed to give some special solutions to equation (4.15) when (a) f is constant and (b) when f is a power function of z. When f is constant the solution is given by equation (4.16):

$$f^{\frac{\beta'}{m}} z = A\, (k\, \alpha\, s_0\, J_0)^{n'} t^{\beta'} \tag{4.16}$$

where

$$A = \left(\frac{1}{\beta'}\right)^{\beta'}, \quad \beta' = m/1 + \alpha m - \alpha, \quad n' = \frac{1-m}{m}\beta' \tag{4.17}$$

In the case where $f = f_0 z^{\phi}$, where $\phi > 0$, the solution to equation (4.15) is given by equation (4.16) as before except that now the constant β' is given by equation (4.18):

$$\beta' = m/1 + \alpha m - \alpha + \phi \tag{4.18}$$

and the constant f on the left hand side of equation (4.16) is now denoted by f_0.

Knowing z(t) one may now calculate the creep strain e^p by use of equations (4.7) and (4.12), in conjunction with equation (4.16). Thus

$$e^p = A^{\alpha} f_0^{\frac{\beta}{m}} (k\alpha)^{n-1} (s_0 J_0)^n t^{\beta} \tag{4.19}$$

where

$$1 + \alpha n' = n, \quad \beta'\alpha = \beta \tag{4.20a,b}$$

Discussion. So far we have represented the creep strain by a single integral. We have also represented the creep function J(z), the strain rate sensitivity function $g(\dot{\zeta})$ and the hardening function $f(\zeta)$ by analytical forms of the power type. By analysis we then arrived at equation (4.19) which is basically of the form

$$e^p = B\, s_0^n\, t^{\beta} \tag{4.21}$$

where B is a constant, whereby the monotonic creep strain depends multiplicatively on the stress amplitude to the power n and the time to the power β. This form has appeared frequently in the literature where it has been arrived at by analysis of the data. It does not for all creep data and certainly not over the entire range of stress.

What is important, however, is that the creep strain depends on time according to a power law (equation (4.21) in accordance with observation as per equation (4.13) while the dependence on stress is of a more general type. One can change the dependence of e^p on s_0 by changing the analytical form of J(z) or $g(\dot{\zeta})$ or both but it seems that this would vitiate the dependence of e^p on a power function of t. Two other avenues are, however, available. One is to introduce a spectrum of intrinsic times, as discussed previously, i.e., a series

of integrals on the right hand side of equation (4.1). The other is to introduce a stress dependence in the hardening function f . This has been found to be the case in other materials such as polymers.

Specifically, if one sets

$$f = f_0(s_0)z^{\phi} \tag{4.22}$$

then under monotonic creep conditions in the presence of constant stress equation (4.19) will have the form given by equation (4.13), for an appropriate choice of the function f.

This approach alone, however, has been found inadequate to describe creep under cyclic piece-wise constant stress histories. This question as well as a constitutive equation involving more than one intrinsic time will be discussed in the next section.

5. Specific Constituitive Equations for 304 Stainless Steel

In the application of the theory to 304 stainless steel at 600°C and specifically to the experimental data generated by Ohno et als. (Ref. [4]), two terms were retained on the right hand side of equation (2.28), i.e.,

$$e^p = J_1(z_1)*ds + J_2(z_2)*ds \tag{5.1}$$

For the purposes of analysis and presentation of the results it is more convenient to write equation (5.1) in the form

$$e^p = e_1^p + e_2^p \tag{5.2}$$

where

$$e_r^p = J_r(z_r)*ds \tag{5.3}$$

r = 1, 2. In this case two hardening functions exist in the sense of equation (5.4)

$$dz_r = \frac{dz}{f_r} \cdot \frac{1}{\xi m} \tag{5.4}$$

where m is a material constant found to be equal to 0.12. Also two creep functions $J_1(z)$ and $J_2(z)$ are needed and these were given the analytical forms shown in equation (5.5):

$$J_1 = J_1^0 z^{\alpha_1}, \quad J_2 = J_2^0 z^{\alpha_2} \tag{5.5 a,b}$$

where $\alpha = 0.836$, $\alpha_2 = 1$. $J_1^0 = 2.34 \times 10^{-3}$ MPa, $J_2^0 = 1.58 \times 10^{-3}$ MPa. It still remains to determine the form of the hardening functions. In order to match the monotonic data f_2 was represented by a power function of the form

$$f_2 = z^{\phi_2} \tag{5.6}$$

where $\phi_2 = 0.196$.

On the other hand f_1 could not be represented as a state function of, say, s and z, or any other variable for that matter. Rather, the experimental cyclic results of Ref. [4], gave strong indication that f_1 should be given in differential form of the type

$$d \log f_1 = dF(|s|, z_1)|_{z_1} \tag{5.7}$$

Note that the right hand side of equation (5.7) is not an exact differential and hence f is a function of the stress history. The physical implication of equation (5.7) is that a change in z_1 does not affect f_1 if during the change the absolute value of the stress s remains constant. A mathematically more explicit form for f_1 is

$$d \log f_1 = \frac{\partial F}{\partial |s|} (|s|, z_1)\, d|s| \tag{5.8}$$

The logarithmic form is not fortuitous but is a consequence of the physics of deformation kinetics and specifically equation (3.25) in view of which

$$\log f_1 = \beta \Delta \varepsilon_0' \tag{5.9}$$

$$d \log f_1 = \beta\, d(\Delta \varepsilon_0') \tag{5.10}$$

The implication is that in mechanism 1 the mean barrier height will change when the absolute value of stress changes but not otherwise. The constituitive description of the material is complete once the function $F(|s|, z_1)$ is known.

The function F is given below for various values of |s| (in MPa):

$$\begin{aligned} F(134.2, z_1) &= 2.25 + 1.3(1 - e^{-30z_1}) \\ F(120, z_1) &= F(134.2, z_1) \\ F(90, z_1) &= 2.19 + 0.9(1 - e^{-50z_1}) \\ F(60, z_1) &= 1.86 + 44(1 - e^{-85z_1}) \end{aligned} \tag{5.11a,b,c,d}$$

In addition the value of the hardening function at zero stress and zero value of z is set at 0.1054. This value together with the relation.

$$\log f(0,|s|_1) - \log f(0,|s|_2) = F(0,|s|_1 - F(0,|s|_2) \qquad (5.12)$$

where s_1 and s_2 are any two stress levels determines f for various values of the initial stress applied at the onset of a creep experiment.

6. Comparison with Piece-wise Constant Stress Experimetns of Ohno et als.

Monotonic Creep Experiments

The strain response to a constant stress history is obtained by application of equation (4.19) in conjunction with equation (5.2). Specifically

$$e^p = \sum_{r=1}^{2} A^{\alpha_r} f_{0r}^{-(\frac{\beta}{n})_r} (k\alpha_r)^{n_r-1} (s_0 J_{0r})^{n_r} t^{\beta_r} \tag{6.1}$$

in the presence of the constraint

$$\beta_1 = \beta_2 = \beta, \; n_1 = n_2 = n, \; m_1 = m_2 = m \tag{6.2}$$

so that equation (6.1) becomes

$$e^p = (s_0)^n t^\beta \sum_{r=1}^{2} A^{\alpha_r} (f_{0r})^{\frac{\beta}{m}} (k\alpha_r)^{n-1} J_{0r}^{n} \tag{6.3}$$

In the case of the linear model (2), f_{02} is a constant. However, in the non-linear model (1), f_{01} is a function of $|s|$. This dependence is determined by adjusting f_0, for various values of $|s|$, so as to obtain optimal agreement between theory and experiment in the case of monotonic creep. The function f_{01} ($|s|$) is shown in Figure 3. With all the other constants known, the descriptive capability of the theory is shown in Figure 4.

Cyclic Creep Experiments

Following Section 2 let e_r^p be the r'th partial shear strain such that

$$e_r = J_r(z_r)*ds \tag{6.4}$$

and

$$e^p = \sum_{r=1}^{m} e_r^p \tag{6.5}$$

where in our case m = 2. For our purposes it is more convenient to write equation (6.4) in the form

$$e_r^p = \int_0^t J_r[z_r(t) - z(t^r)] \frac{ds}{dt^r}\, dt' \tag{6.6}$$

in the specific case of piece-wise constant stress histories of the type considered by Ohno et als.

$$\frac{ds}{dt} = s_0\{\delta(t) - a\,\delta(t-t_1) + a\,\delta(t-t_2) \ldots .\} \tag{6.7}$$

where $\delta(t)$ is the Dirac delta-function, s_0 is the initial stress amplitude and a is a constant. In this set of experiments two parameters s_0 and "a" define the history of stress - in addition to the reversal times t_1, t_2 ... t_n. Substitution of equation (6.7) in equation (6.6) and integration gives the explicit result

$$e_r^p = s_0\{J_r(z_r) + a \sum_{n=1}^{N} (-1)^r J_r(z_r - z_{rn})\} \tag{6.8}$$

or

$$e_r^p = s_0\, y(z_r) \tag{6.9}$$

where $y(z_r)$ represents the bracket on the right hand side of equation (6.8). We differentiate equation (6.9) to obtain

$$\dot{e}_r^p = s_0\, \hat{y}(z_r)\, \dot{z}_r \tag{6.10}$$

where $\hat{y}_r = \frac{dy}{dz_r}$. Use of equation (5.4) then gives the result

$$\dot{e}_r^p = s_0\, \hat{y}_r \frac{\dot{\zeta}}{f_r z^m} \tag{6.11}$$

Now we take absolute values of both sides of equation (6.11) and use equation (4.3) to obtain

$$f_r \dot{\zeta}^m = s_0 \, k|\hat{y}| \tag{6.12}$$

But in view of equation (5.4)

$$\dot{\zeta} = (f_r \dot{z}_r)^{\frac{1}{1-m}} \tag{6.13}$$

Equations (6.12) and (6.13) combine to give the following differential relation between dz_r and dt

$$dt = \frac{f_r^{\frac{1}{m}} \, dz_r}{|k s_0 \hat{y}_r|^{\frac{1-m}{m}}} \tag{6.14}$$

Integration of equation (6.14) gives the relation between z_r and t. Substitution of $z_r(t)$ in equation (6.8) then gives the desired relation $e_r^p(t)$ and, therefore, $e^p(t)$ upon use of equation (6.5).

In our particular case

$$J_r = J_{0r} \, z_r^{\alpha_r} \tag{6.15}$$

and

$$y_r = \alpha_r \, J_{0r} \, z_r^{\alpha_1} + \sum_{n=1}^{N} (-1)^r \, J_{0r} \, (a_r - a_{rn})^{\alpha_r} \tag{6.16}$$

In Figures 5, 6 and 7 we show the experimental values of $e^p(t)$ obtained in Ref. [4] for the stress histories shown. Also shown are the analytical functions $e^p(t)$ obtained (a) by the use of the present theory and (b) as reported by Ohno et als. in Ref. [4] using their own theory.

The most significant difference in the predictive capability of the two theories lies in their depiction of the creep recovery slope at points of stress reversal. The endochronic theory predicts an infinite slope, in agreement with experiment, while the theory by Ohno et als. depicts a finite much shallower slope. Overall the predictive capability of the endochronic theory is very good for the type of stress histories discussed here.

7. Creep in Tension-Torsion

In this section, we examine this problem in the complex case where both the torsion and tension histories are piece wise constant junctions of time. In addition in the complexity of the stress histories, we have the added coupling effect which is observed experimentally. In other words, the cyclic creep in torsion is affected by the presence of tension. It will show that this effect is accounted for satisfactorily by the definition of intrinsic time. In this section we shall address the experiments of ohms [4] where cyclic creep in shear is carried out at constant tensile stress.

The basic equations are:

$$\underline{e}_N^b = \sum_{r=1}^{2} \underline{e}_N{}_r^b \tag{7.1}$$

$$\underline{e}_N = \Sigma(Z_r) * d\underline{S}_N \tag{7.2}$$

$$dZ_r = \frac{d\xi}{fr} \cdot \frac{1}{\xi^{rm}} \tag{7.3}$$

$$dS = ||d\underline{e}_N^p|| \tag{7.4}$$

$$J_r = J_r^o \, Z^{\alpha r} \tag{7.5}$$

$$f_r = Z^{\phi r} \tag{7.6}$$

Thus the actual solid is represented by two inelastic model solids in series. The pertinent material functions and constants are the following:

$$\alpha_1 = 0.836, \quad J_1^o = 2.34 \times 10^{-3} \text{ MPa}$$

$$\alpha_2 = 1.0 \quad J_2^o = 1.58 \times 10^{-3} \text{ MPa}$$

$$m_1 = m_2 = 0.12$$

$$\phi_1 = 0, \quad \phi_2 = 0.196$$

In this section f_1 is a constant for simplicity while in section 6 it was an elaborate function designed to match the experimental data as closely as possible. Thus in this section, the effectiveness of the theory is demonstrated without the need for the complexity of representation of f_1 adopted in section 6.

The stress histories involved in the experiments of Ref. 4 are of the type

$$\sigma_{ij}(k) = \sigma_{ij}^o \, H_a(t) \tag{7.7}$$

where

$$H_a(t) = H(t) - a \sum_{r=1}^{n} H(t - rt_o) \tag{7.8}$$

and H(t) denotes the Heaviside step function.

In the following denote the axial stress by α_a, the axial creep strain by ε^p, creep strain by e^p. In all the experiments considered below

$$\alpha_1 = \sigma_1^o \, H(t) \tag{7.9}$$

while

$$s = s^{o} H_a(t) \tag{7.10}$$

for values of a equal to 0, 1.5 and 2. Plastic (inelastic) incompressibility is assumed; i.e.

$$\varepsilon^{p}_{pk} = 0 \tag{7.10}$$

In the presence of equation (7.10), equations (7.1) and (7.2) become

$$e^{p}_{r} = J_r(Zr) * ds \tag{7.11}$$

$$e^{p}_{1r} = \frac{2}{3} J_r(Zr) * d6 \tag{7.12}$$

substition of equation (7.8) in equation (7.11) gives the explicit result:

$$e^{p}_{r} = s_0 \{J_r(Z_r) + a \sum_{n=1}^{N} (-1)^n J_r(Z_r - Z_{rn})\} \tag{7.13}$$

$$e^{pr}_{1} = \frac{2}{3} 6_1 J_r(Z_r) \tag{7.14}$$

The creep strains of e^p and ε^p were then determined numerically following the method given in detail in section 6. The results are shown in Figures 8, 9 and 10 for corresponding values of a=1, 1.5 and 2. Comparison with data shows good qualitative agreement. However a refinement of the representation of the hardening properties of the material seems pertinent.

The work of this section was done co-jointly by K.C. Valanis and S.D. Lee. The latter is a graduate student in Civil Engineering at the University of Cincinnati.

8. Large Deformation Theory

In this section we extend the theory to the domain of large deformation. This is an important development because high temperature processes, during which materials are strain rate sensitive, involve large deformations. Our target here is metals.

A great deal of effort has been expended in recent years to develop constitutive eqations pertaining to large deformation of metals. The problems that one encounters in the formulation of small deformation theories are magnified when large deformations are involved. When the problem is approached from a yield surface point of view, one has to be concerned with the evolution of its geometry in stress space as the material deforms and its translation in stress space (i.e., a constitutive description of the back stress - which has been the central problem in classical plasticity).

In addition, and irrespective of one's approach, the question of appropriate separation of the increment of plastic strain (defined in large deformation terms) into elastic and plastic parts must be addressed and resolved. How this is to be done is a matter of differing opinion. Of course over and above these considerations, the principle of isotropy of space must must apply. This last requirement creates other difficulties associated with "objective rates" when incremental theories are considered. In strictly mathematical theories the choice of a physically "correct" objective stress rate (say) is not obvious a priori.

In the present paper we side-step a number of the above problems by utilizing the concepts of endochronic plasticity in conjunction with the theory of internal variables to arrive at a constitutive equation of the hereditary type whereby the stress tensor (in terms of its <u>covariant</u> components in the material frame) is a quadratic functional of the history of the Right Cauchy-Green tensor. Plastic incompressibility is assumed and the elastic deformation is neglected relative to the large plastic deformations considered in the paper.

The theory is applicable to both strain rate dependent and strain rate independent processes. In the applications a constant strain rate has been assumed. This is equivalent to a constant plastic strain rate, in the light of the assumption that the elastic component of strain is negligible.

A number of solutions of practical interest have been obtained in closed form or by finite element techniques in strictly Lagrangian terms thus obviating the numerical difficulties associated with Eulerian formulations. Also difficulties associated with objective rates are not encountered because of the integral form of the constitutive equation. Solutions associated with bending, torsion and inflation are obtained in closed form. Finite element solutions pertaining to forging of blocks have also been obtained and will be discussed.

The constitutive equation was first tested by application to the simple homogeneous extension of a bar in the presence of a memory kernel that gives rise to asymptotically constant Cauchy stress. Monotonic behavior was observed with no instabilities. The Piola stress first increased and then decreased with stretch as observed in experiment. The problem of plastic flow in a tube (extrusion problem) was then solved in closed form. Substantially flat displacement profiles were obtained, in agreement with observed behavior.

The problem of the large inflation of a thick sphere was then solved again in closed form revealing a geometric instability at a critical value of the internal pressure, as is commonly observed. Finally the finite bending of a beam was solved revealing the observed shift of the neutral axis toward the compressive side and strongly non-linear stress distribution within the beam.

The "upsetting" of a block, i.e., forging by means of a vertically applied displacement, was solved by finite element methods. The initial barrelling eventually gave way to a bone-shaped configuration and the vertical stress at the outside boundary went from compressive to tensile as expected. The ease of the computation is emphasized.

The body of this work, which served as the Ph.D. thesis of Dr. J.

Wang, is not given in this section, but is appended as Appendix I.

References

1. Valanis, K.C., "Endochronic Theory with Proper Hysteresis Closure Properties," Systems, Science and Software, LaJolla, CA, EPRI Report NP-1388, 1980.

2. Valanis, K.C., and Lee, C.F., "Some Recent Developments of the Endochronic Theory with Applications," Nuclear Engineering and Design, 69, pp. 327-344, (1982).

3. Valanis, K.C., and Lee, C.F., "Endochronic Theory of Cyclic Plasticity with Applications," J. of Appl. Mech. Trans. ASME (to appear).

4. Ohno, J., Murakami, S. and Veno, T., "A Constitutive Model of Creep Describing Creep Recovery and Material Softening Caused by Stress Reversals," Journal of Eng. Mat. and Technol., 107, 1, (1985).

5. Chaboche, J.L., Dang Van, K., and Cordier, K., "Modelization of the Strain Memory Effect on the Cyclic Hardening of 316 Stainless Steel," Trans. 5th SMIRT, L11/3, Aug. 1979, Berlin, Germany.

6. Krieg, R.D., Swearengen, J.C., and Rohde, R.W., "A Physically-Based Internal Variable Model for Rate--Dependent Plasticity," in Inelastic Behavior of Pressure Vessels and Piping Components, ed. T.Y. Chang and E. Krempl, ASME PVP-028, pp. 15-28, (1978).

7. Malvern, L.E., "The Propagation of Longitudinal Waves of Plastic Deformation in a Bar of Material Exhibiting a Strain-Rate Effect," J. Appl. Mech., 18, pp. 203-208, (1951).

8. Haisler, W., "Application of an Uncoupled Elastic--Plastic Creek Constitutive Model to Metals at High Temperatures," in NASA Symposium on Nonlinear Constitutive Relations for High Temperature Applications, May 19-20, (1982). The University of Akron, Akron, Ohio, pp. 185-189.

9. Bradley, W.L., and Yuen, S., "A New Coupled Viscoplastic Constitutive Model," in NASA Symposium on Nonlinear Constitutive Relations for High Temperature Applications, May 19-20, (1982). The University of Akron, Akron, Ohio, pp. 217-233.

10. Cescotto, S., and Leckie, F.A., "Determination of Unified Constitutive Equations for Metals at High Temperature," Proceedings Int. Conf. on Constitutive Laws for Engineering Materials, ed. C.S. Desai and R.H. Gallagher, Jan. 10-14, (1983), Tucson, Arizona, pp. 105-111.

11. Krempl, E., "The Role of Servocontrolled Testing in the Development of the Theory of Viscoplasticity Based on Total Strain and Overstress," ASTM STP 765, pp. 5-28, (1982).

12. Walker, K.P., "Research and Development Program for Nonlinear Structural Modeling with Advanced Time--Temperature Dependent Constitutive Relationships," NASA CR-165533, Nov. 1981.

13. Miller, A.K., "An Inelastic Constitutive Model for Monotonic Cyclic, and Creep Deformation: Part I--Equations Development and Analytical Procedures, Part II--Application to Type 304 Stainless Steel," J. of Eng. Mat. Techn. Trans. ASME, 98, pp. 97-133, (1976).

14. Hart, E.W., "Constitutive Relations for the Nonelastic Deformation of Metals," J. Engn. Mat. Techn. Trans. ASME, 98, pp. 193-202, (1976).

15. Ohashi, Y., Ohno, N. and Kawai, K., "Evaluation of Creep Constitutive Equations for Type 304 Stainless Steel Under Repeated Multiaxial Loading," J. Eng. Mat. and Technol., 104, 159, (1982).

16. Murakami, S. and Ohno, N., "A Constitutive Equation of Creep Based on the Concept of a Creep Hardening Surface," Int. J. Solids and Struct., 18, 597, (1982).

17. Krausz, A.S. and Faucher, B., "A Kinetics Approach to the Derivation and Measurement of the Constitutive Equations of Time Dependent Deformation," STP 765, ASTM (1982).

18. Wu, H.C. and Yip, M.C., "Strain Rate and Strain Rate History Effects on the Dynamic Behavior of Metallic Materials," Int. J. Solids and Structures, 16, pp. 515-536, (1980).

19. Wu, H.C. and Yip, M.C., "Endochronic Description of Cyclic Hardening Behavior for Metallic Materials," J. Appl. Mech. Trans. ASME, pp. 212-217, (1981).

20. Lin, H.C. and Wu, H.C., "On the Rate-Dependent Endochronic Theory of Viscoplasticity and its Application to Plastic-Wave Propagation," Int. J. Solids and Structures, 19, pp. 587-599, (1983).

22. Valanis, K.C., "Proper Tensorial Formulation of the Internal Variable Theory," Archives of Mechanics, 29, 173, (1977).

23. Valanis, K.C., "Fundamental Consequences of a New Intrinsic Time Measure: Plasticity as a Limit of the Endochronic Theory," Arch. of Mech., 32, pp. 171-191, (1980).

24. Kraus, A.S. and Eyring, H., "Deformation Kinetics," Wiley, N.Y. (1975).

25. Valanis, K.C. and Lalwani, S., "Thermodynamics of Internal Variables in the Content of the Absolute Reaction Rate Theory," J. Chem. Phys., 67, 3980, (1977).

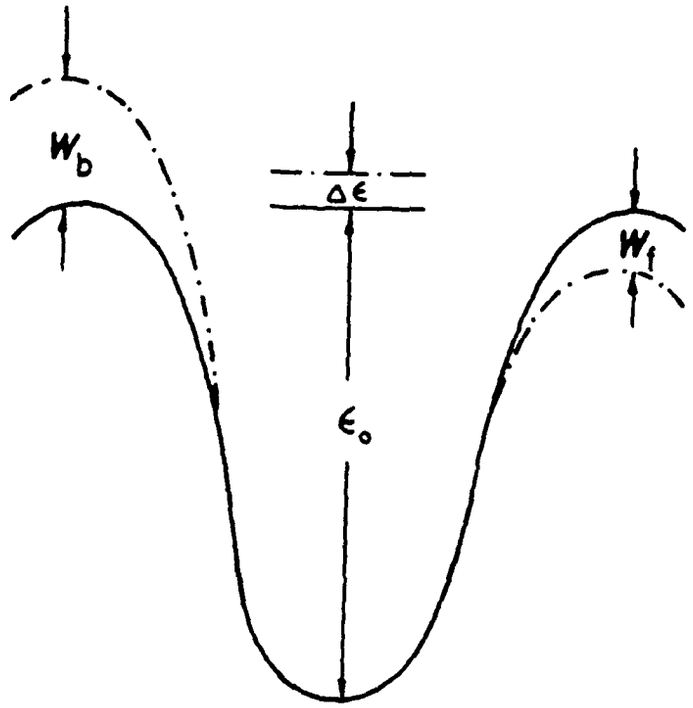

Fig. 1 Initial and Disturbed Barrier Surface

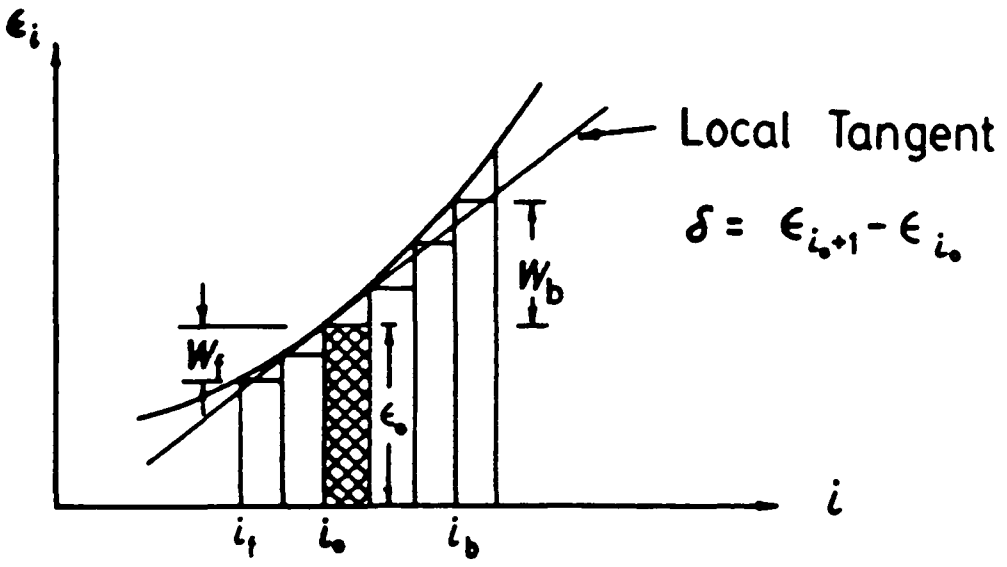

Fig. 2 Energy Distribution in Vicinity of ε_0

$$\epsilon_i = \epsilon_{i_0} + (i - i_0)\,\delta$$

$$W_b = (i_b - i_0)\,\delta$$

$$W_f = (i_0 - i_f)\,\delta$$

$$\epsilon_0 = \epsilon_{i_0}$$

$$P_f - P_b = \frac{2\,e^{-\beta\epsilon_0}}{1 - e^{-\beta\delta}}\, e^{-\beta\Delta\epsilon} \sinh \beta\bar{W}$$

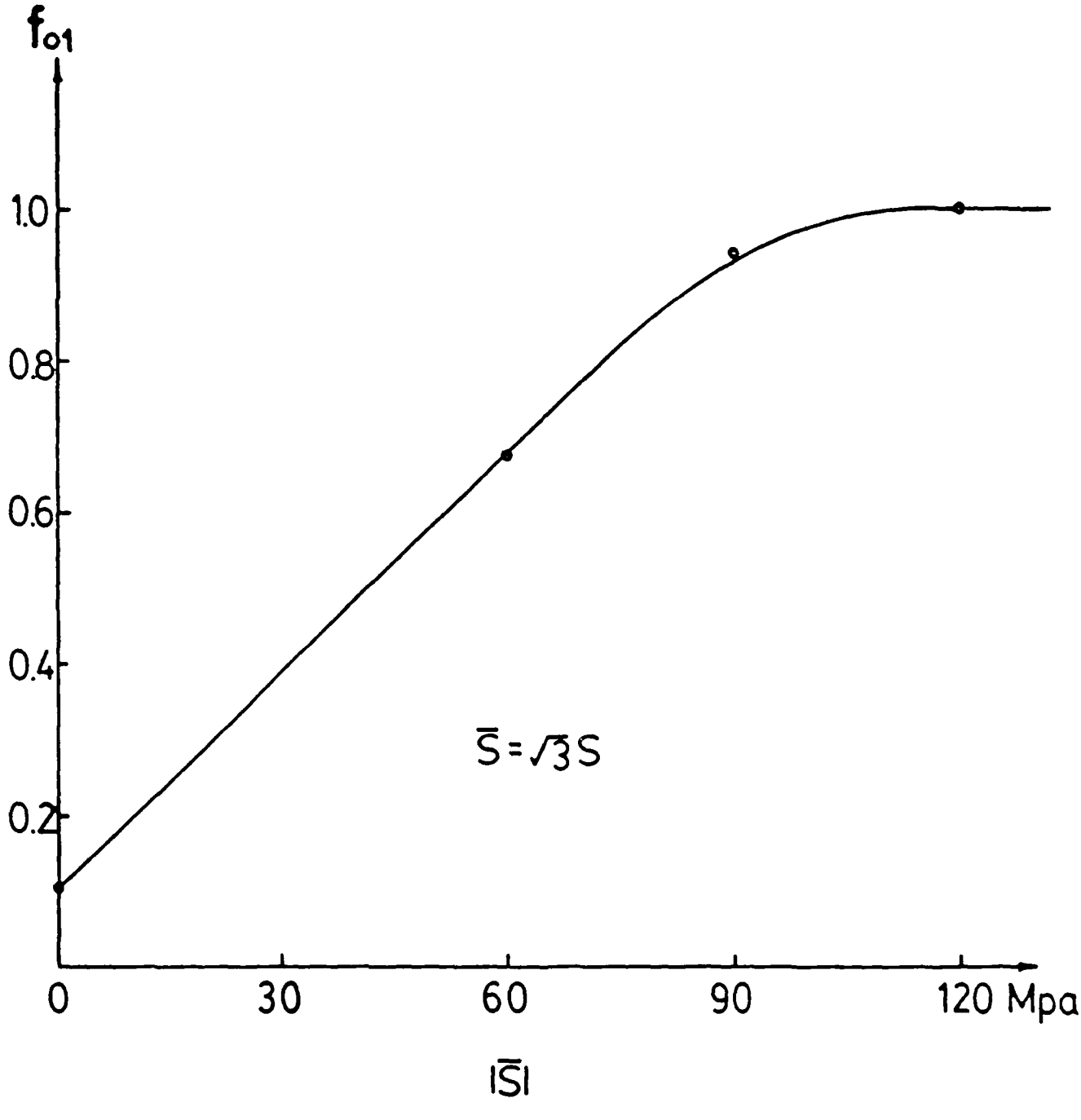

Fig. 3 Relation of $f_{o1}(|\bar{S}|)$

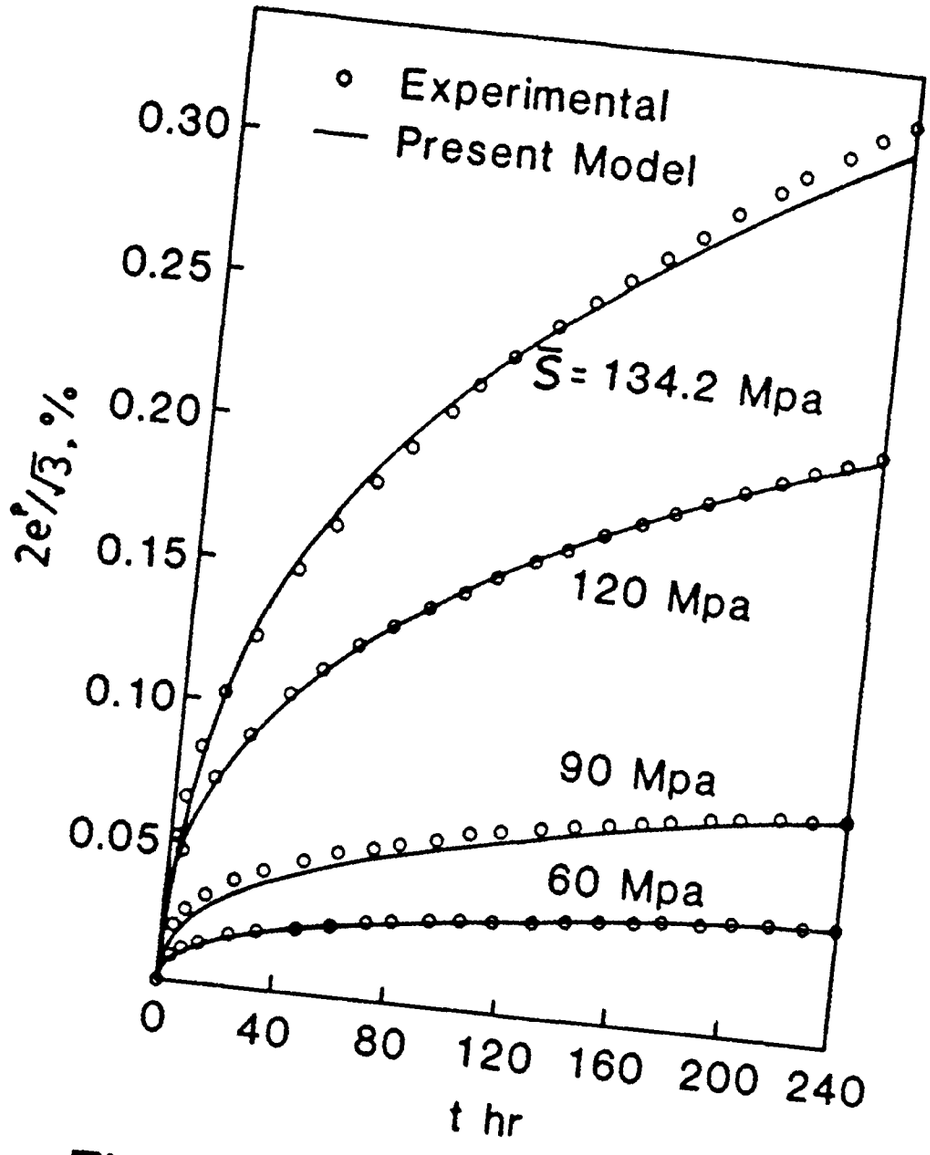

Fig. 4 Monotonic Creep Tests

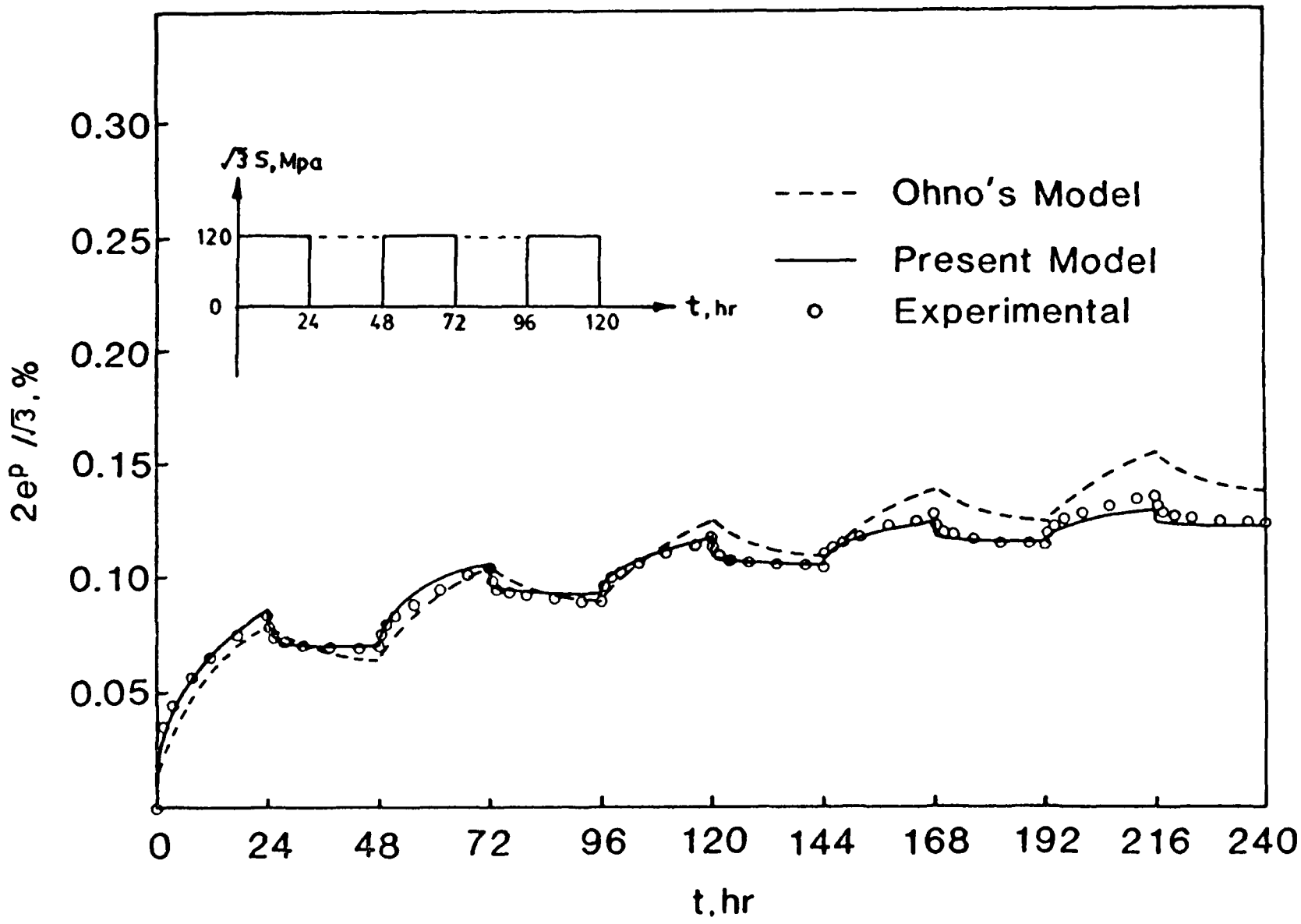

Fig. 5 Creep Strain Response to Piece-wise Constant Shear Stress History ($\sqrt{3}$ S = 120 Mpa, a = 1.0)

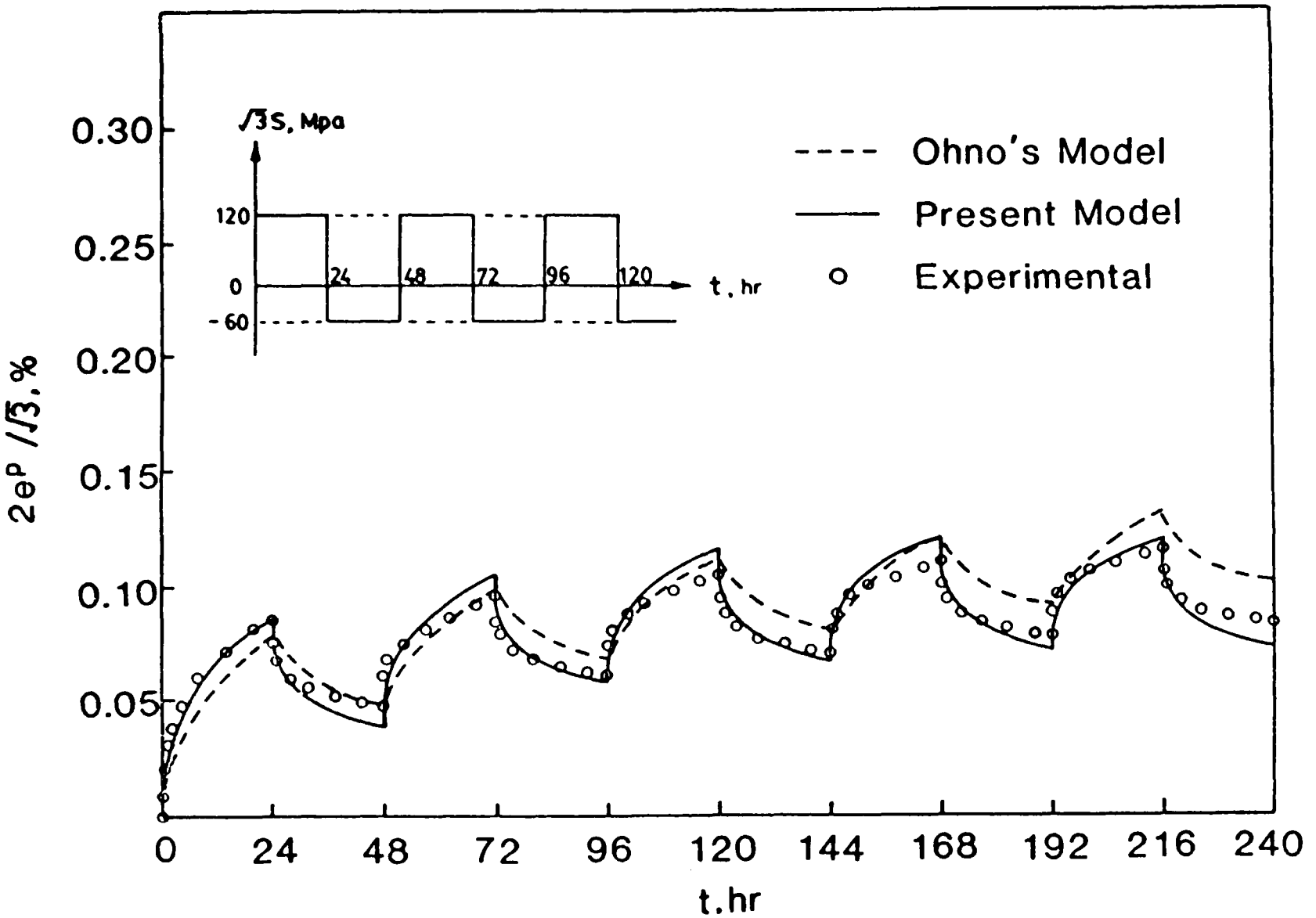

Fig. 6 Creep Strain Response to Piece-wise Constant Shear Stress History ($\sqrt{3}$ S = 120 Mpa, a = 1.5)

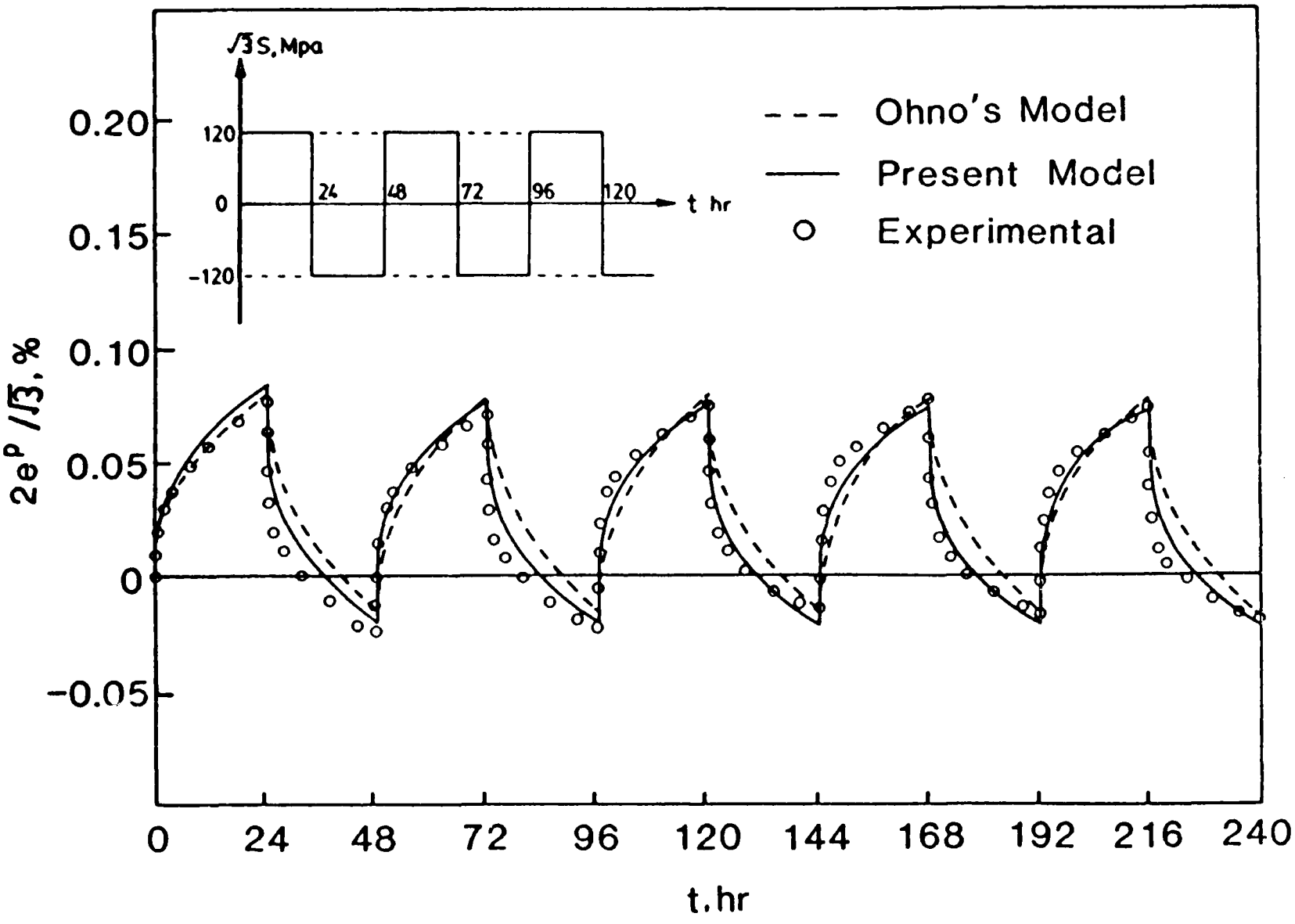

Fig.7 Creep Strain Response to Piece-wise Constant Shear Stress History ($\sqrt{3}S = 120$ Mpa, $a = 2.0$)

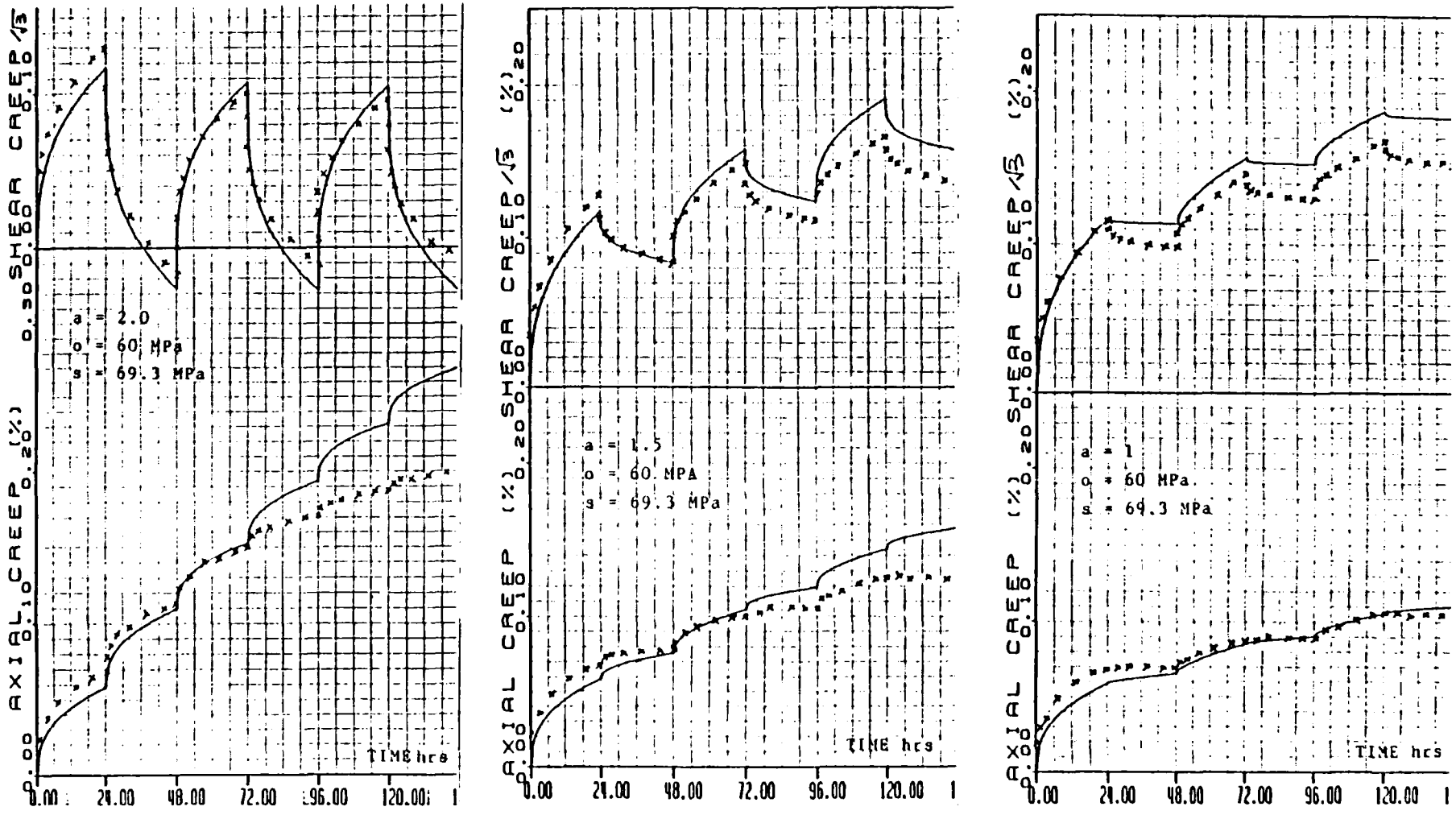

Fig.'s 8, 9 and 10. Torsional and Axial Creep Strain Response in the Presence of Piece-wise Constant Torsion and Constant Tension.

MAILING LIST

NAME	STREET ADDRESS AND AFFILIATION	CITY	STATE	ZIPCODE
Dr. Charles D. Babcock	2392 Morslay Road	Altadena	CA	91001
Dr. Paul Cernocky	Shell Development Co., PO Box 481	Houston	TX	30332
Dr. Peter C T Chen	Watervliet Arsenal, US Army R&D Comm LCW	Watervliet	NY	12189
Dr. R M Christensen	Lawrence Livermore Lab, PO Box 808 (L-338)	Livermore	CA	94550
Prof. Y F Dafalias	Dept. of Civil Engng, Univ. of California-Davis	Davis	CA	95616
Dr. L W Davison	Solid Mechs Dept 1530, Sandia Natl Labs	Albuquerque	NM	87185
Dr. John K. Dienes	Theoret Div., MS 216, Los Alamos Scient Lab	Los Alamos	NM	87545
Dr. Stanley Fistedis	Reactor Analy & Safety Div., Argonne Nat'l Lab	Argonne	IL	60439
Prof. J E Fitzgerald	Sch CE, Georgia Tech	Atlanta	GA	30332
Prof. M E Gurtin	Mathematics, Carnegie-Mellon Univ.	Pittsburgh	PA	15213
Prof. Leonard Herrmann	CE Dept. Bainer Hall, Univ. of California	Davis	CA	95616
Dr. Walter Herrmann	Org 1500, Sandia Nat'l Labs	Albuquerque	NM	87185
Prof. T J R Hughes	Applied Mechanics, Duran 281, Stanford Univ.	Stanford	CA	94305
Melvin F. Kanninen	Eng & Matls, Southwest Res Inst, 6220 Culebra Road	San Antonio	TX	78284
Prof. Dusan Krajcinovic	Civil Engr. P O Box 4348 Univ of Ill.	Chicago	IL	60680
Prof. F A Leckie	T&AM, 296 Tlabot Lab Univ of Ill, 104 S. Wright	Urbana	IL	61801
Dr. J K Lee	Engr Mechs, Ohio State Univ	Columbus	OH	43210
Prof. Frederick F. Ling	ME AE & Mech, RPI	Troy	NY	12181
Mr. J Lubliner	CE Dept. Univ of California	Berkeley	CA	94720
Prof. L E Malvern	Engr Sci Dept, 231 Aero Bldg, Univ of Florida	Gainesville	FL	32611
Prof. X Markenscoff	Mech & Environ Engng, Univ. of California	Santa Barbara	CA	93106
Prof. S Nemat-Nasser	Civil Engng, Northwestern Univ.	Evanston	IL	60201
Prof. J Tinsley Oden	Ticom WRW 305, Univ of Texas @ Austin	Austin	TX	78712
Dr. Steven Peng	Jet Propulsion Lab, 67/201 Caltech Bldg.	Pasadena	CA	91103

NAME	STREET ADDRESS AND AFFILIATION	CITY	STATE	ZIPCODE
Dr. Jerry T Pendera	Inst for Experimental Mechs, Univ. of Waterloo	Waterloo, Ont	CANADA	N2L 3G1
Prof. Karl S. Pister	CE Dept, Univ of California	Berkeley	CA	94720
J W Rudnicki	Civil Engng, Northwestern Univ	Evanston	IL	60201
Prof. Jerome L Sackman	Civil Engng, Univ. of California	Berkeley	CA	94720
Dr. Anthony San-Miguel	2775 Mesa Verde Dr East, Apt P-212	Costa Mesa	CA	92626
Prof. S S Sternstein	Mata Engr Dept. RPI	Troy	NY	12181
Prof. Gerald A Wempner	Engng Sci & Mechanics, Georgia Tech	Atlanta	GA	30332
Prof. Kaspar J. William	Campus Box 428, Univ of Colorado	Boulder	CO	80309
Mr. Lawrence K Yu	Intl Paper Co. Box 797	Tuxedo Park	NY	10987

APPENDIX I

ENDOCHRONIC CONSTITUTIVE EQUATION OF FINITE PLASTICITY WITH APPLICATIONS

TABLE OF CONTENTS

LIST OF FIGURES

ABSTRACT

The object of this research is an extensive study of an endochronic constitutive relation for both incompressible and compressible materials undergoing finite plastic deformation. Attention, in this dissertation, has been paid to the foundation, application, and computational capability of the theory.

In the first part of this dissertation the endochronic constitutive relation of plasticity for incompressible finite deformation, as proposed by Valanis in 1978, is reviewed. This relation is formulated in the material frame of reference which is convenient for problems involving a definite initial configuration such as a solid as opposed to a fluid. A set of academic and practical problems of interest, consisting of finite plastic uniform extension, finite plastic shear flow in a pipe, finite plastic torsion, finite plastic bending, and finite plastic spherical expansion, are solved analytically. Closed form solutions are obtained for all problems by the use of a semi-inverse method.

In the second part of this dissertation the theory is extended to account for plastic compressibility. incompressibility is pivotal in the development of classical theory of plasticity. However, it is only an assumption and a simplification of the actual situation. In the endochronic theory, plastic compressibility can be accommodated. This is done by modifying the free energy density function of the plastic deformation process by adding a term $\psi_0(I_3)$ which reflects the compressible plastic

deformation and then developing the constitutive relation for a special functional form of $\psi_0(I_3)$.

To solve more general engineering problems, a numerical method is developed using the powerful finite element technique for boundary value problems for both compressible and incompressible materials. In the compressible case, a special form of ψ_0 is used to demonstrate the application of the theory. The finite element formulation is referred to the material system, by using a Lagrangian formulation.

A computer code is then established to solve a plane strain boundary value problem in the presence of compressible plastic deformation by the use of linear triangular elements. A specific problem associated with a metal forging process, that of "upsetting" a block is analyzed numerically using the code. All relevant parameters of the problem are investigated. The results obtained give a very reasonable description of the forging process.

The study of this dissertation shows that the endochronic theory, which is based on a sound thermodynamic foundation, also has a powerful computational capability for solving practical engineering problems that involve large plastic deformation.

CHAPTER 1 - INTRODUCTION

Finite plasticity as a subject dealing with a time-independent, rate-independent, large permanent strain during a deformation process, has very significant application in engineering problems. In ductile metals, under favorable conditions, plastic deformation can continue to a very large extent without failure. For instance, except for castings, which are formed from the liquid state, all metal products are subjected to at least one metal forming process during their manufacture. In metal forming processes such as forging, drawing, extrusion, rolling, stamping and cutting, etc., the products suffer a considerable shape change. The deformation is substantially permanent and involves predominantly large plastic strains. Other processes include the plastic bending of beams and plates, the overstraining of spheres and cylinders which are widely used as pressure vessels in the chemical industry for example. A thorough understanding of the mechanics involved in large plastic deformation is very important to engineering application and design. Moreover, the advancement of many branches of solid mechanics such as fracture and fatigue as well as soil mechanics, rock mechanics, geophysics, and geology, etc., is closely related to the development of a sound plasticity theory. Recently with the availability of high-speed computing facilities and the development of the sophisticated material testing machines, many researchers have been motivated to develop more advanced theories of plasticity. Hence many of the

simplifying assumptions in plasticity and many empirical formulations are no longer necessary.

A difficult element of classical plasticity is the concept of the yield surface, which leads to experimental and numerical difficulties in attempts to describe and analyze the two- or three- dimensional response of a material. Valanis [1,2] circumvented this difficulty by proposing, in 1971, the endochronic theory, which does not require the concept of yield for the description of plastic behavior of materials. During about 15 years' development, a number of publications documented the potential of the theory to describe the mechanical response of materials under conditions of small plastic deformation and proved that the endochronic theory of plasticity was able to predict not only the salient features of the plastic behavior of materials, but also a number of observed features of plasticity that lay beyond the scope of the existing plasticity theories. It is natural then to extend the endochronic theory to the other subjects in plasticity such as problems of large deformation, rate-dependence, and thermomechanical coupling, etc. In this dissertation, we study extensively how the endochronic theory can be applied to problems in the domain of large plastic deformation and how it can be used to solve relevant engineering problems. Before proceeding with the development of the theory, we will review briefly the history of the classical and endochronic theories of plasticity.

Plasticity as a science is generally regarded to have begun in 1864 when Tresca [3] published a preliminary account of his experimental results on punching and extrusion and formulated a yield criterion which states that a metal yields plastically when the maximum shear stress attains a

critical value. Early contributions to the theory of plasticity were also due to Saint-Venant [4] and Levy [5], who in 1870 applied the Tresca yield criterion to establish relations between stress and plastic strain-rate for two-dimensional and three-dimensional plastic deformation.

In the following 60 years development of the theory of plasticity was slow. After 1921, there were important contributions from Von Mises [6], Hencky [7], and Prandtl [8]. Von Mises suggested a yield criterion on the basis of purely mathematical considerations and Hencky later interpreted that this yield criterion implies that yielding occurs when the elastic shear-strain energy reached a critical value. Prandtl showed the plane plastic strain problem was hyperbolic and calculated the loads needed to indent a planar surface. Hencky continued Prandtl's work and discovered simple geometrical properties of the field of slip-lines in a state of plane plastic strain. Lode [9] and Taylor and Quinney [10] carried out experiments on various metals under combined tension and internal pressure. The effective application of plasticity theory to technological processes began in 1925 when Von Karman [11] analysed the stress distribution during the rolling of metal strip by an elementary method. In the following year Siebel [12] and Sachs [13] presented similar theories for wire drawing.

About 1950, the classical mathematical theory of plasticity entered a fully developed period. D.C. Drucker [14] generalized the meaning of work hardening and related it to the stability of plastic deformation by postulating that (1) the work done by an external agency during the application of additional stresses is positive for a working-hardening material, and (2) the net work done by an external agency during a cycle of

addition and removal of stresses in a material undergoing plastic deformation is positive. This led to the normality of plastic strain rate vector with respect to the yield surface and convexity of the yield surface. The Von Mises flow rule was then derived, which provided the relationship between the loading (yielding) function and plastic flow. In 1961, Ilyushin [15] stated his postulate of plasticity, which he claimed to be a generalization of Drucker's postulate. A third aspect of the classical plastic theory, besides the initial yield criteria and an associated flow rule, includes the isotropic hardening rule by Hill [16] and Hodger [17], kinematic hardening rule by Prager [18], modified kinematic hardening rule by Ziegler [19], and Mroz's rule of hardening moduli [20].

The theories to describe the relation between stresses and strains are of two general classes, which are total strain (deformation) theory and incremental strain (flow) theory. The total deformation theory is not physically sound because it cannot account for history effects in the mechanical response of dissipative materials. Thus, preference is given to the flow theory, which is still useful in some problems [21,22]. Based on the classical theory, a number of researchers proposed different constitutive relations for large plastic deformation problems. They include Hill [23,24], Rice [25,26], Mandel [27,28], Lee [29,30], and Green and Naghdi [31]. However, the existing results in the literature showed anomalous solutions to analysis of necking and localization in metal and peculiar results for predic ion of oscillatory shear stress due to a monotonically increasing simple shear strain [32-35] when the kinematic hardending rules are used.

In the late 1960s, the formulation of constitutive theories of viscoelastic materials from concepts of irreversible thermodynamics and internal state variables reached an advanced level of development [36]. On the basis of this success, the theory of plasticity was re-examined along the lines of irreversible thermodynamics, since by nature plastic deformation should be considered as an irreversible thermodynamic process. In 1971, Valanis [1,2] proposed a new approach, called endochronic theory, for describing the behavior of viscoplastic material. The theory was developed on the concept of stress and free energy being a functional of the entire histories of deformation and temperature based on thermodynamics and internal variables. Two new concepts were drawn in the development of the theory, which are (1) the concept of intrinsic time, defined as the norm of the increment of the total strain tensor. It is a scale with respect to which the memory of a material of its past deformation history can be measured and (2) the concept of the description of plasticity without a yield surface. The application of the theory was given by Valanis [2,37]. Wu and Lin [38] used the theory to obtained the simple wave solution of a thin-walled tube subject to combined step loading. Valanis and Wu [39] showed that the theory is able to predict cyclic creep and relaxation of metals. Wu and Lin [40] illustrated how the strain rate effects could be included in the theory. Bazant [41], Bazant and Bhat [42], and Bazant and Krizek [43] modeled the inelastic properties of geological materials including sand, rocks and concrete using the theory.

The theory was attacked by Sandler [44] on the basis of a conjecture that the theory might give rise to numerical instabilities in the solution

of wave propagation problems and also on its prediction of unloading-reloading behavior which violates Drucker's postulate of material stability. To these arguments, Valanis and Read [45] claimed that the instability is due to the non-uniqueness of the solution of posed problem and not the fault of the endochronic model. They also claimed that Drucker's postulate is not of thermodynamic origin and can be violated by the standard frictional physical systems.

A more serious concern, however, was the openess of the hysteresis loops. Therefore, the new endochronic theory was developed [45-47]. In new theory, a new intrinsic time was defined in the plastic strain space, and a weakly singular kernel function was introduced. It was shown that various versions of the classical plasticity theory are asymptotic cases of the endochronic theory. Idealized plasticity models are shown to be constitutive subsets of the general theory. In particular, the kinematic model, the isotropic hardening model, as well as their combinations are derivable from the general theory. The new theory has been applied to situations involving unloading and cyclic behavior of materials [45,48]. Lin and Wu [49] applied the theory to the viscoplastic wave propagation problem of a thin-walled tube subjected to impact loading. Valanis and Fan [50] analyzed the cyclic elastic-plastic strain fields in a notched plate. Pindera and Herakovick [51] applied the theory to model the response of unidirectional composites under off-axis tensile load.

In 1978, Valanis proposed an extension of endochronic theory that can apply to problems of large plastic deformation [52]. He developed a constitutive relation for incompressible materials and used it to analyze a

problem of simple shear. Recently Valanis and Wang [53] used the constitutive relation to analyze the problem of finite plastic bending. Further applications of the theory to a set of special engineering problems,including closed form solutions, will be presented in this dissertation.

CHAPTER 2 - ENDOCHRONIC CONSTITUTIVE RELATION OF INCOMPRESSIBLE PLASTICITY WITH FINITE DEFORMATION

An endochronic constitutive relation applicable to problems of large plastic deformation was proposed by Valanis [52] very much along the lines of the endochronic constitutive theory of small plastic deformation [1-2, 46-47], which is founded on irreversible thermodynamics of internal variables and the notion of intrinsic time. In reference [52], the endochronic constitutive relation of plasticity was derived for an incompressible, isotropic, and isothermal material in the spatial frame. In this chapter the derivation of the constitutive equation for large plastic deformation is reviewed in the material frame of reference, since in the next chapter the theory will be used to analyze a set of problems which involve definite initial configurations.

2.1 Review of the Endochronic Constitutive Equation

Let R_x be a material region with a surface S_x, in an initial unstressed state. In this state the geometry of R_x is defined with respect to a fixed Cartesian 'material' frame, X^α . The deformed region R_y with a surface S_y is defined with respect to Cartesian 'spatial' frame, Y_i. The deformation of R_x is defined through the one-to-one mapping $R_x \rightarrow R_y$ such that

$$Y_i = Y_i(X^\alpha, t) \quad . \tag{2.1.1}$$

In the following when quantities are referred to coordinates X^{α}, their indices will be the lower case Greek letters; and when they are referred to coordinates Y_i, their indices will be the lower case english letters.

The deformation tensor $C_{\alpha\beta}$ and the deformation rate tensor d_{ij} are defined by

$$C_{\alpha\beta} = \frac{\partial Y_i}{\partial X^{\alpha}} \frac{\partial Y_i}{\partial X^{\beta}} \qquad (2.1.2)$$

and

$$d_{ij} = 1/2 \left(\frac{\partial v_i}{\partial Y_j} + \frac{\partial v_j}{\partial Y_i} \right) \quad . \qquad (2.1.3)$$

where v_i is the velocity of a particle.

In their local forms, the fundamental laws of thermodynamics in the material coordinate frame are:

the first law,

$$\dot{\varepsilon} = (\rho_o/2\rho)\, T^{\alpha\beta}\dot{C}_{\alpha\beta} - h^{\alpha}{}_{,\alpha} + \dot{Q} \quad , \qquad (2.1.4)$$

the rate of dissipation inequality,

$$\theta\dot{\Upsilon} = (\rho_o/\rho)\, T^{\alpha\beta}\, \dot{C}_{\alpha\beta} - \dot{\Psi} - \eta\dot{\theta} \geq 0 \quad , \qquad (2.1.5)$$

and the heat conduction inequality,

$$-h^{\alpha}\theta_{,\alpha} \geq 0 \quad , \qquad (2.1.6)$$

where ε denotes the internal energy per unit mass, $T^{\alpha\beta}$ the contravariant components of the stress tensor in the material system, Ψ the free energy density per unit mass, θ the absolute temperature, h^{α} the heat flux vector, $\dot{Q}$ the rate of heat supply, Υ the irreversible entropy, η the entropy, ρ_o and

ρ the density of the medium in the undeformed and deformed configurations, respectively, and the dot denotes the time derivative.

In the internal variable formalism an assumption is made that the thermodynamic state of a body undergoing an irreversible process can be specified by the current values of $C_{\alpha\beta}$ and θ as well as n internal variables $\underset{\sim}{q}_r$ (not necessarily observable), which could be scalars, vectors or tensors in the material frame or the spatial frame, depending on the transformation laws that they are assigned to satisfy. Thus the free energy Ψ is set to be a function of $C_{\alpha\beta}$, θ, and $\underset{\sim}{q}_r$. Inequality (2.1.5) then becomes,

$$\theta\dot{\Upsilon} = [(\rho_o/2\rho)\, T^{\alpha\beta} - \frac{\partial\Psi}{\partial C_{\alpha\beta}}]\, \dot{C}_{\alpha\beta} - (\frac{\partial\Psi}{\partial\theta} + \eta)\dot{\theta} - \frac{\partial\Psi}{\partial \underset{\sim}{q}_r}\, \dot{\underset{\sim}{q}}_r \geq 0 \quad . \qquad (2.1.7)$$

Since $C_{\alpha\beta}$, $\underset{\sim}{q}_r$, and θ are independent of each other, the following relations must hold to preserve the dissipation inequality for an arbitrary process:

$$T^{\alpha\beta} = 2\, \frac{\rho}{\rho_o}\, \frac{\partial\Psi}{\partial C_{\alpha\beta}} \quad , \qquad (2.1.8)$$

$$\eta = -\, \frac{\partial\Psi}{\partial\theta} \quad , \qquad (2.1.9)$$

$$-\, \frac{\partial\Psi}{\partial \underset{\sim}{q}_r}\, \dot{\underset{\sim}{q}}_r \geq 0 \quad . \qquad (2.1.10)$$

For incompressible materials ($|C_{\alpha\beta}| = 1$), eq.(2.1.8) becomes

$$T^{\alpha\beta} = 2\, \frac{\partial\Psi}{\partial C_{\alpha\beta}} - P\, C^{\alpha\beta} \quad , \qquad (2.1.11)$$

where P is an arbitrary hydrostatic pressure.

The reduced dissipation inequality (2.1.10) admits the internal constitutive equation:

$$-\frac{\partial \Psi}{\partial \underline{q}_r} = \underline{\underline{b}}_r \cdot \dot{\underline{q}}_r \qquad \text{(no sum on r)} \quad , \qquad (2.1.12)$$

where $\underline{\underline{b}}_r$ are positive definite fourth order tensors.

The unique feature of the endochronic theory (see Valanis [45-47]) is in the definition an intrinsic time scale as the distance in plastic strain space between two <u>plastic</u> deformation events, and the stipulation that the stress be a function of the history of plastic deformation, measured with respect to the intrinsic time scale. In the case of large plastic deformation of metals one can afford to ignore the contribution of the elastic deformation, which is small, and thus define the intrinsic time in terms of the total deformation. Where plastic fluids are concerned, e.g., metals whose deformation is so large that they have lost cognizance of their original configuration [52], one then defines the rate of change of the intrinsic time in terms of the total deformation rate tensor d_{ij}. More specifically,

$$\left(\frac{d\xi}{dt}\right)^2 = P_{ijkl} d_{ij} d_{kl} \quad , \qquad (2.1.13)$$

where P_{ijkl} should be an isotropic non-dimensional function of d_{ij} for a rate independent material.

The simplest form of P_{ijkl} is a constant tensor

$$P_{ijkl} = p_1 \delta_{ij}\delta_{kl} + p_2 \delta_{ik}\delta_{jl} \quad , \qquad (2.1.14)$$

where p_1 and p_2 are positive non-dimensional constants. Eq.(2.1.13) in conjunction with eq.(2.1.14) yields the result:

$$\left(\frac{d\zeta}{dt}\right)^2 = p_1 d_{ii} d_{jj} + p_2 d_{ij} d_{ij} \quad . \qquad (2.1.15)$$

When incompressibility applies, d_{ii} vanishes and

$$\left(\frac{d\zeta}{dt}\right)^2 = p_2 d_{ij} d_{ij} \quad , \qquad (2.1.16)$$

An intrinsic time scale z is defined to account for the hardening or softening character of a material,

$$z = \int_0^\zeta \frac{d\zeta'}{f(\zeta')} \quad , \qquad (2.1.17)$$

where $f(\zeta)$ is a positive function of ζ. If no hardening (or softening) takes place $f(\zeta)=1$.

In the present form of the theory (see Ref.[52]), the free energy density is specified as a quadratic function of $\underset{\sim}{q}_r$ according to eq.(2.1.18):

$$\Psi = \Psi_0 + A^r q_i^r + 1/2\, C^{(r)} q_{ij}^r q_{ij}^r \quad , \qquad (2.1.18)$$

where Ψ_0 , A^r, and $C^{(r)}$ are constants and q_{ij}^r are the components of $\underset{\sim}{q}^r$ in the spatial frame.

The implication of eq.(2.1.18) is that in the spatial frame the free energy density does not depend explicitly on the deformation, a property that one associates with a "plastic fluid", i.e., a material that is so deformed that its structure in the reference configuration plays no role in the determination of the Cauchy stress. Note that the form of Ψ in eq.(2.1.18) satisfies material objectivity and material isotropy in the reference state.

Eq.(2.1.18) is now expressed in terms of the covariant components of $\underset{\sim}{q}_r$ in the material frame and it is these that will play the role of independent variables in the thermodynamic formulation. Thus

$$\Psi = \Psi_0 + A^r q^r_{\alpha\beta} C^{\alpha\beta} + 1/2\, C^{(r)} q^r_{\alpha\beta} q^r_{\gamma\delta} C^{\alpha\gamma} C^{\beta\delta} \quad , \qquad (2.1.19)$$

where $$q^r_{\alpha\beta} = \frac{\partial Y_i}{\partial X^\alpha} \frac{\partial Y_j}{\partial X^\beta} q^r_{ij} \quad . \qquad (2.1.19a)$$

Note that contravariant and mixed components of $\underset{\sim}{q}_r$ in the material system can be defined by the relations

$$q^{\alpha\beta}_{(r)} = \frac{\partial X^\alpha}{\partial Y_i} \frac{\partial X^\beta}{\partial Y_j} q^{(r)}_{ij} \quad , \qquad (2.1.19b)$$

$$q^{\alpha}_{(r)\beta} = \frac{\partial X^\alpha}{\partial Y_i} \frac{\partial Y_j}{\partial X^\beta} q^{(r)}_{ij} \quad , \qquad (2.1.19c)$$

$$q^{(r)\beta}_{\alpha} = \frac{\partial Y_i}{\partial X^\alpha} \frac{\partial X^\beta}{\partial Y_j} q^{(r)}_{ij} \quad . \qquad (2.1.19d)$$

The internal constitutive equation (2.1.12) is now written in the specific form

$$b^{(r)} \hat{q}^{(r)}_{\alpha\beta} + \frac{\partial \Psi}{\partial q^{\alpha\beta}_{(r)}} = 0 \quad , \qquad (2.1.20)$$

where $b^{(r)}$ are scalars and the roof denotes the derivative with respect to z. It implies that the endochronic rate of change of the covariant components of $q^{(r)}$ should be proportional to the covariant components of the internal

stress tensor $\frac{\partial \Psi}{q_{(r)}^{\alpha\beta}}$, in which case $\underset{=}{b}^{(r)}$ is of the form:

$$b^{(r)}_{\alpha\beta\gamma\delta} = b^{(r)} \delta_{\alpha\gamma}\, \delta_{\beta\delta} \quad . \tag{2.1.20a}$$

The solution of eq.(2.1.20) in conjunction with the form of Ψ in eq.(2.1.19) and the initial condition on $q_{\alpha\beta}$ ($q_{\alpha\beta}|_0 = \delta_{\alpha\beta}$), dictated by the fact that the Cauchy stress in the reference state can be at most a hydrostatic pressure, is given by

$$q^{(r)}_{\alpha\beta} = \frac{A^{(r)}}{C^{(r)}} C_{\alpha\beta} + \frac{A^{(r)}}{C^{(r)}} \int_0^z e^{-\alpha_r (z-z')} \hat{C}_{\alpha\beta}(z')\, dz' \quad , \tag{2.1.21}$$

where $\alpha_r = \frac{C^{(r)}}{b^{(r)}}$.

On the other hand eq.(2.1.11) in conjunction with eq.(2.1.19) gives

$$T^{\alpha\beta} = -P\, C^{\alpha\beta} - 2\left(A^{(r)} q^{\alpha\beta}_{(r)} + C^{(r)} q^{(r)\alpha}_{\ \ \beta'} q^{(r)\beta'\beta}\right) \tag{2.1.22}$$

or

$$T_{\alpha\beta} = -P\, C_{\alpha\beta} - 2\left(A^{(r)} q^{(r)}_{\alpha\beta} + C^{(r)} q^{(r)}_{\alpha\beta'} q^{(r)\beta'}_{\ \ \beta}\right) \quad . \tag{2.1.23}$$

Substitution of eq.(2.1.21) into eq.(2.1.23) gives the following relation for the covariant components of the stress

$$T_{\alpha\beta} = -P\, C_{\alpha\beta} + \int_0^z G(z-z') \frac{dC_{\alpha\beta}}{dz'}\, dz' -$$

$$-C^{\mu\nu} \int_0^z \int_0^z G(2z-z_1-z_2) \frac{dC_{\alpha\mu}}{dz_1} \frac{dC_{\beta\nu}}{dz_2}\, dz_1 dz_2 \quad . \tag{2.1.24}$$

It was found from an analysis of the problems of simple extension and simple shearing that the contribution to the stress of the second integral relative to that of the first integral is of the order of $1/\alpha^2$ where α is of

the order of one hundred, this being the ratio of the elastic modulus to the maximum stress (in tension or in shear). In the subsequent analysis the double integral was ignored with the result that the covariant components of stress in the material frame of reference are given in terms of a linear history integral of the right Cauchy-Green tensor $C_{\alpha\beta}$. Thus

$$T_{\alpha\beta} = -P\, C_{\alpha\beta} + \int_0^z G(z-z')\, \hat{C}_{\alpha\beta}(z')\, dz' \quad , \qquad (2.1.25)$$

where

$$G(z) = 2 \sum_r \frac{A^{(r)}}{C^{(r)}} e^{-\alpha_r z} \quad . \qquad (2.1.25a)$$

For an extensive discussion see Ref.[52].

2.2 Description of Constitutive Equation in Curvilinear Systems

In order to describe the deformation in a curvilinear system, we set ϕ^β and θ_j to be curvilinear coordinates for the material system X^α and the spatial system Y_i, respectively, as shown in Fig.1.

For the material system, we have the relation,

$$\phi^\beta = \phi^\beta(X^\alpha) \quad . \qquad (2.2.1)$$

The corresponding covariant and contravariant metric tensors $G_{\alpha\beta}$ and $G^{\alpha\beta}$ are given by eq. (2.2.2):

$$G_{\alpha\beta} = \frac{\partial X^k}{\partial \phi^\alpha} \frac{\partial X^k}{\partial \phi^\beta} \qquad (2.2.2a)$$

and

$$G^{\alpha\beta} = (1/|G|)\ (\text{cofactor of } G_{\alpha\beta}) \qquad (2.2.2b)$$

where $|G|$ is the determinant of $G_{\alpha\beta}$.

The corresponding relations for the spatial frame are

$$\theta_j = \theta_j(Y_i) \quad , \tag{2.2.3}$$

$$g_{kl} = \frac{\partial Y_i}{\partial \theta_k} \frac{\partial Y_i}{\partial \theta_l} \tag{2.2.4a}$$

and

$$g^{kl} = (1/|g|) \text{ (cofactor of } g_{kl}) \tag{2.2.4b}$$

The deformation map (2.1.1) can be then written through eq.(2.2.1) and (2.2.3) in terms of one of the following alternatives, depending on the problem at hand:

$$Y_i = Y_i(\theta^\beta, t) \quad , \tag{2.2.5}$$

$$\theta_j = \theta_j(X^\alpha, t) \tag{2.2.6}$$

and

$$\theta_j = \theta_j(\phi^\beta, t) \tag{2.2.7}$$

The Cauchy-Green deformation tensor $C_{\alpha\beta}$ and its curvilinear counterpart $\bar{C}_{\mu\nu}$ are given below:

$$C_{\alpha\beta} = g_{kl} \frac{\partial \theta_k}{\partial X^\alpha} \frac{\partial \theta_l}{\partial X^\beta} \tag{2.2.8}$$

or in matrix form

$$[C] = [F]^T [g] [F] \quad , \tag{2.2.8a}$$

where the deformation gradient matrix [F] is given by eq.(2.2.9).

$$F_{k\alpha} = \frac{\partial \theta_k}{\partial X^\alpha} \quad , \tag{2.2.9}$$

also,

$$\tilde{C}_{\mu\nu} = g_{kl} \frac{\partial \theta_k}{\partial \phi^\mu} \frac{\partial \theta_l}{\partial \phi^\nu} \tag{2.2.10}$$

or

$$[\tilde{C}] = [\tilde{F}]^T [g] [\tilde{F}] \quad , \tag{2.2.10a}$$

where

$$\tilde{F}_{k\mu} = \frac{\partial \theta_k}{\partial \phi^\mu} \quad . \tag{2.2.11}$$

We now prove the following relations, as these will be of interest in what follows:

(1) The incompressibility condition is given by

$$|\tilde{C}_{\mu\nu}| = |C_{kl}| \quad . \tag{2.2.12}$$

Proof: From the tensor transformation,

$$\tilde{C}_{\mu\nu} = C_{\alpha\beta} \frac{\partial X^\alpha}{\partial \phi^\mu} \frac{\partial X^\beta}{\partial \phi^\nu} \quad . \tag{2.2.13}$$

Then

$$|\tilde{C}_{\mu\nu}| = \left| \left(\frac{\partial X^\alpha}{\partial \phi^\mu}\right)^T \right| \cdot |C_{\alpha\beta}| \cdot \left| \frac{\partial X^\beta}{\partial \phi^\nu} \right| = |h^T| \cdot |h| \tag{2.2.14}$$

where $|C_{\alpha\beta}| = 1$ is unity

and

$$|h| = \left| \frac{\partial X^\beta}{\partial \phi^\nu} \right| \quad . \tag{2.2.15}$$

The proof is completed by noting eq.(2.2.2a).

(2) The deformation-rate tensor d_{ij} is also given by

$$d_{ij} = 1/2 \frac{\partial X^{\alpha}}{\partial Y_j} \frac{\partial X^{\beta}}{\partial Y_i} \dot{C}_{\alpha\beta} \quad . \tag{2.2.16}$$

Proof: The rate of change of $C_{\alpha\beta}$ is

$$\dot{C}_{\alpha\beta} = \frac{\partial v_i}{\partial X^{\alpha}} \frac{\partial Y_i}{\partial X^{\beta}} + \frac{\partial Y_i}{\partial X^{\alpha}} \frac{\partial v_i}{\partial X^{\beta}} = \left(\frac{\partial v_i}{\partial Y_j} + \frac{\partial v_j}{\partial Y_i} \right) \frac{\partial Y_j}{\partial X^{\alpha}} \frac{\partial Y_i}{\partial X^{\beta}}$$

$$= 2 \, d_{ij} \frac{\partial Y_j}{\partial X^{\alpha}} \frac{\partial Y_i}{\partial X^{\beta}} \tag{2.2.17}$$

from which eq.(2.2.16) follows easily.

(3) The intrinsic time scale can be obtained by means of the following relation, derived by direct substitution of (2.2.16) into eq.(2.1.16).

$$\left(\frac{d\zeta}{dt} \right)^2 = (P_2 \, C^{-1}_{\gamma\alpha} \, \dot{C}_{\alpha\beta} \, C^{-1}_{\beta\eta} \, \dot{C}_{\eta\gamma})/4 \tag{2.2.18}$$

or

$$(d\zeta)^2 = (p_2 tr([D]))/4 \quad , \tag{2.2.19}$$

where

$$[D] = [C]^{-1} \, d[C] \, [C]^{-1} \, d[C] \quad . \tag{2.2.20}$$

In the same manner, we also can obtain $d\zeta$ from eq.(2.2.12)

$$(d\zeta)^2 = (p_2 tr([\bar{D}]))/4 \tag{2.2.21}$$

where

$$[\bar{D}] = [\bar{C}]^{-1} \, d[\bar{C}] \, [\bar{C}]^{-1} \, d[\bar{C}] \quad . \tag{2.2.22}$$

The constitutive eq.(2.1.25), upon use of the tensor transformation,

$$\tau_{\mu\nu} = T_{\alpha\beta} \frac{\partial \phi^{\alpha}}{\partial X^{\mu}} \frac{\partial \phi^{\beta}}{\partial X^{\nu}} \tag{2.2.23}$$

can be described in the curvilinear system as

$$\tau_{\mu\nu} = -P \tilde{C}_{\mu\nu} + \int_0^z G(z-z') \hat{\tilde{C}}_{\mu\nu}(z') \, dz' \tag{2.2.24}$$

or

$$[\tilde{\tau}] = -P [\tilde{C}] + \int_0^z G(z-z') [\hat{\tilde{C}}(z')] \, dz' \, . \tag{2.2.25}$$

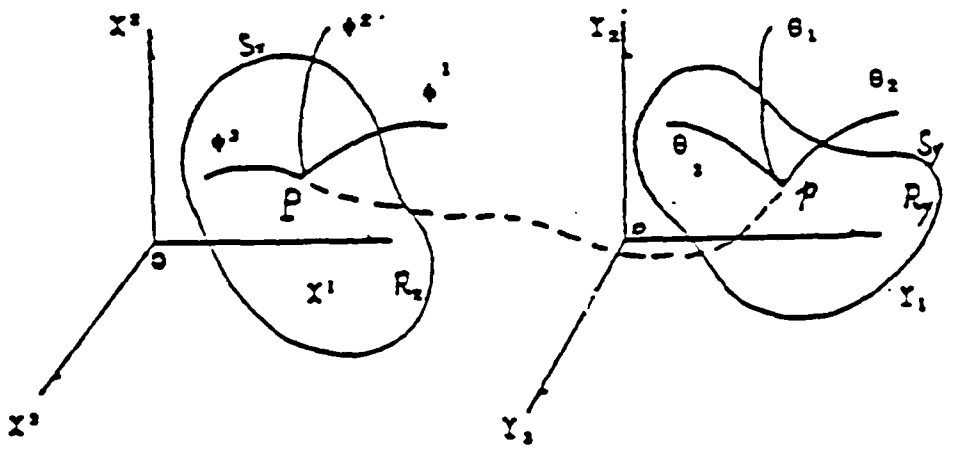

Fig.1 Coordinate systems

CHAPTER 3 - CLOSED FORM SOLUTIONS

To illustrate the application of the theory to the domain of finite plastic deformation, in this chapter the theory will be used to analyze a set of special and yet practical problems. These problems are:

(1) large plastic uniform extension of a cuboid;

(2) large plastic shear flow in a circular tube;

(3) large plastic torsion of a circular bar;

(4) large plastic bending of a block;

(5) large plastic expansion of a sphere.

Closed form solutions for all problems are obtained. To our knowledge, this is the first time in the field that this set of problem are solved in closed form solutions. In the course of obtaining the solutions the semi-inverse method is used. The deformation field is derived from the condition of incompressibility to within a set of unknown parameters, which are then determined by satisfying the equilibrium and boundary conditions.

In order to find the complete solutions for these problems, we need to know the kernel function $G(z)$ in the constitutive equations (2.1.25), (2.2.24), and (2.2.25). In the development of the endochronic theory of plasticity in the region of infinitesimal deformation, the kernel function was discussed thoroughly. There, $G(z)$ was required to be weakly singular at the origin but integrable in the domain $0 \leq z \leq \infty$, i.e., $G(0)=\infty$ and $\int_0^z G(z)dz < \infty$. This requirement leads to the following consequences: (1) it gives rise to closed hysteresis loops, (2) it ensures initially elastic unloading, i.e., initially zero rate of dissipation upon unloading, but (3) it implies an

infinitesimally small elastic domain. Two explicit algebraic forms were discussed at great length in [45]. They are

$$\text{(i)} \qquad G(z) = \frac{\rho_0}{z^{\omega}} \sum_{1}^{n} G_r e^{-\alpha_r z} \tag{3.1}$$

where $0<\omega<1$, $\rho_0>0$, $G_r>0$, and $\alpha_r \geq 0$ for all r, and

$$\text{(ii)} \qquad G(z) = \sum_{1}^{\infty} G_r e^{-\alpha_r z} \tag{3.2}$$

with the conditions that G_r and α_r be positive for all r,

$$\sum_{1}^{\infty} G_r = \infty \,, \tag{3.3a}$$

and

$$\sum_{1}^{\infty} G_r/\alpha_r < \infty \tag{3.3a}$$

The determination of the material functions is very important in order that the plasticity theory can be developed and applied. It is a task involving a considerable amount of experimental investigation and theoretical analysis. This is not a object of the present dissertation. In a recent work [54], the kernel function was determined by a strain controlled cyclic test. The kernel function G(z) was given by the slope of the cyclic plastic strain-stress curve for the shear test at a steady state. The hardening function $f(\zeta)$ of eq.(2.1.17) was determined from reversals of the cyclic shear test. Fan [55] determined by an approximate method the material functions which were convenient for engineering application.

In this work, to demonstrate the application of the theory, eq.(3.1) or eq.(3.2) are not applied to a specific material in detail. Instead, just for a convenience of calculation, an approximate form

$$G(z)=G_0 e^{-\alpha z} \qquad (3.4)$$

will be taken in problems of uniform extension, bending, and expansion, while

$$G(z)=\rho_0/z^{\omega} \qquad (3.5)$$

in the problems of shear flow and torsion. These kernel functions represent simple and yet realistic cases [52,53]. For numerical calculation, α will be set to 200 (this number is characteristic of pure aluminum with a tensile modulus of 10^7 lb/in^2 and an ultimate stress of 50×10^3lb/in^2, α being their ratio.) and ω to 0.86 (from [48] for normalized mild steel).

3.1. Large Uniform Plastic Extension

Uniform extension of a unit cube is considered. Taking Cartesian coordinates x^{α} and y_i (which parallel the sides of the undeformed and deformed bodies) as the material and the spatial coordinates, respectively, the deformation field can be expressed by the following relations:

$$y_1 = \lambda_1(t)x^1, \quad y_2 = \lambda_2(t)x^2, \quad y_3 = \lambda_3(t)x^3 \qquad (3.1.1)$$

where λ_1, λ_2, and λ_3 are the stretches in the x^1, x^2, and x^3 directions respectively, $\lambda_1>1$ corresponding to extension and $0<\lambda_i<1$ to compression.

For a particular case of simple extension under a force parallel to the x^1 direction of the cube, as shown in Fig.2, we have $\lambda_1>1$ and $0<\lambda_2=\lambda_3<1$.

The Cauchy-Green deformation tensor is

$$[C] = \begin{bmatrix} \lambda_1^2 & 0 & 0 \\ 0 & \lambda_2^2 & 0 \\ 0 & 0 & \lambda_2^2 \end{bmatrix} \quad . \qquad (3.1.2)$$

For incompressible material $|C| = \lambda_1^2 \lambda_2^4 = 1$, i.e. $\lambda_2 = (1/\lambda_1)^{1/2}$. Hence the deformation for an incompressible cube becomes

$$y_1 = \lambda_1 x^1 \ , \quad y_2 = (1/\lambda_1)^{1/2} x^2 \ , \quad y_3 = (1/\lambda_1)^{1/2} x^3 \quad . \qquad (3.1.3)$$

The Cauchy-Green deformation tensor now becomes

$$[C] = \begin{bmatrix} \lambda_1^2 & 0 & 0 \\ 0 & 1/\lambda_1 & 0 \\ 0 & 0 & 1/\lambda_1 \end{bmatrix} \quad . \qquad (3.1.4)$$

Then the inverse and the increment of Cauchy-Green tensor are given by.

$$[C]^{-1} = \begin{bmatrix} 1/\lambda_1^2 & 0 & 0 \\ 0 & \lambda_1 & 0 \\ 0 & 0 & \lambda_1 \end{bmatrix} \qquad (3.1.5)$$

and

$$d[C] = \begin{bmatrix} 2\lambda_1 d\lambda_1 & 0 & 0 \\ 0 & -\lambda_1^{-2} d\lambda_1 & 0 \\ 0 & 0 & -\lambda_1^{-2} d\lambda_1 \end{bmatrix} \quad . \qquad (3.1.6)$$

With direct substitution of eq.(3.1.5) and eq.(3.1.6) into eq.(2.2.20), the intrinsic time is obtained as

$$(d\zeta)^2 = 3p_2/2\ (d\lambda_1/\lambda_1)^2 \quad . \qquad (3.1.7)$$

Setting p_2 equal to 2/3 (the actual value of p_2 is immaterial for all problems in this paper), $(d\zeta)^2 = (d\lambda_1/\lambda_1)^2$. For monotonic extension, $d\zeta = d\lambda_1/\lambda_1$. Upon integration, $\zeta = \ln(\lambda_1) + c$, where c is an arbitrary constant. The condition $\zeta = 0$ for $\lambda_1 = 1$ requires that $c = 0$ and $\zeta = \ln(\lambda_1)$. Neglecting hardening (or softening) effects in the material, $f(\zeta) = 1$ and dz and z are obtained as shown in eq.(3.1.8).

$$dz = d\lambda_1/\lambda_1 \quad , \quad z = \ln(\lambda_1) \quad . \qquad (3.1.8)$$

With the help of eq.(3.1.8) $[\hat{C}]$ is given below,

$$[\hat{C}] = \begin{bmatrix} 2\lambda_1^2 & 0 & 0 \\ 0 & -\lambda_1^{-1} & 0 \\ 0 & 0 & -\lambda_1^{-1} \end{bmatrix} \quad . \qquad (3.1.9)$$

Setting $G = G_0 e^{-\alpha z}$, the stresses are obtained upon use of the constitutive equation (2.1.25) as follows,

$$\tau_{11} = \lambda_1^2 \left[-P + \frac{2G_2}{(\alpha+2)} (1 - 1/\lambda_1^{\alpha+2})\right] \quad , \qquad (3.1.10a)$$

$$\tau_{22} = \tau_{33} = 1/\lambda_1 \left[-P - \frac{G_0}{(\alpha-1)} (1 - 1/\lambda_1^{\alpha-1})\right] \qquad (3.1.10b)$$

and

$$\tau_{12} = \tau_{23} = \tau_{13} = 0 \quad . \qquad (3.1.10c)$$

The components of the stresses in spatial coordinates are given by

$$T_{11} = -P + \frac{2G_0}{(\alpha+2)} (1 - 1/\lambda_1^{\alpha+2}) \quad , \qquad (3.1.11a)$$

$$T_{22} = T_{33} = -P - \frac{G_0}{(\alpha-1)} (1 - 1/\lambda_1^{\alpha-1}) \qquad (3.1.11b)$$

and

$$T_{12} = T_{23} = T_{13} = 0 \quad . \qquad (3.1.11c)$$

In the absence of body forces, equilibrium in the deformed body with the stresses in eq.(3.1.11) gives $\partial p/\partial y_1 = \partial P/\partial y_2 = \partial p/\partial y_3 = 0$, i.e., P is a constant. This constant is determined by satisfying the boundary conditions. In the present case, T_{22} and T_{33} are zero at the edges in y_2 and y_3 directions. Hence,

$$P = -\frac{G_0}{(\alpha-1)} (1 - 1/\lambda_1^{\alpha-1}) \quad . \qquad (3.1.12)$$

Substituting eq.(3.1.12) into eq.(3.1.11), the only no-vanishing stress T_{11} (normalized by G_0) is given below,

$$T_{11}/G_0 = \frac{2}{\alpha+2} (1 - 1/\lambda_1^{\alpha+2}) + \frac{1}{\alpha-1} (1 - 1/\lambda_1^{\alpha-1}) \quad , \qquad (3.1.13)$$

while the resultant force in y_1 direction is given by

$$F/G_0 = T_{11}\lambda_2^2/G_0 = \frac{3\alpha}{(\alpha+2)(\alpha-1)}(1/\lambda_1) - \frac{2}{\alpha+2}(1/\lambda_1^{\alpha+3}) - \frac{1}{\alpha-1}(1/\lambda_1^{\alpha}) \quad . \qquad (3.1.14)$$

When λ_1 becomes very large , T_{11} approaches a constant given by

$$T_{11} = \frac{3\alpha G_0}{(\alpha+2)\ (\alpha-1)} \quad . \qquad (3.1.12)$$

However, since the cross sectional area of the cuboid decreases with λ_1, the resultant force will decrease after a critical value of λ_1 and will go to zero as λ_1 goes to infinity. The variation of T_{11} and F with λ_1 are shown in Fig.3 and 4.

3.2. Large plastic flow in a circular tube (pipe flow)

Consider a case of pipe flow in which each point in the material moves parallel to the axis of the pipe through a distance f(r) depending only upon the radial position of the point.

Taking the cylindrical polar coordinates $\phi^{\alpha}(R,\theta,Z)$ in the undeformed body and $\theta_j(r,\theta,w)$ in the deformed body, the deformation field is expressed as follows:

$$r=R, \qquad \theta=\theta, \qquad w=-K(t)f(r)+Z \quad . \qquad (3.2.1)$$

where K is a positive function and the deformation corresponding to positive stresses is shown in Fig.5.

The metric tensor in the material system is

$$[G_{\alpha\beta}] = \begin{bmatrix} 1 & 0 & 0 \\ 0 & R^2 & 0 \\ 0 & 0 & 1 \end{bmatrix} \quad , \quad |G_{\alpha\beta}| = R^2 \qquad (3.2.2)$$

and in spatial system

$$[g_{kl}] = \begin{bmatrix} 1 & 0 & 0 \\ 0 & r^2 & 0 \\ 0 & 0 & 1 \end{bmatrix} \quad , \quad |g_{kl}| = r^2 \quad . \qquad (3.2.3)$$

The deformation gradient is

$$[\bar{F}] = \begin{bmatrix} 1 & 0 & 0 \\ 0 & 1 & 0 \\ -Kf' & 0 & 1 \end{bmatrix} \quad . \qquad (3.2.4)$$

where $f' = df/dr$. The Cauchy-Green deformation tensor, derived by use of eq.(2.2.10a), is

$$[\bar{C}_{\mu\nu}] = \begin{bmatrix} 1+K^2f'^2 & 0 & -Kf' \\ 0 & r^2 & 0 \\ -Kf' & 0 & 1 \end{bmatrix} \quad , \quad |\bar{C}_{\mu\nu}| = r^2 \quad . \qquad (3.2.5)$$

The incompressibility condition is satisfied automatically since $|\bar{C}_{\mu\nu}| = |G_{kl}|$. The inverse and the increment of $[\bar{C}_{\mu\nu}]$ are

$$[\bar{C}_{\mu\nu}]^{-1} = \begin{bmatrix} 1 & 0 & Kf' \\ 0 & 1/r^2 & 0 \\ Kf' & 0 & 1+K^2f'^2 \end{bmatrix} \qquad (3.2.6)$$

and

$$d[\bar{C}_{\mu\nu}] = \begin{bmatrix} 2Kf'^2dK & 0 & -f'dK \\ 0 & 0 & 0 \\ -f'dK & 0 & 0 \end{bmatrix} \quad . \qquad (3.2.7)$$

The intrinsic time can be found from eq.(2.2.22) to be

$$(d\zeta)^2 = (f'dK)^2 \quad , \qquad (3.2.8)$$

where p_2 has been set to 2. For monotonic shearing, $d\zeta = f'dK$. After an integration and imposition of the initial condition, $\zeta = 0$, at $K = 0$, it follows that $\zeta = f'K$. Upon neglecting the effect of hardening (or softening) of the material, dz and z are

$$dz = f'dK \quad \text{and} \quad z = f'K \quad . \qquad (3.2.9)$$

Now The Cauchy-Green deformation tensor is rewritten with the help of eq.(3.2.9) in the form

$$[\tilde{C}_{\mu\nu}] = \begin{bmatrix} 1+z^2 & 0 & -z \\ 0 & r^2 & 0 \\ -z & 0 & 1 \end{bmatrix} \qquad (3.2.10))$$

and $d[\tilde{C}]/dz$ is obtained in the form

$$d[\tilde{C}]/dz = \begin{bmatrix} 2z & 0 & -1 \\ 0 & 0 & 0 \\ -1 & 0 & 0 \end{bmatrix} \quad . \qquad (3.2.11)$$

Setting $G(z) = \rho_0/z^{\alpha}$, the stresses are obtained by use of the constitutive equation (2.2.25) in the form

$$\tilde{\tau}_{RR} = -P(1+z^2) + 2\rho_0/(1-\alpha)/(2-\alpha)\, z^{(2-\alpha)} \quad , \qquad (3.2.12a)$$

$$\tilde{\tau}_{RZ} = Pz - \rho_0/(1-\alpha)\, z^{(1-\alpha)} \qquad (3.2.12b)$$

and

$$\tilde{\tau}_{\theta\theta} = -Pr^2 \quad , \quad \tilde{\tau}_{ZZ} = -P \quad , \quad \tilde{\tau}_{R\theta} = \tilde{\tau}_{\theta Z} = 0 \quad . \qquad (3.2.12c)$$

The components of stress in the spatial curvilinear system $\bar{T}$ are given by

$$\bar{T}_{rr} = -P - 2\rho_0/(2-\alpha)\, z^{(2-\alpha)} \quad , \quad \bar{T}_{\theta\theta} = -Pr^2 \quad , \quad \bar{T}_{ww} = -P \quad , \tag{3.2.13}$$

$$\bar{T}_{rw} = -\rho_0/(1-\alpha)\, z^{(1-\alpha)} \quad \text{and} \quad \bar{T}_{r\theta} = \bar{T}_{\theta w} = 0$$

while the physical components of stress in the spatial system are given by

$$\sigma_{rr} = -P + g_1 \quad , \quad \sigma_{\theta\theta} = \sigma_{ww} = -P \quad ,$$

$$\sigma_{rw} = g_2 \quad \text{and} \quad \sigma_{r\theta} = \sigma_{\theta w} = 0 \tag{3.2.14}$$

where

$$g_1 = -2\rho_0/(2-\alpha)\, z^{(2-\alpha)} = -2\rho_0/(2-\alpha)\, (f'K)^{(2-\alpha)} \tag{3.2.14a}$$

and

$$g_2 = -\rho_0/(1-\alpha)\, z^{(1-\alpha)} = -\rho_0/(1-\alpha)(f'K)^{(1-\alpha)} \tag{3.2.14b}$$

In the absence of body forces the equations of equilibrium along with the stresses of eqs.(3.2.14) give the relations,

$$-\partial P/\partial r + \partial g_1/\partial r + g_1/r = 0 \quad , \tag{3.2.15a}$$

$$-\partial P/\partial w + \partial g_2/\partial r + g_2/r = 0 \tag{3.2.15b}$$

and

$$-\partial P/\partial \theta = 0 \tag{3.2.15c}$$

The last equation requires that P be a function of r and w only. Since g_1 depends on r only, equation (3.2.15a) requires $\partial^2 P/\partial r \partial w = 0$. Thus,

$$P = C_0 w + Y(r) \quad , \tag{3.2.16}$$

where C_0 is a constant of integration. From equation (3.2.15b),

$$g_2 = C_1/r + C_0 r/2 \quad , \tag{3.2.17}$$

where C_1 is another constant of integration. To ensure a finite solution at $r=0$, C_1 must be zero in eq.(3.2.17),

$$g_2 = C_0 r/2 \quad . \tag{3.2.18}$$

Recalling the expression of g_2 in eq.(3.2.14a), it follows that

$$C_0 r/2 = -\rho_0/(1-\alpha)\ z^{(1-\alpha)} \quad . \tag{3.2.19}$$

Solving for z from eq.(3.2.19), one obtains

$$z = [-C_0(1-\alpha)/2\rho_0]^{1/(1-\alpha)} r^{1/(1-\alpha)} \quad . \tag{3.2.20}$$

Introducing z into g_1 in (3.2.14a) and then substituting g_1 and P in eq.(3.2.16) into the first equation of (3.2.15),

$$\frac{\partial P}{\partial r} = \frac{\partial Y(r)}{\partial r} = \frac{2\rho_0}{2-\alpha} \left\{\frac{-C_0(1-\alpha)}{2\rho_0}\right\}^{(2-\alpha)/(1-\alpha)} \left\{\frac{3-\alpha}{1-\alpha}\right\} r^{(2-\alpha)/(1-\alpha)} . \tag{3.2.21}$$

After integration of eq.(3.2.21), the pressure P is obtained as

$$P = C_0 w + D - \frac{2\rho_0(3-2\alpha)}{(2-\alpha)^2} \left\{\frac{-C_0(1-\alpha)}{2\rho_0}\right\}^{(2-\alpha)/(1-\alpha)} r^{(4-3\alpha)/(1-\alpha)} \quad , \tag{3.2.22}$$

where D is a constant of integration. The constants C_0 and D are determined by imposing the boundary conditions.

A case of pipe flow with the following boundary conditions is now considered:

$$\text{(i) at } w=0, \qquad -F = \int_0^a 2\pi r \sigma_{ww}|_{w=0} dr \quad ,$$

$$\text{(ii) at } w=L \qquad 0 = \int_0^a 2\pi r \sigma_{ww}|_{w=L} dr \tag{3.2.23}$$

and

$$\text{(iii) at } r=a \qquad f(a)=0 \quad .$$

Upon satisfying the boundary conditions (i) and (ii) in eq.(3.2.23) the following equations are obtained:

$$-F = -D\pi a^2 + \frac{4\rho_o(3-2\alpha)(1-\alpha)}{(2-\alpha)^2\,(4-3\alpha)} \left\{\frac{-C_o(1-\alpha)}{2\rho_o}\right\}^{(2-\alpha)/(1-\alpha)} a^{(4-3\alpha)/(1-\alpha)} \tag{3.2.24}$$

and

$$0 = -D\pi a^2 - C_o L\pi a^2 + \frac{4\rho_o(3-2\alpha)(1-\alpha)}{(2-\alpha)^2\,(4-3\alpha)} \left\{\frac{-C_o(1-\alpha)}{2\rho_o}\right\}^{(2-\alpha)/(1-\alpha)} a^{(4-3\alpha)/(1-\alpha)}$$

Solving the simultaneous equations (3.2.24), The constants C_o and D are obtained as

$$C_o = -F/(L\pi a^2)$$

and (3.2.25)

$$D = F/(\pi a^2) + \frac{4\rho_o(3-2\alpha)(1-\alpha)}{(2-\alpha)^2(4-3\alpha)} \left\{\frac{-C_o(1-\alpha)}{2\rho_o}\right\}^{(2-\alpha)(1-\alpha)} r^{(2-\alpha)(1-\alpha)} .$$

Finally, the following non-vanishing stresses are obtained and are given by eq.(3.2.26)

$$\sigma_{rw}/\rho_o = -\beta(r/L)/2 \tag{3.2.26a}$$

$$\sigma_{ww}/\rho_o = \sigma_{\theta\theta}/\rho_o = \beta(w/L-1) - 2(3+2\alpha)/(2-\alpha)^2[(1-\alpha)/2\cdot\beta]^{(2-\alpha)/(1-\alpha)} \cdot$$

$$\cdot\{2(1-\alpha)/(4-3\alpha)(\alpha/L)^{(2-\alpha)/(1-\alpha)} - (r/L)^{(2-\alpha)/(1-\alpha)}\}$$

and (3.2.26b)

$$\sigma_{rr}/\rho_o = \sigma_{ww}/\rho_o - 2/(2-\alpha)[(1-\alpha)/2\cdot\beta]^{(2-\alpha)/(1-\alpha)} (r/L)^{(2-\alpha)/(1-\alpha)}$$

where (3.2.26c)

$$\beta = F/(\pi\rho_o a^2) \quad . \tag{3.2.26}$$

The displacement in the w direction, $u_3 = w - Z = -Kf(r)$, can be obtained by an integration of the expression $z = Kf'(r)$ in eq.(3.2.20) and is given by

$$Kf = [F(1-\alpha)/(2L\pi a^2\rho_o)]^{1/(1-\alpha)}[(1-\alpha)/(2-\alpha)]r^{(2-\alpha)/(1-\alpha)} + C_3 \quad . \qquad (3.2.27)$$

Imposing the boundary condition (iii) in eq.(3.2.23) gives the integration constant C_3,

$$C_3 = -[F(1-\alpha)/(2L\pi a^2\rho_o)]^{1/(1-\alpha)}[(1-\alpha)/(2-\alpha)]a^{(2-\alpha)/(1-\alpha)} \qquad (3.2.28)$$

Hence the displacement u_3, normalized by a, the radius of pipe, becomes

$$u_3/a = -\frac{(1-\alpha)}{(2-\alpha)}[(1-\alpha)/2\cdot\beta]^{1/(1-\alpha)}\{(r/a)(r/L)^{1/(1-\alpha)} - (a/L)^{1/(1-\alpha)}\} \quad . \qquad (3.2.29)$$

It is noticed that u_3 reaches a maximum value at r=0, which is

$$u_3(0)/a = \frac{(1-\alpha)}{(2-\alpha)}[a(1-\alpha)/2L]^{1/(1-\alpha)}\beta^{1/(1-\alpha)} \quad . \qquad (3.2.30)$$

The above solutions can be used to analyze the process of metal extrusion in a cylindrical die. The condition to move a bar of length L and radius a is given by $\sigma_{rw} = (\sigma_{rw})_c$ at r=a. $(\sigma_{rw})_c$ is the factor representing the surface condition between the metal and the die. When F increases until F_c, σ_{rw} reaches the critical value $(\sigma_{rw})_c$ at r=a, The metal bar starts to move in the die with the shape of u_3 corresponding to F_c.

$$F_c = 2L\pi a(\sigma_{rw})_c \qquad (3.2.31a)$$

$$u_3/a = -\frac{(1-\alpha)}{(2-\alpha)}[(1-\alpha)/2\cdot\beta_c]^{1/(1-\alpha)}\{(r/a)(r/L)^{1/(1-\alpha)} - (a/L)^{1/(1-\alpha)}\}$$

where $\qquad (3.2.31b)$

$$\beta_c = F_c/(\pi\rho_o a^2) \quad .$$

With α= 0.86 a numerical example is given as follows. Fig.6 shows the deformation profile for various parameter β. Fig.7 gives the relation between deformation u_3 and the parameter β , i.e., the applied force, at r=0. σ_{rw} is a linear distribution over the cross section of the pipe, σ_{rw}=0 at r=0 and σ_{rw}= βa/2L at r=a. The distribution of σ_{ww} and σ_{rr} over the cross sections w=0, and w/L=0.5, are given in Fig.8 for the case of a/L=0.2, and β=70.

3.3. Large plastic torsion of circular bar

Consider a uniform solid circular bar of radius a. The one end of the bar is fixed. The other end is subjected to an angle of twist due to applied torque T. The bar is also assumed to be constrained axially, thus allowing the possible development of an axial force F. The deformation field is the following:

$$r=R \quad ,$$

$$\theta=\Theta+k(t)Z \qquad (3.3.1)$$

and $$w=Z \quad ,$$

where (R,Θ,Z) and (r,θ,w) are the cylindrical coordinates for the material and spatial system, respectively. Eq.(3.3.1) implies that the planes perpendicular to the axis of the bar are rotated in their own planes through an angle proportional to the distance of the plane from the fixed end, k is the twist per unit length.

The metric tensor in the material system is

$$[G_{\alpha\beta}] = \begin{bmatrix} 1 & 0 & 0 \\ 0 & R^2 & 0 \\ 0 & 0 & 1 \end{bmatrix} \qquad |G_{\alpha\beta}|=R^2 \qquad (3.3.2)$$

and in spatial system

$$[g_{kl}] = \begin{bmatrix} 1 & 0 & 0 \\ 0 & r^2 & 0 \\ 0 & 0 & 1 \end{bmatrix} \quad , \quad |g_{kl}| = r^2 \quad . \qquad (3.3.3))$$

The deformation gradient is given below,

$$[\tilde{F}] = \begin{bmatrix} 1 & 0 & 0 \\ 0 & 1 & k \\ 0 & 0 & 1 \end{bmatrix} \quad . \qquad (3.3.4)$$

The Cauchy-Green deformation tensor can be derived by use of eq.(2.2.10a),

$$[\tilde{C}_{\mu\nu}] = \begin{bmatrix} 1 & 0 & 0 \\ 0 & r^2 & r^2k \\ 0 & r^2k & r^2k^2+1 \end{bmatrix} \quad , \quad |\tilde{C}_{\mu\nu}| = r^2 \quad . \qquad (3.3.5)$$

The incompressibility is again satisfied since $|C_{\mu\nu}| = |G_{kl}|$. The inverse and the increment of $[C_{\mu\nu}]$ are given by

$$[\tilde{C}_{\mu\nu}]^{-1} = 1/r^2 \begin{bmatrix} r^2 & 0 & 0 \\ 0 & r^2k^2+1 & -r^2k \\ 0 & -r^2k & r^2 \end{bmatrix} \qquad (3.3.6)$$

and

$$d[\tilde{C}_{\mu\nu}] = r^2dk \begin{bmatrix} 0 & 0 & 0 \\ 0 & 0 & 1 \\ 0 & 1 & 2k \end{bmatrix} \quad . \qquad (3.3.7)$$

The intrinsic time can be obtained as

$$(d\zeta)^2 = (r\dot{k})^2 \quad , \tag{3.3.8}$$

where P_2 has been set to 2. Under the condition of monotonic torsion, $d\zeta = rdk$. After integration and consideration of a zero strain initial condition, $\zeta = rk$. Neglecting hardening and softening effects, dz and z are given below,

$$dz = rdk, \qquad z = rk \quad . \tag{3.3.9}$$

Hence, the Cauchy-Green deformation tensor can be written as

$$[\tilde{C}_{\mu\nu}] = \begin{bmatrix} 1 & 0 & 0 \\ 0 & r^2 & rz \\ 0 & rz & z^2+1 \end{bmatrix} \quad . \tag{3.3.10}$$

Then,

$$[\hat{\tilde{C}}_{\mu\nu}] = \begin{bmatrix} 0 & 0 & 0 \\ 0 & 0 & r \\ 0 & r & 2z \end{bmatrix} \quad . \tag{3.3.11}$$

Again taking $G(z) = \rho_0/z^{\alpha}$, the following stresses are obtained after substitution of eq.(3.3.10) and eq.(3.3.11) into eq.(2.2.25) and then integrating the resultant equations,

$$\bar{\tau}_{RR} = -P \quad , \quad \bar{\tau}_{\theta\theta} = -Pr^2, \quad \bar{\tau}_{R\theta} = \bar{\tau}_{RZ} = 0 \quad ,$$

$$\bar{\tau}_{ZZ} = -P(z^2+1) + \frac{2\rho_o}{(1-\alpha)(2-\alpha)} z^{(2-\alpha)} \qquad (3.3.12)$$

and $$\bar{\tau}_{\theta Z} = -Prz + [\rho_o/(1-\alpha)] \cdot r \cdot z^{(1-\alpha)}$$

The stresses in the spatial curvilinear system $\bar{T}$ can be obtained by tensor transformation as follows:

$$\bar{T}_{rr} = -P \ , \ \bar{T}_{\theta\theta} = -Pr^2 \ , \ \bar{T}_{ww} = -P - [2\rho_o/(2-\alpha)]z^{(2-\alpha} \ ,$$

$$\bar{T}_{\theta w} = [\rho_o/(1-\alpha)] \cdot r \cdot z^{(1-\alpha)} \quad \text{and} \quad \bar{T}_{r\theta} = \bar{T}_{rw} = 0 \qquad (3.3.13)$$

The physical components of the stresses in the spatial system are

$$\sigma_{rr} = \sigma_{\theta\theta} = -P \ , \quad \sigma_{ww} = -1 - [2\rho_o/(2-\alpha)] \ z^{(2-\alpha)},$$

$$\sigma_{\theta w} = [\rho_o/(1-\alpha)] \ z^{(1-\alpha)} \text{and} \quad \sigma_{r\theta} = \sigma_{rw} = 0 \qquad (3.3.14)$$

When body forces are zero, the equilibrium equations with the stresses in eq.(3.3.14) give $\partial p/\partial r = 0$, $\partial p/\partial \theta = 0$, and $\partial p/\partial z = 0$. This states that P is a constant. If the surface of the cylinder r=a is to be free of tractions, $\sigma_{rr} = 0$ there. Hence P must be equal to zero. Consequently, the following non-vanishing stresses yield

$$\sigma_{\theta w} = [\rho_o/(1-\alpha)](rk)^{(1-\alpha)} \qquad (3.3.15a)$$

$$\sigma_{ww} = [-2\rho_o/(2-\alpha)](rk)^{(2-\alpha)} \qquad (3.3.15b)$$

Clearly there is no any integration constant available, the forces at the ends can no longer be controlled for the prescribed deformation field. The resultant force F which is needed to maintain the length of the bar during the deformation can be calculated as

AD-A194 167 AN ENDOCHRONIC RATE-SENSITIVE CONSTITUTIVE EQUATION FOR METALS APPLICATIO..(U) CINCINNATI UNIV OH K C VALANIS 01 MAR 88 ARO-21663.2-EG DAAG29-85-K-0017 2/3

UNCLASSIFIED F/G 11/6.1 NL

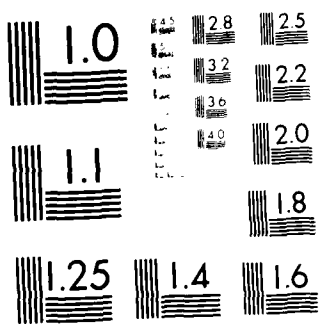

$$F/(\rho_0 a^2) = (\int_0^a |\sigma_{ww}| 2\pi r dr)/(\rho_0 a^2) = \frac{4\pi}{(2-\alpha)(4-\alpha)}(ka)^{(2-\alpha)} \qquad (3.3.16)$$

while the resultant torque as

$$T/(\rho_0 a^3) = (\int_0^a 2\pi \sigma_{\theta w} r^2 dr)/(\rho_0 a^3) = \frac{2\pi}{(1-\alpha)(4-\alpha)}(ka)^{(1-\alpha)} \quad . \qquad (3.3.17)$$

Solving for k from (3.3.17), the twist per unit length is obtained and given by eq.(3.3.18),

$$k = 1/a \left[T/(\rho_0 a^3) \frac{(1-\alpha)(4-\alpha)}{2\pi}\right]^{1/(1-\alpha)} \qquad (3.3.18)$$

The total twist angle at any station w can be obtained as

$$\Delta\theta = \theta - \Theta = kz = (w/a)\left[T/(\rho_0 a^3) \frac{(1-\alpha)(4-\alpha)}{2\pi}\right]^{1/(1-\alpha)} . \qquad (3.3.19)$$

The numerical results with α=0.86 are given in Fig.10 - Fig.13. Fig.10 and Fig.11 show the variations of the torque and axial force vs. the twist, respectively. The distributions of $\sigma_{w\theta}$ and σ_{ww} over the cross section are given in Fig.12 and Fig.13. It is interesting to observe that for relative small k ($k \ll 1$) the torque increases more rapidly than the axial force, however for relative large k ($k > 1$) the axial force increases much faster than the torque. For the elastic case when α=0, in eq.(3.3.17) and eq.(3.3.16)

$$T = (\pi \rho_0 a^4/2)k \ , \qquad F = (\pi \rho_0 a^4/2)k^2 \qquad (3.3.20)$$

For infinitesimal deformation, $k \ll 1$, F vanishes. The results agree with those from the theory of elementary mechanics of materials.

3.4. Large Plastic Bending of a Block

Let a block, bounded by the planes $X^1_1 = a_1$, $X^1_2 = a_2$; and $X^2 = \pm b$; $X^3 = \pm c$ in the undeformed state, be deformed symmetrically with respect to X^1 axis into a portion of a cylinder as shown in Fig.14. Letting $\theta_j(r,\theta,w)$ be coordinates in deformed state, the deformation map can be stipulated by

$$r = r(X^1,t) \quad ,$$

$$\theta = \theta(X^2,t) \qquad (3.4.1)$$

and $$w = w(X^3,t)$$

It will be shown presently that the condition of incompressibility restricts the deformation given by eq.(3.4.1) to a form where a plane of constant X^1 deforms to a surface of constant r; a plane of constant X^2 to a plane of constant θ; and a plane of constant X^3 to a plane of constant w.

The metric tensors in the spatial system are

$$[g_{kl}] = \begin{bmatrix} 1 & 0 & 0 \\ 0 & r^2 & 0 \\ 0 & 0 & 1 \end{bmatrix} \quad \text{and} \quad [g^{kl}] = \begin{bmatrix} 1 & 0 & 0 \\ 0 & 1/r^2 & 0 \\ 0 & 0 & 1 \end{bmatrix} \quad . \qquad (3.4.2)$$

The deformation gradient matrix is

$$[F] = \begin{bmatrix} dr/dX^1 & 0 & 0 \\ 0 & d\theta/dX^2 & 0 \\ 0 & 0 & dw/dX^3 \end{bmatrix} \quad .$$

Hence the Cauchy-Green tensor is

$$[C] = \begin{bmatrix} (dr/dX^1)^2 & 0 & 0 \\ 0 & r^2(d\theta/dX^2)^2 & 0 \\ 0 & 0 & (dw/dX^3)^2 \end{bmatrix} . \qquad (3.4.3)$$

The incompressibility requires that

$$(r\ dr/dX^1)(d\theta/dX^2)(dw/dX^3) = 1 \quad . \qquad (3.4.4)$$

Since r depends on X^1 and t only; θ on X^2 and t; and w on X^3 and t, the following must be true at all times,

$$r\ dr/dX^1 = c_1(t), \qquad d\theta/dX^2 = c_2(t), \qquad dw/dX^3 = c_3(t)$$

$$\text{and} \qquad c_1(t)\ c_2(t)\ c_3(t) = 1 \qquad (3.4.5)$$

Integration of eq.s(3.4.5) give the following deformation field,

$$r^2/2 = c_1X^1 + A_1(t) \quad ,$$

$$\theta = c_2X^2 + A_2(t) \qquad (3.4.6)$$

$$\text{and} \qquad w = c_3X^3 + A_3(t)$$

where A_1, A_2, and A_3 are the constants of the integrals.

Considering the plane strain condition (c_3=1, A_3=0) and excluding rigid body rotation (A_2=0), the deformation field becomes

$$r^2/2 = R\ X^1 + A(t) \quad ,$$

$$\theta = (1/R)\ X^2 \qquad (3.4.7)$$

$$\text{and} \qquad w = X^3 \quad .$$

where the facts that c_2 is the curvature and c_1 the radius of curvature of the deformed cylinder have been used. The Cauchy-Green tensor and its inverse now become

$$[C] = \begin{bmatrix} 1/Q^2 & 0 & 0 \\ 0 & Q^2 & 0 \\ 0 & 0 & 1 \end{bmatrix} \quad \text{and} \quad [C]^{-1} = \begin{bmatrix} Q^2 & 0 & 0 \\ 0 & 1/Q^2 & 0 \\ 0 & 0 & 1 \end{bmatrix} , \tag{3.4.8}$$

where $Q = r/R$. The increment of [C] is

$$d[C] = \begin{bmatrix} -2Q^{-3}dQ & 0 & 0 \\ 0 & 2QdQ & 0 \\ 0 & 0 & 0 \end{bmatrix} . \tag{3.4.9}$$

The intrinsic time can be obtained from eq.(2.2.15) and eq.(2.2.16) whereby

$$(d\zeta)^2 = [(1/Q)dQ]^2 , \tag{3.4.10}$$

where p_2 in eq.(2.2.15) has been set equal to 1/2.

For monotonic bending $d\zeta = (1/Q)dQ$ and then $\zeta = \ln(Q)+c$ after integration. Since $\zeta=0$, for $Q=1$, hence $c=0$. Neglecting hardening or softening effects, $f=1$ and dz and z can be derived as shown in eq.(3.4.11),

$$dz = (1/Q)dQ \quad , \quad z = \ln(Q) \quad . \tag{3.4.11}$$

With the help of (3.4.11) $\hat{C}$ is given below:

$$[\hat{C}] = Q \begin{bmatrix} -2Q^{-3} & 0 & 0 \\ 0 & 2Q & 0 \\ 0 & 0 & 0 \end{bmatrix} . \tag{3.4.12}$$

Taking $G(z) = G_0 e^{-\alpha z}$, the stresses are obtained, upon use of the constitutive eq.(2.1.25),

$$T_{11} = (1/Q^2)[-P-(2G_0/(\alpha-2))(1-1/Q^{(\alpha-2)})] \quad ,$$

$$T_{22} = Q^2[-P+(2G_0/(\alpha+2))(1-1/Q^{(\alpha+2)})] \quad , \qquad (3.4.13)$$

$$T_{33} = -P, \quad \text{and} \quad T_{12} = T_{23} = T_{13} = 0 \quad .$$

The components of stress in the spatial curvilinear system are given by eq.(3.4.14),

$$\bar{T}_{rr} = -P -(2G_0/(\alpha-2))(1-1/Q^{(\alpha-2)}) \quad ,$$

$$\bar{T}_{\theta\theta} = r^2[-P+(2G_0/(\alpha+2))(1-1/Q^{(\alpha+2)})] \quad , \qquad (3.4.14)$$

$$\bar{T}_{ww} = -P \quad , \quad \text{and} \quad \bar{T}_{r\theta} = \bar{T}_{rw} = \bar{T}_{w\theta} = 0 \quad .$$

while the physical components of stress in the spatial system are given by eq.(3.4.15),

$$\sigma_{rr} = -P-(2G_0/(\alpha-2)(1-1/Q^{(\alpha-2)}) \quad ,$$

$$\sigma_{\theta\theta} = -P+(2G_0/(\alpha+2)(1-1/Q^{(\alpha+2)}) \quad , \qquad (3.4.15)$$

$$\sigma_{ww} = -P \quad \text{and} \quad \sigma_{r\theta} = \sigma_{wr} = \sigma_{\theta w} = 0 \quad ,$$

where P will be determined from the equilibrium equations and the boundary conditions.

When body forces are absent, two of the three equations of equilibrium, in the θ and w directions, are satisfied identically if the stresses in (3.4.15) are functions of r only. The remaining equilibrium condition is given by eq.(3.4.16):

$$\frac{d}{dr}(\sigma_{rr}) + \frac{\sigma_{rr}-\sigma_{\theta\theta}}{r} = 0 \quad . \tag{3.4.16}$$

Substituting the expressions for the stresses in eq.(3.4.15) into eq.(3.4.16) and integrating, the following relation for P is obtained,

$$P = -\frac{2G_0}{\alpha-2}\{1+(R/r)^{(\alpha-2)}\} + 2G_0\{-2\alpha/(\alpha^2-4)\ln(r/c) - 1/(\alpha-2)^2(R/r)^{(\alpha-2)} - 1/(\alpha+2)^2(R/r)^{(\alpha+2)}\} \quad , \tag{3.4.17}$$

where c is the constant of integration.

Normalized by $2G_0$, the non-vanishing stresses in (3.4.15) with the help of eq.(3.4.17) become

$$\sigma_{rr}/2G_0 = 2\alpha/(\alpha^2-4)\ln(r/c) + 1/(\alpha+2)^2(R/r)^{(\alpha+2)} + 1/(\alpha+2)^2(R/r)^{(\alpha+2)}, \tag{3.4.18a}$$

$$\sigma_{\theta\theta}/2G_0 = 2\alpha/(\alpha^2-4)[1+\ln(r/c)] - (\alpha-3)/(\alpha-2)^2(R/r)^{(\alpha-2)} - (\alpha+1)/(\alpha+2)^2(R/r)^{(\alpha+2)} \quad , \tag{3.4.18b}$$

$$\sigma_{ww}/2G_0 = 1/(\alpha-2) + 2\alpha/(\alpha^2-4)\ln(r/c) - (\alpha-3)/(\alpha-2)^2(R/r)^{(\alpha-2)} + 1/(\alpha+2)^2(R/r)^{(\alpha+2)} \quad , \tag{3.4.18c}$$

where the constant c will be determined from the boundary conditions.

Suppose that the undeformed surfaces of the block $a_1=0$, $a_2=H$, $b=L/2$, and $c=1/2$ in Fig.2 map into the deformed surfaces $r=r_1$, $r=r_2$, and $\theta=\theta_0$. The following geometrical restrictions must hold:

(a) $R=(r_2^2-r_1^2)/(2H)$;

(b) $\theta_0=L/2R$ and in the case in which the beam is bent as a circle, $R/H=L/(2H\pi)$. (3.4.19)

(c) $A=(r_1^2+r_2^2)/4RH$

The boundary conditions appropriate to the bending of the block are the following:

(1) $\sigma_{rr}= f_1$ at $r=r_1$; $\sigma_{rr}= f_2$ at $r=r_2$;

(2) the resultant moment and the resultant force acting on the surface initially at $X^2 = \pm b/2$, are

$$M = \int_{r_1}^{r_2} \sigma_{\theta\theta} r dr \qquad (3.4.20a)$$

$$F = \int_{r_1}^{r_2} \sigma_{\theta\theta}\, dr = \int_{r_1}^{r_2} d(r\sigma_{rr}) = r_2 f_2 - r_1 f_1 \qquad (3.4.20b)$$

Upon satisfying the boundary conditions stipulated in eq.'s(3.4.20a,b) we obtain the following <u>five</u> equations relating the <u>six</u> variables r_1, r_2, c, R, M, and F.

$$2\alpha/(\alpha^2-4)\ln(\eta_1/d)+1/(\alpha-2)^2(\eta/\eta_1)^{(\alpha-2)}+1/(\alpha+2)^2(\eta/\eta_1)^{(\alpha+2)} = g_1$$

$$2\alpha/(\alpha^2-4)\ln(\eta_2/d)+1/(\alpha-2)^2(\eta/\eta_2)^{(\alpha-2)}+1/(\alpha+2)^2(\eta/\eta_2)^{(\alpha+2)} = g_2$$

$$\begin{aligned} T = {} & 2\alpha/(\alpha^2-4)[(\eta_2^2/2)\ln(\eta_2/d)-(\eta_1^2/2)\ln(\eta_1/d)+(\eta_2^2-\eta_1^2)/4] \\ & +(\alpha-3)/(\alpha-2)^2/(\alpha-4)[(\eta/\eta_2)^{(\alpha-2)}\eta_2^2 - (\eta/\eta_1)^{(\alpha-2)}\eta_1^2] \\ & +(\alpha+1)/(\alpha+2)^2/\alpha\,[(\eta/\eta_2)^{(\alpha+2)}\eta_2^2 - (\eta/\eta_1)^{(\alpha+2)}\eta_1^2] \end{aligned} \qquad (3.4.21)$$

$$S = \eta_2 g_2 - \eta_1 g_1$$

$$\eta = (\eta_2^2 - \eta_1^2)/2$$

where

$$\eta_1 = r_1/H \ , \quad \eta_2 = r_2/H \ , \ \eta = R/H \ , \ T = M/(2G_0H^2), \ d = c/H$$

$$S = F/(2G_0H) \ , \ g_1 = f_1/(2G_0), \text{ and } g_2 = f_2/(2G_0) \qquad (3.4.22)$$

The problem of interest here is the one in which the radial boundary stresses f_1 and f_2 are equal to zero. The solution then reduces to assigning a value to R, the radius of curvature of the neutral axis. Eq.'s(3.4.21) then determines the deformed radii r_1 and r_2, the constant of integration c, the moment M and the end force F which is zero in this case.

Specific cases

case (i): A very thin beam.

As the first example, consider a pure bending of very thin beam. Let ξ be the distance from the neutral axis. Then $r=R+\xi$, and $\xi/R<<1$. Employing the Taylor expansion,

$$(R/r)^{(\alpha-2)} \simeq 1-(\alpha-2)(\xi/R); \quad (R/r)^{(\alpha+2)} \simeq 1-(\alpha+2)(\xi/R) \qquad (3.4.23)$$

The non-zero stresses (3.4.15) become

$$\sigma_{rr} = -P-2G_0\xi/R \ ; \quad \sigma_{\theta\theta} = -P+2G_0\xi/R \ ; \quad \sigma_{ww} = -P \qquad (3.4.24)$$

Satisfaction of the equilibrium eq.(3.4.16) gives the pressure as

$$P = -2G_0\xi/R + c \qquad (3.4.25)$$

Introducing (3.4.25) into (3.4.24),

$$\sigma_{rr} = -c \quad , \quad \sigma_{\theta\theta} = 4G_0\xi/R - c \quad , \quad \sigma_{ww} = 2G_0\xi/R - c \quad . \qquad (3.4.26)$$

The boundary condition, $\sigma_{rr}=0$, at $\xi=\xi_1,\xi_2$ gives the integration constant $c=0$; and the condition of zero resultant force at the ends of θ-direction yields $\xi_1=-\xi_2=h/2$,where h is the deformed thickness of the beam. Then,

$$\sigma_{\theta\theta} = 4G_0\xi/R \ , \quad \sigma_{ww} = 2G_0\xi/R \ , \quad M = G_0h^3/(3R). \qquad (3.4.27)$$

The results here are the same as those in the elastic deformation of pure bending except the stress in w-direction which is required to produce plane strain conditions in the presence of incompressibility. Evidently the strains in this case are extremely small resulting in an elastic solution.

Case(ii): A thick beam.

Now consider an example of pure bending of a thick beam. In this case the zero resultant force F=0 and $f_1=f_2=0$. Therefore, $g_1=g_2=0$. thus,

$$2\alpha/(\alpha^2-4)\ln(\eta_1/d)+1/(\alpha-2)^2(\eta/\eta_1)^{(\alpha-2)}+1/(\alpha+2)^2(\eta/\eta_1)^{(\alpha+2)} = 0$$

$$2\alpha/(\alpha^2-4)\ln(\eta_2/d)+1/(\alpha-2)^2(\eta/\eta_2)^{(\alpha-2)}+1/(\alpha+2)^2(\eta/\eta_2)^{(\alpha+2)} = 0$$

$$\eta = (\eta_2^2 - \eta_1^2)/2 \qquad (3.4.28)$$

$$T = 2\alpha/(\alpha^2-4)[(\eta_2^2/2)\ln(\eta_2/d)-(\eta_1^2/2)\ln(\eta_1/d)+(\eta_2^2-\eta_1^2)/4]$$

$$+(\alpha-3)/(\alpha-2)^2/(\alpha-4)[(\eta/\eta_2)^{(\alpha-2)}\eta_2^2 - (\eta/\eta_1)^{(\alpha-2)}\eta_1^2]$$

$$+(\alpha+1)/(\alpha+2)^2/\alpha\,[(\eta/\eta_2)^{(\alpha+2)}\eta_2^2 - (\eta/\eta_1)^{(\alpha+2)}\eta_1^2]$$

Eq.(3.4.28) is a set of non-linear equations. The following procedure is used to get some numerical results for this set of equations.

(1). Eliminate the constant d from the first two equations of (3.4.28) to get one equation involving unknown η_1, η_2, and η.

(2). Use the Newton iteration to solve η_1 and η_2 for given η from the resulting equation from step (1) and the third equation in (3.4.28), which are,

$$2\alpha/(\alpha^2-4)\ln(\eta_1)+1/(\alpha-2)^2(\eta/\eta_1)^{(\alpha-2)}+1/(\alpha+2)^2(\eta/\eta_1)^{(\alpha+2)}=$$

$$2\alpha/(\alpha^2-4)\ln(\eta_2)+1/(\alpha-2)^2(\eta/\eta_2)^{(\alpha-2)}+1/(\alpha+2)^2(\eta/\eta_2)^{(\alpha+2)}$$

$$\eta = (\eta_2^2 - \eta_1^2)/2 \qquad (3.4.29)$$

(3). Obtain the constant d for corresponding η, η_1, and η_2 from either one of the first two equations in (3.4.28).

(4). Obtain T from the last equation in (3.4.28) for corresponding η, η_1, η_2, and d.

Before formulating the numerical solution scheme, the existence and the uniqueness of eq.(3.4.29) is first discussed. Look at the following function,

$$f(x)=2\alpha/(\alpha^2-4)\ln x+1/(\alpha-2)^2(\eta/x)^{(\alpha-2)}+1/(\alpha+2)^2(\eta/x)^{(\alpha+2)} \qquad (3.4.30)$$

where x may be η_1 and η_2. For given η, when x approaches zero, f(x) goes to infinity. When x tends to infinity, f(x) goes to infinity. f(x) has one and only one minimum at x_m approximately equal to η, since α is a large number ranging from 100 to 200, $x_m=\eta$ is the root of following equation,

$$f(x)' = [2\alpha/(\alpha^2-4) - (\eta/x_m)^{(\alpha-2)}/(\alpha-2) + (\eta/x_m)^{(\alpha+2)}/(\alpha+2)]/x_m = 0 \qquad (3.4.31)$$

Fig.15 depicts the character of function f(x). It can be seen that for a value of f(x), there are two roots(except the case in which the minimum is also the root) corresponding to η_1 and η_2. One-one relation I is shown in Fig.16 from the first equation (3.4.29). On the other hand another one-one relation II is also shown in Fig.16 for positive η_1 and η_2 from the second equation of (3.4.29). The intersect of I and II gives the solution η_1 and η_2 for given η.

The Newton iteration scheme [56] for (3.4.29) can be written as

$$\begin{bmatrix} \eta_1 \\ \eta_2 \end{bmatrix}_{i+1} = \begin{bmatrix} \eta_1 \\ \eta_2 \end{bmatrix}_i \begin{bmatrix} \partial\phi_1/\partial\eta_1 & \partial\phi_1/\partial\eta_2 \\ \partial\phi_2/\partial\eta_1 & \partial\phi_2/\partial\eta_2 \end{bmatrix}_i^{-1} \begin{bmatrix} \phi_1 \\ \phi_2 \end{bmatrix}_i , \qquad (3.4.32)$$

where ϕ_1 and ϕ_2 are

$$\phi_1 = 2\alpha/(\alpha^2-4)\ln(\eta_1/\eta_2) + [(\eta/\eta_1)^{(\alpha-2)} - (\eta/\eta_2)^{(\alpha-2)}]/(\alpha-2)^2 + \\ + [(\eta/\eta_1)^{(\alpha+2)} - (\eta/\eta_2)^{(\alpha+2)}]/(\alpha+2)^2 \qquad (3.4.33)$$

and $\phi_2 = 2\eta - \eta_2^2 + \eta_1^2$

Numerical results were obtained after setting α=200. Fig.17 shows the variation of moment with the curvature. There is a softening effect in the sense that the moment decreases with increase in curvature after a critical value of the curvature has been reached. However this is a geometric phenomenon since all stresses increase monotonically with curvature. Fig.18

shows the variation of σ_{rr} with curvature at the neutral axis while in Fig.19 and 20 we show $\sigma_{\theta\theta}$ at $r=r_1$ and $r=r_2$. As the curvature increases the neutral axis moves closer to the compressive surface of the beam thereby requiring a large compressive tangential stress to maintain moment equilibrium. The material can sustain a large compressive stress by virtue of its incompressibility. Fig.s 21-23 show the distribution of $\sigma_{\theta\theta}$ over the cross-section of the the beam for values of R/H of 50, 5, and 1. The stress $\sigma_{\theta\theta}$ is zero at the neutral axis as expected. Fig.s 24-26 show the distribution of σ_{rr} over the depth of the beam for values of R/H of 50, 5, and 1. Observe that σ_{rr} is about two orders of magnitude smaller than $\sigma_{\theta\theta}$ and reaches maximum value at the neutral axis.

3.5. Symmetrical expansion of a thick spherical shell

Identify the curvilinear coordinate systems ϕ^α in undeformed body and θ_j in deformed body with the system of the spherical coordinates (R,Φ,Θ) and (r,ϕ,θ), respectively. The deformation of the symmetrical expansion of a thick spherical shell can be described as

$$r = r(R,t) \ , \quad \phi = \Phi \ , \quad \theta = \Theta \ . \qquad (3.5.1)$$

In the material system metric tensors is

$$[G_{\alpha\beta}] = \begin{bmatrix} 1 & 0 & 0 \\ 0 & R^2 & 0 \\ 0 & 0 & (R\sin\Phi)^2 \end{bmatrix} \ , \quad |G_{\alpha\beta}| = R^4\sin^2\Phi \qquad (3.5.2)$$

and in spatial system

$$[g_{\alpha\beta}] = \begin{bmatrix} 1 & 0 & 0 \\ 0 & r^2 & 0 \\ 0 & 0 & (r\sin\phi)^2 \end{bmatrix} \quad , \quad |g_{\alpha\beta}| = r^4\sin^2\phi \quad . \quad (3.5.3)$$

The deformation gradient matrix is given below,

$$[\bar{F}] = \begin{bmatrix} r' & 0 & 0 \\ 0 & 1 & 0 \\ 0 & 0 & 1 \end{bmatrix} \quad , \qquad (3.2.4)$$

where $r' = dr/dR$. The Cauchy-Green deformation tensor is

$$[\tilde{C}] = \begin{bmatrix} r' & 0 & 0 \\ 0 & r^2 & 0 \\ 0 & 0 & (r\sin\phi)^2 \end{bmatrix} \quad , \quad |\tilde{C}| = r'^2 r^4 \sin^2\phi \quad . \quad (3.5.5)$$

For incompressible material,

$$r'^2 r^4 = R^4 \quad , \quad \text{i.e.,} \quad r^2 dr = \pm R^2 dR \quad . \quad (3.5.6)$$

Positive sign in eq.(3.5.6) is taken for expansion of the sphere. After an integration, $r^3 = R^3 + A(t)$. Therefore, the deformation (3.5.1) becomes

$$r = [R^3 + A(t)]^{1/3}, \quad \phi = \Phi \ , \quad \theta = \Theta \quad . \quad (3.5.7)$$

Consequently, the Cauchy-Green deformation tensor becomes

$$[\tilde{C}] = \begin{bmatrix} R^4/r^4 & 0 & 0 \\ 0 & r^2 & 0 \\ 0 & 0 & (r\sin\phi)^2 \end{bmatrix} \quad , \quad |\tilde{C}| = r'^2 r^4 \sin^2\phi \quad . \quad (3.5.8)$$

Then the inverse of the Cauchy-Green tensor is

$$[\tilde{C}]^{-1} = \begin{bmatrix} r^*/R^* & 0 & 0 \\ 0 & 1/r^2 & 0 \\ 0 & 0 & 1/(r\sin\phi)^2 \end{bmatrix} \qquad (3.5.9)$$

while the increment is

$$d[\tilde{C}] = \begin{bmatrix} -4(R^*/r^5)dr & 0 & 0 \\ 0 & 2rdr & 0 \\ 0 & 0 & 2r\sin^2\phi dr \end{bmatrix} . \qquad (3.5.10)$$

The intrinsic time can be obtained by substitution of eq.(3.5.9), eq.(3.5.10) into eq.(2.2.22) as

$$(d\zeta)^2=(dr/r)^2 \quad , \qquad (3.5.11)$$

where p_2 has been set to 1/6. For monotonic expansion, $d\zeta=dr/r$. After an integration, $\zeta=\ln(kr)$, where k is a constant of integration. Since $\zeta=0$, for $r=R$, hence $kR=1$, i.e., $k=1/R$. Neglecting the hardening and softening effect, dz and z are obtained as follows,

$$dz=dr/r \ , \qquad z=\ln(r/R) \quad . \qquad (3.5.12)$$

With the help of eq.(3.5.12) $d[C]/dz$ is given below,

$$d[\tilde{C}]/dz = \begin{bmatrix} -4(R^*/r^*) & 0 & 0 \\ 0 & 2r^2 & 0 \\ 0 & 0 & 2r^2\sin^2\phi \end{bmatrix} . \qquad (3.5.13)$$

Taking $G=G_0e^{-\alpha z}$, the following stresses are derived by use of the constitutive equation (2.2.25),

$$\tilde{\tau}_{RR}= (R/r)^{*}\{-P - \frac{4G_0}{(\alpha-4)}[1-(R/r)^{\alpha-4}]\} \quad ,$$

$$\tilde{\tau}_{\phi\phi}= r^2\{-P + \frac{2G_0}{(\alpha+2)}[1-(R/r)^{\alpha+2}]\} \quad ,$$

$$\tilde{\tau}_{\theta\theta}= r^2\sin^2\phi \{-P + \frac{2G_0}{(\alpha+2)}[1-(R/r)^{\alpha+2}]\} \qquad (3.5.14)$$

and $\tilde{\tau}_{R\theta}= \tilde{\tau}_{\phi\theta}= \tilde{\tau}_{\phi R}= 0$

The components of stresses in spatial curvilinear system are

$$\tilde{T}_{rr}= -P - \frac{4G_0}{(\alpha-4)}[1-(R/r)^{\alpha-4}] \quad ,$$

$$\tilde{T}_{\phi\phi}= r^2\{-P + \frac{2G_0}{(\alpha+2)}[1-(R/r)^{\alpha+2}]\} \quad ,$$

$$\tilde{T}_{\theta\theta}= r^2\sin^2\phi \{-P + \frac{2G_0}{(\alpha+2)}[1-(R/r)^{\alpha+2}]\} \qquad (3.5.15)$$

and $\tilde{T}_{r\theta}= \tilde{T}_{\phi\theta}= \tilde{T}_{\phi r}= 0$

The physical components of the stresses are

$$\sigma_{rr}= -P - \frac{4G_0}{(\alpha-4)}[1-(R/r)^{\alpha-4}] \quad ,$$

$$\sigma_{\phi\phi}= \sigma_{\theta\theta}= -P + \frac{2G_0}{(\alpha+2)}[1-(R/r)^{\alpha+2}] \qquad (3.5.16)$$

and $\sigma_{r\theta}= \sigma_{\phi\theta}= \sigma_{\phi r}= 0$

For the symmetrical expansion, the equilibrium equations in spherical system with the absence of the body forces are

$$(1/r^2)\,\frac{\partial}{\partial r}\,(r^2\sigma_{rr}) - (1/r)(\sigma_{\phi\phi} + \sigma_{\theta\theta}) = 0$$

and $$\frac{\partial}{\partial\theta}\,(\sigma_{\theta\theta}) = \frac{\partial}{\partial\phi}\,(\sigma_{\phi\phi}) = 0 \qquad (3.5.17)$$

After substitution of eq.(3.5.16) into (3.5.17), the last equation of (3.5.17) becomes $\partial P/\partial\theta = \partial P/\partial\phi = 0$. It follows that $P = P(r)$. And the first equation of (3.5.17) becomes

$$\frac{dP}{dr} = -\frac{4G_o}{(\alpha-4)}\,\frac{d}{dr}\,[1-(R/r)^{\alpha-4}] - \frac{2G_o}{r}\left\{\frac{3\alpha}{(\alpha-4)(\alpha+2)} - \frac{2}{(\alpha-4)}(R/r)^{\alpha-4} - \frac{2}{(\alpha+2)}(R/r)^{\alpha+2}\right\} \qquad (3.5.18)$$

The integration of (3.5.11) yields the following,

$$P = -\frac{4G_o}{(\alpha-4)}\,[1-(R/r)^{\alpha-4}] - 4G_oQ(R/r) + c \quad , \qquad (3.5.19)$$

where c is the constant of integration and

$$Q(R/r) = \int_{R_1/r_1}^{R/r}\left\{\frac{3\alpha}{(\alpha-4)(\alpha+2)} - \frac{2}{(\alpha-4)}\,s^{\alpha-4} - \frac{1}{(\alpha+2)}\,s^{\alpha+2}\right\}\,\frac{s^2}{(1-s^3)}\,ds \quad , \qquad (3.5.19a)$$

where R_1 and r_1 are inner radii of undeformed and deformed sphere, respectively. With the help of (3.5.19), the following non-vanishing stresses are obtained,

$$\sigma_{rr} = 4G_oQ(R/r) - c \quad ,$$

$$\sigma_{\phi\phi} = \sigma_{\theta\theta} = \sigma_{rr} + \frac{4G_o}{(\alpha-4)}\,[1-(R/r)^{\alpha-4}] + \frac{2G_o}{(\alpha+2)}\,[1-(R/r)^{\alpha+2}] \qquad (3.5.20)$$

Consider the following boundary conditions in the resent problem,

(i) $\sigma_{rr} = P_1$, at $r = r_1$,

(ii) $\sigma_{rr} = P_2$, at $r = r_2$. (3.5.21)

Upon satisfying the condition (i) in eq.(3.5.21), $c=-P_1$. Applying the condition (ii),

$$P_2 - P_1 = 4G_0Q(R_2/r_2) \quad . \tag{3.5.22}$$

From the geometrical condition $r^3=R^3+a(t)$,

$$r_1^3 - R_1^3 = r_2^3 - R_2^3 = r^3 - R^3 \quad , \tag{3.5.23}$$

where R_2 and r_2 are the outer radii of the undeformed and deformed sphere respectively. After a few steps of simple algebra manipulation, the following relation is derived,

$$R/r = \frac{K}{[K^3-1 + 1/(R_1/r_1)^3]^{1/3}} \quad , \tag{3.5.24}$$

where $K=R/R_1$. Eq.s (3.5.22), (3.5.24), (3.5.20) and (3.5.19a) with the known P_1, P_2, R_1 and R_2 give the complete solution. It can be seen from (3.5.22) that when $P_1=P_2$, $Q(R_2/r_2)=0$. Since the integrand of eq.(3.5.19a) is monotonic increasing function it follows that $R_1/r_1=R_2/r_2$. This is true if only if $R_1/r_1= R_2/r_2=1$. This is the condition under which no deformation takes place. This agrees with the incompressibility assumption. Some numerical solutions with $R_2/R_1=1.5$ and $\alpha=200$ are given in Fig.28-30. Fig.28 shows the variation of $(P_2- P_1)$ with respect to r_1/R_1. The former decreases after a critical value of r_1/R_1. Fig.29 shows the distribution of the σ_{rr} along r-direction for a case $P_1/4G_0=0.0051$ and $P_2=0$ while Fig.30 shows the distribution of $\sigma_{\theta\theta}$ and $\sigma_{\phi\phi}$ along r-direction for the same case.

In this chapter, the closed form solutions for five special problems were obtained, in which the prescribed deformation field has one undetermined parameter. But for more complicated problems it can be expected that the numerical solutions are necessary. In next chapter, the numerical method with finite element technique for the boundary value problem will be formulated for both incompressible and compressible plasticity.

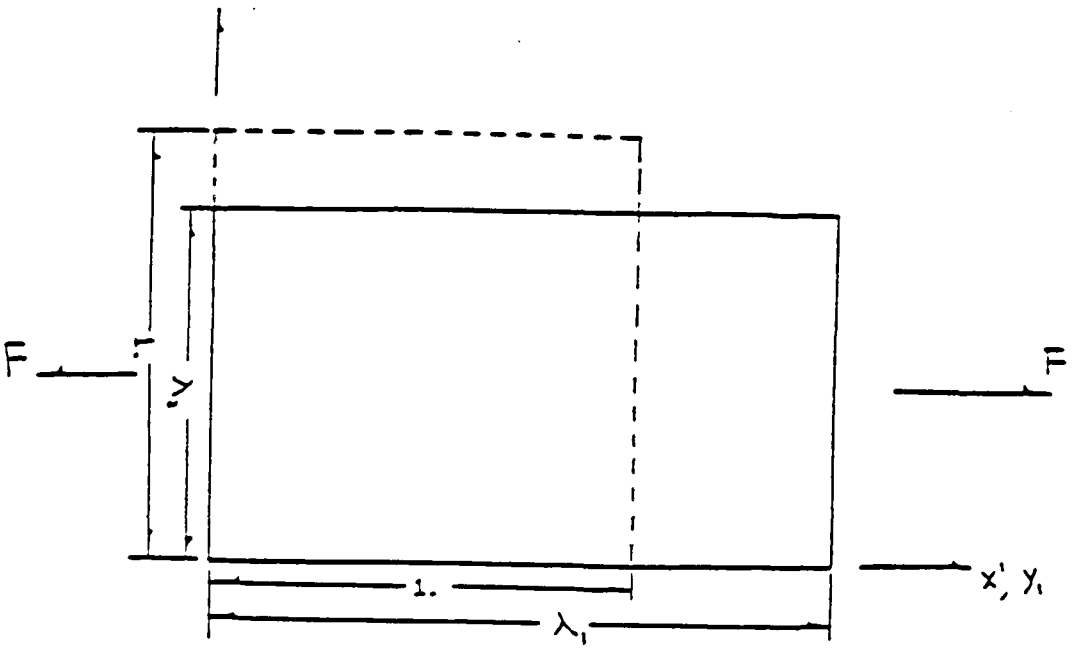

Fig.2 Uniform extension

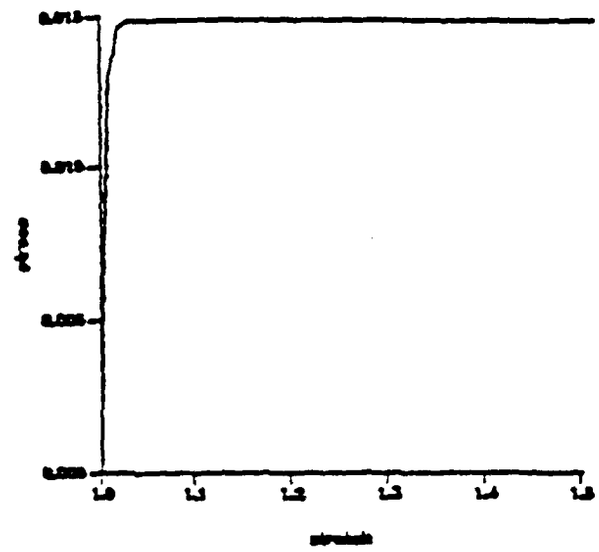

Fig.3 The variation of Stress T_{11} vs. the stretch λ_1 for α=200

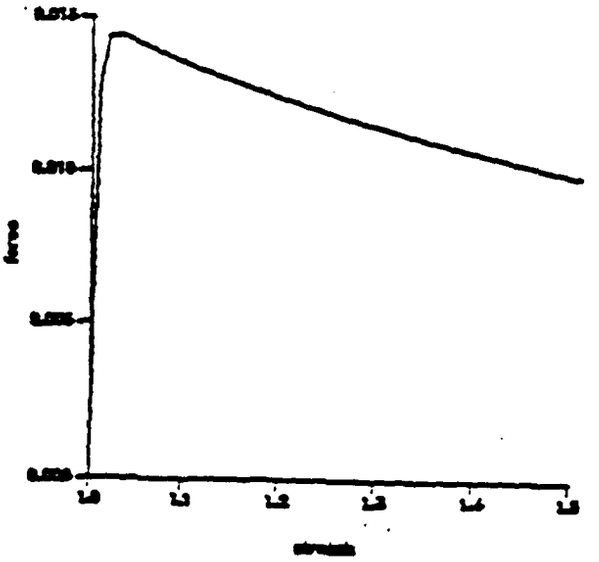

Fig.4 The variation of the resultant force F vs. the stretch λ_1 for α=200

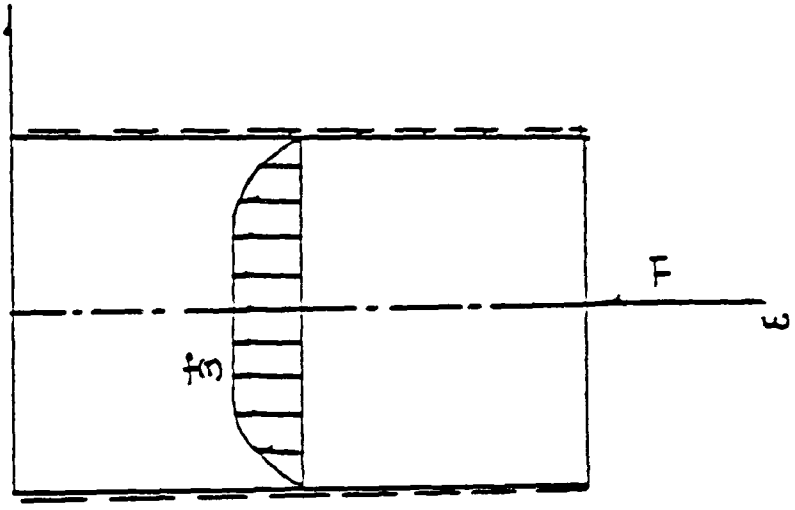

Fig.5 Pipe flow

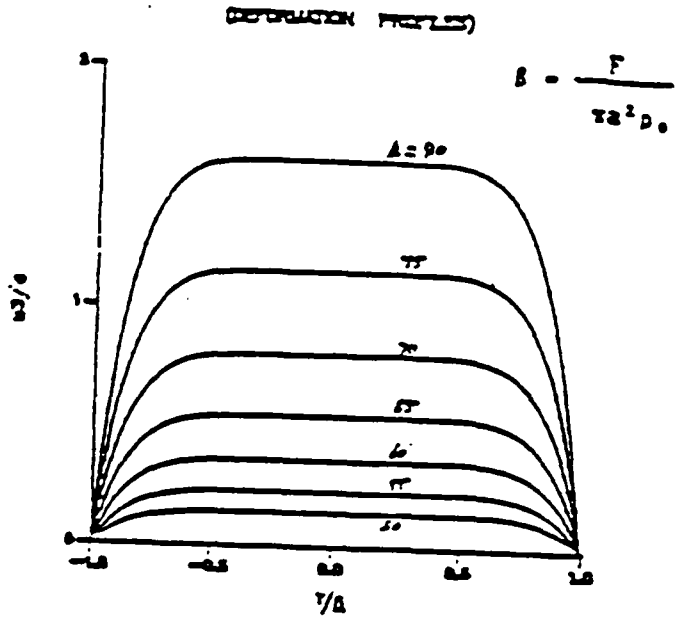

Fig.6 The deformation profile for various parameter β.

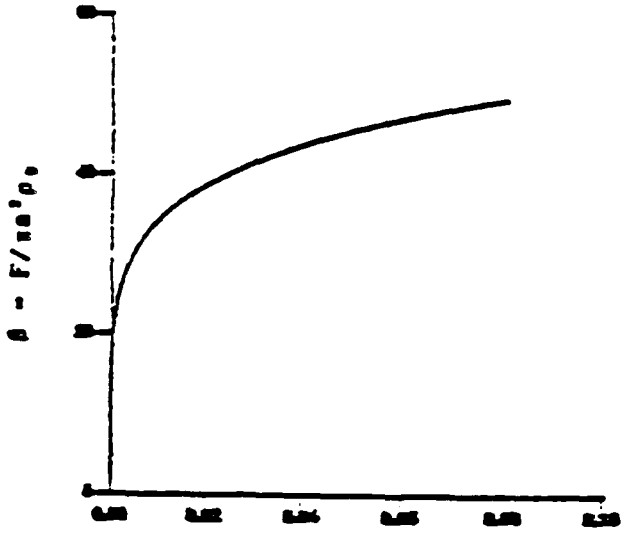

Fig.7 The relation between deformation u_3 and the the parameter β (r=0).

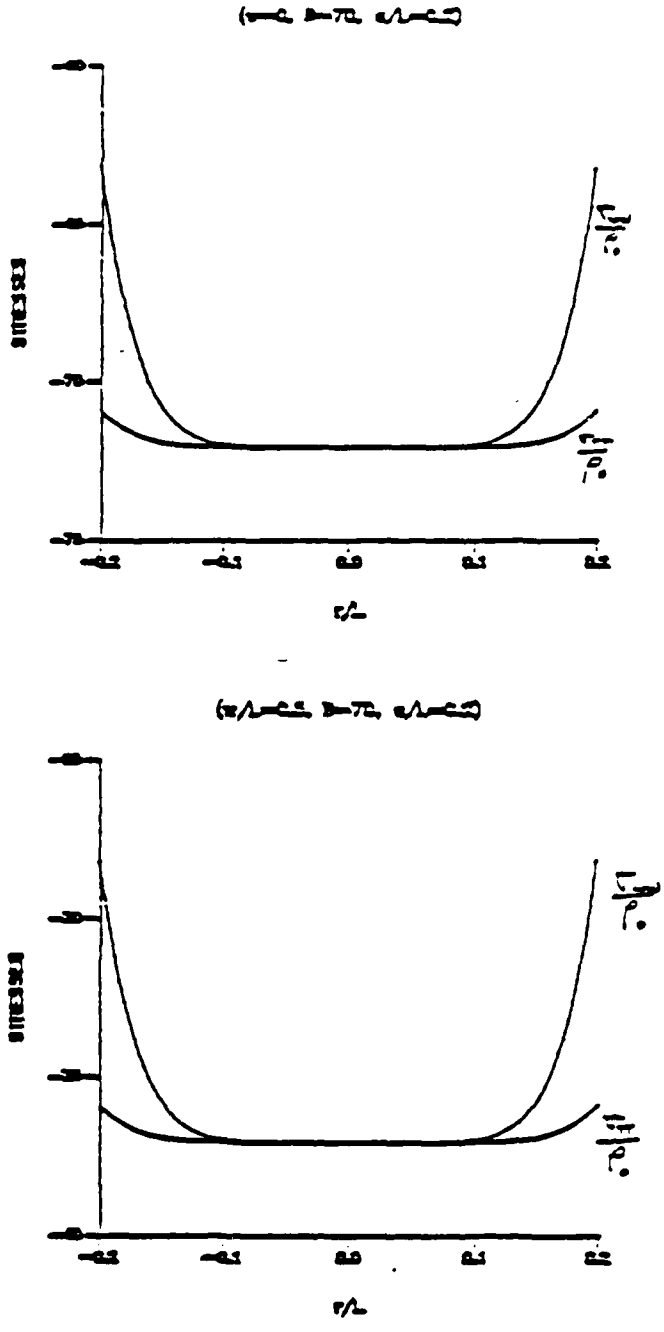

Fig.8 The distribution of σ_{rr} and σ_{ww} over the cross sections w=0, w/L=0.5.

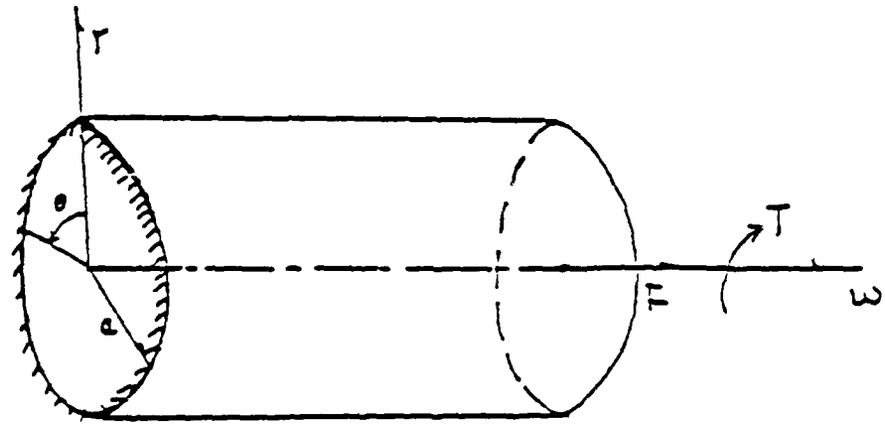

Fig.9 Torsion of a bar

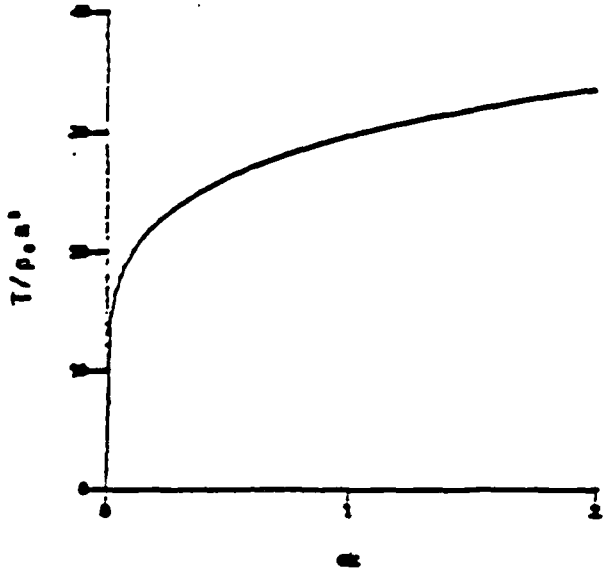

Fig.10 The relation between torque and twist.

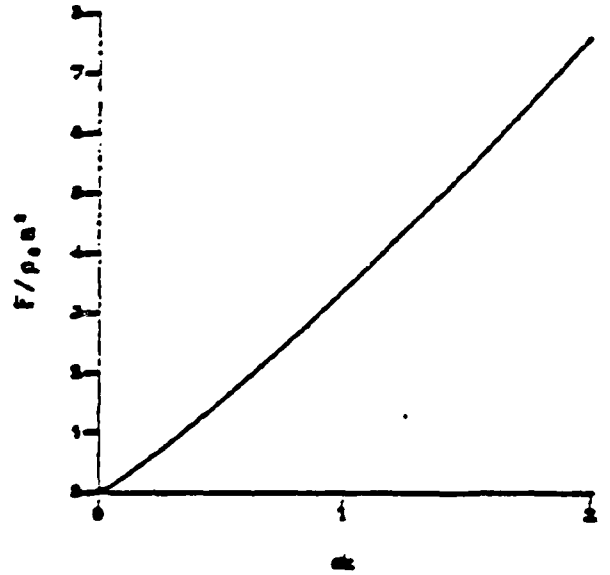

Fig.11 The relation between axial force and twist.

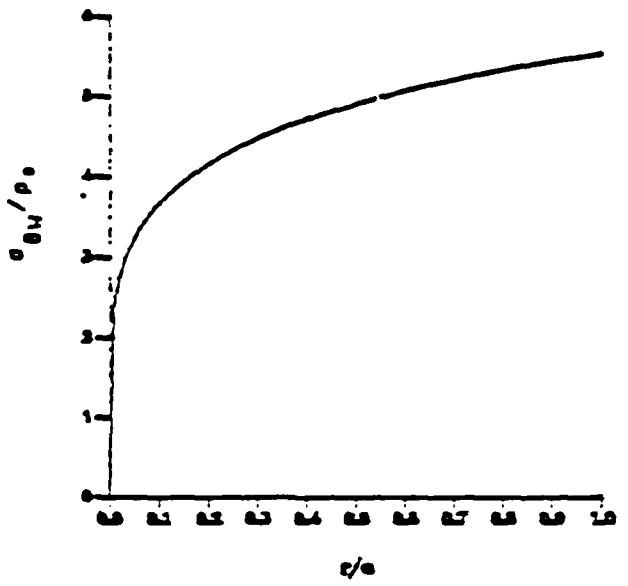

Fig.12 The distribution of $\sigma_{w\theta}$ over cross section for ak=1.

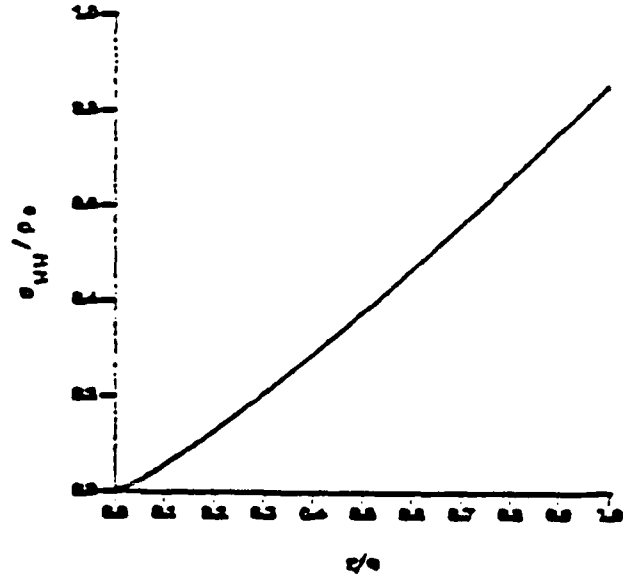

Fig.13 The distribution of σ_{ww} over cross section for ak=1.

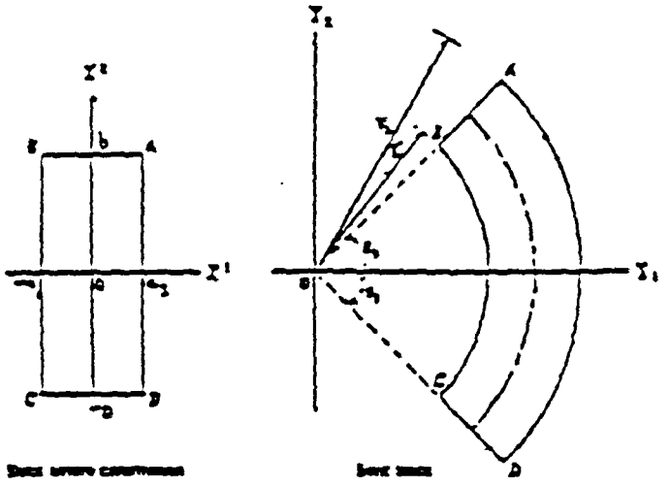

Fig.14 Bending of a block

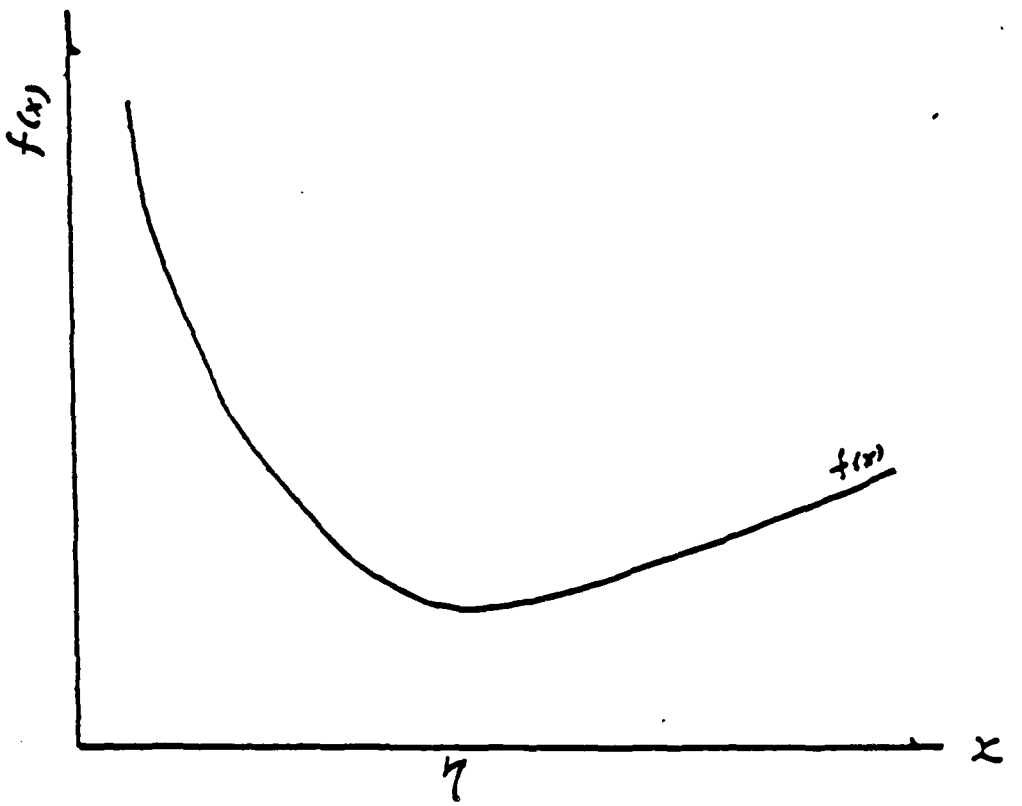

$$f(x)=2\alpha/(\alpha^2-4)\ln x-1/(\alpha-2)^2(\eta/x)^{(\alpha-2)}+1/((\alpha+2)^2(\eta/x)^{(\alpha+2)}$$

Fig.15 Typical plot of f(x)

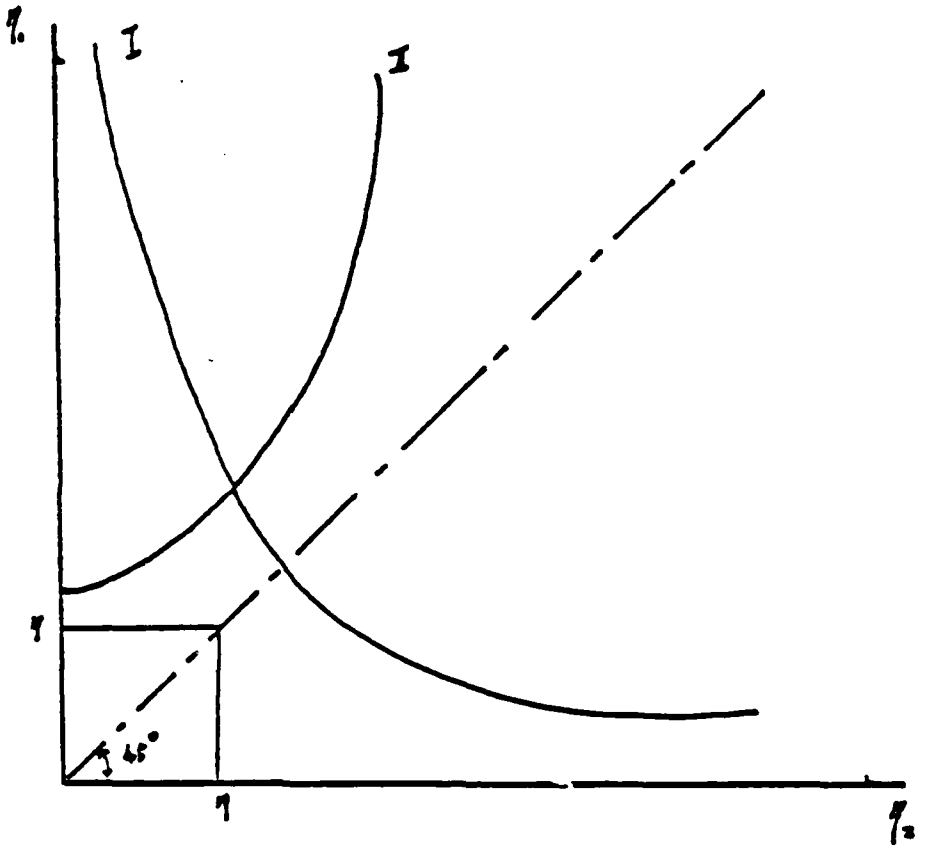

$$I=2\alpha/(\alpha^2-4)\ln(\eta_1/\eta_2)+1/(\alpha-2)^2[(\eta/\eta_1)^{(\alpha-2)}-(\eta/\eta_2)^{(\alpha-2)}]$$
$$+1/(\alpha+2)^2[(\eta/\eta_1)^{(\alpha+2)}-(\eta/\eta_2)^{(\alpha+2)}]$$

$$II=(\eta_2^2-\eta_1^2)/2$$

Fig.16 The plot of function I and II

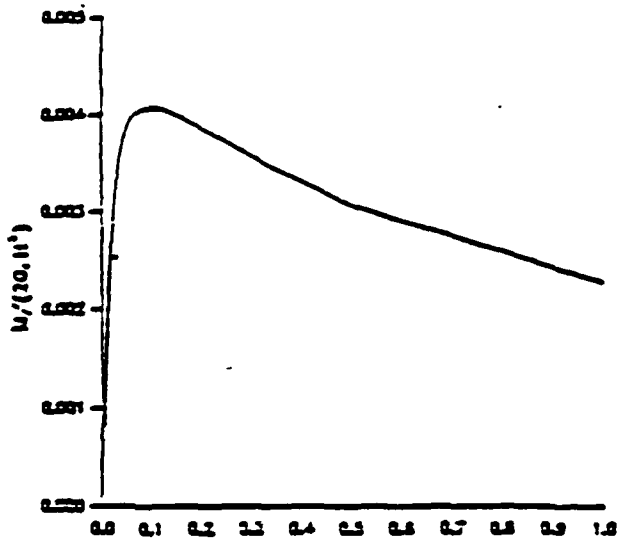

1/R

Fig.17 The variation of applied moment with the curvature for α=200

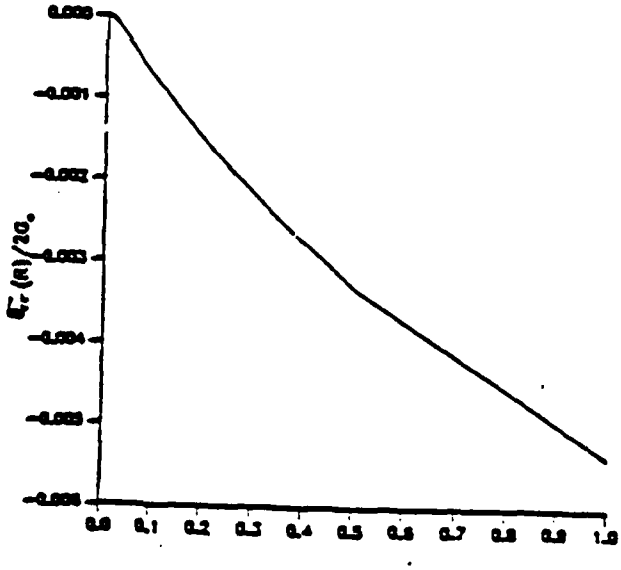

1/R

Fig.18 Stress σ_{rr} at neutral axis vs. the curvature for α=200

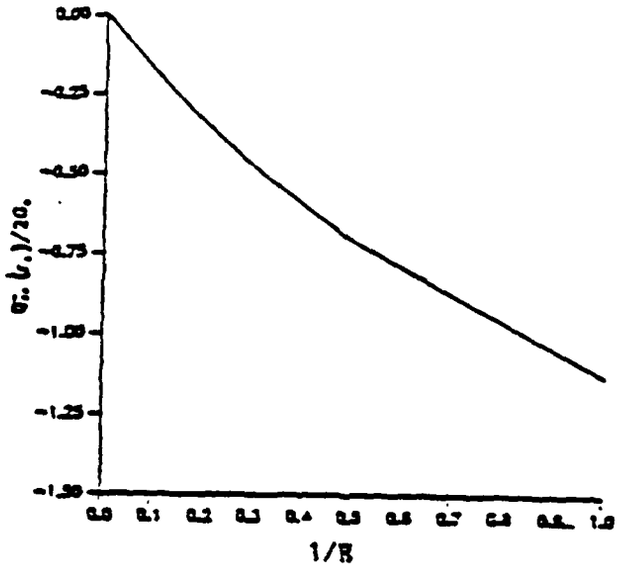

Fig.19 The variation of Stress $-\sigma_{\theta\theta}$ at $r=r_1$ for $\alpha=200$

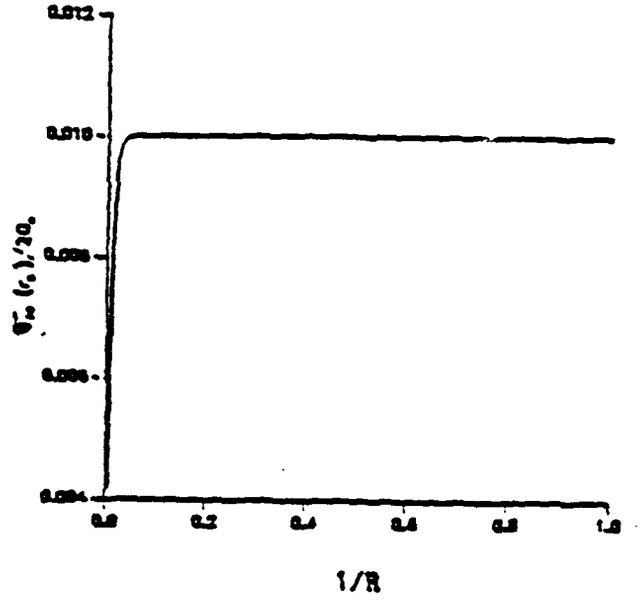

Fig.20 The variation of Stress $\sigma_{\theta\theta}$ at $r=r_2$ for $\alpha=200$

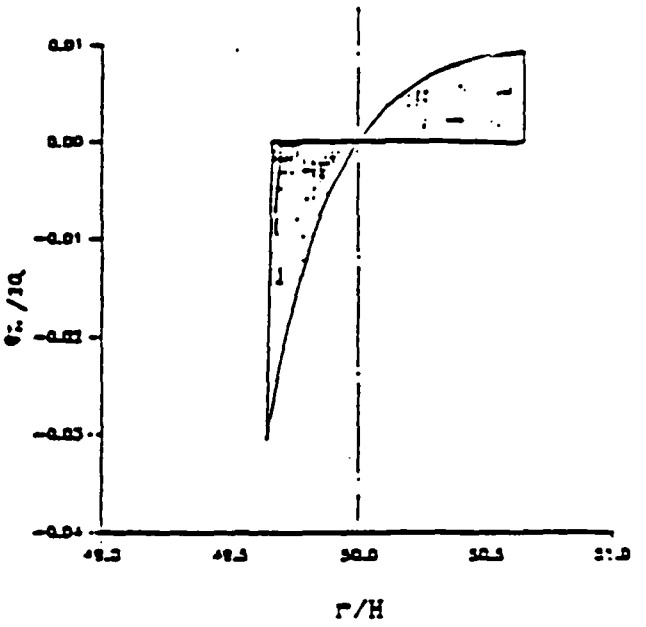

Fig.21 The distribution of $\sigma_{\theta\theta}$ over cross section for R/H=50 and α=200

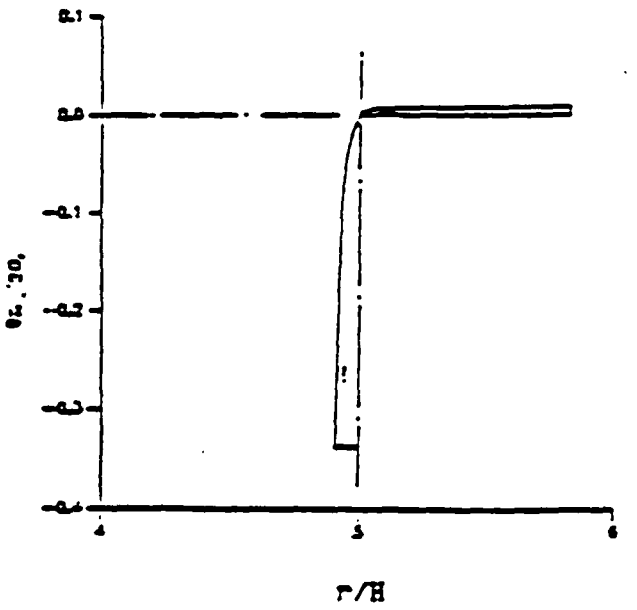

Fig.22 The distribution of $\sigma_{\theta\theta}$ over cross section for R/H=5 and α=200

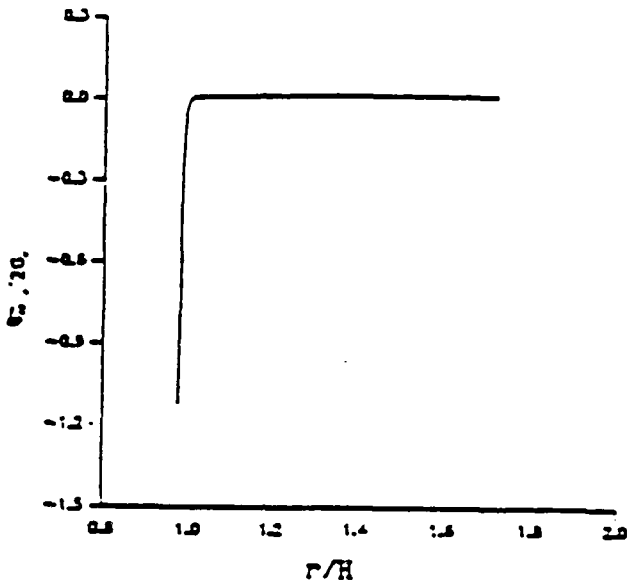

Fig.23 The distribution of $\sigma_{\theta\theta}$ over cross section for R/H=1 and α=200

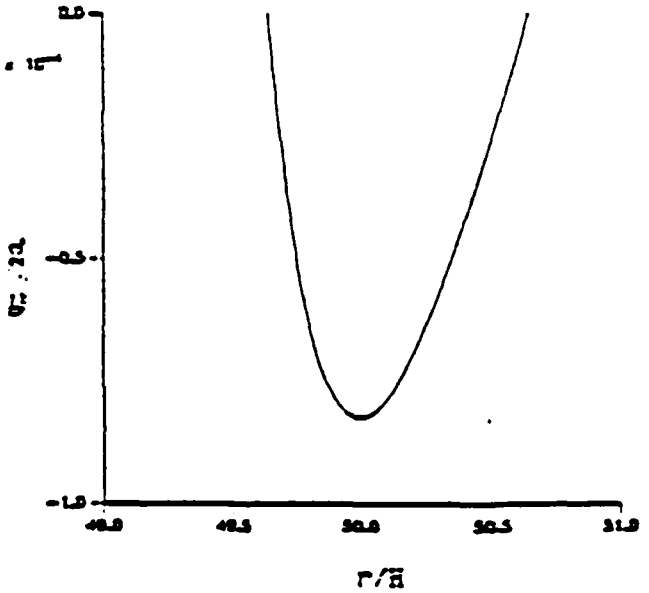

Fig.24 The distribution of σ_{rr} over cross section for R/H=50 and α=200

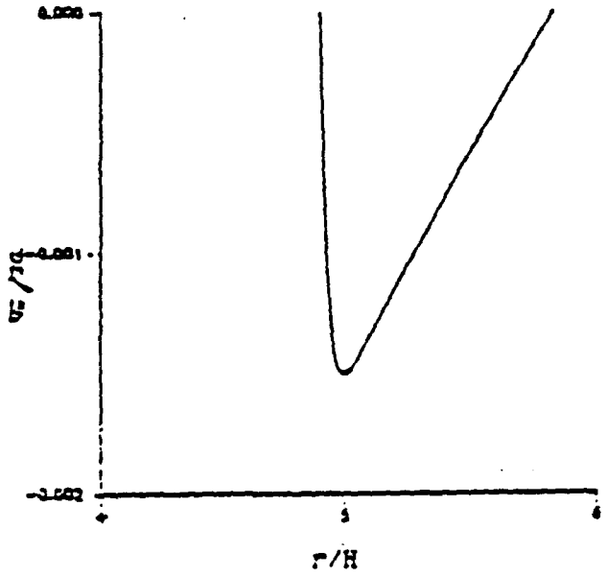

Fig.25 The distribution of σ_{rr} over cross section for R/H=5 and α=200

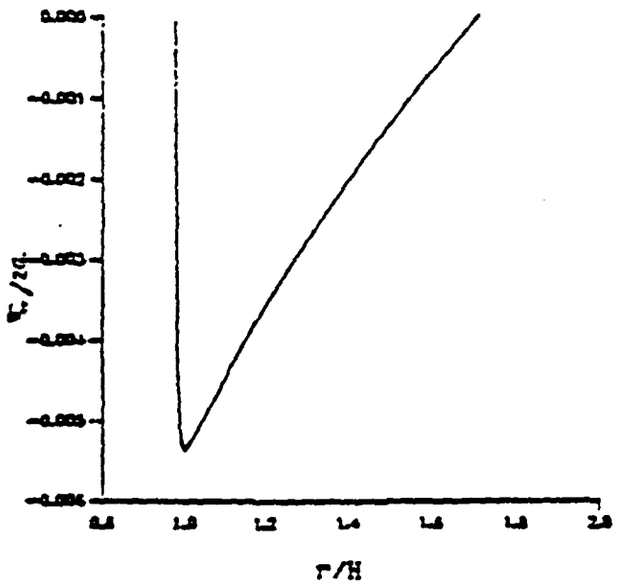

Fig.26 The distribution of σ_{rr} over cross section for R/H=1 and α=200

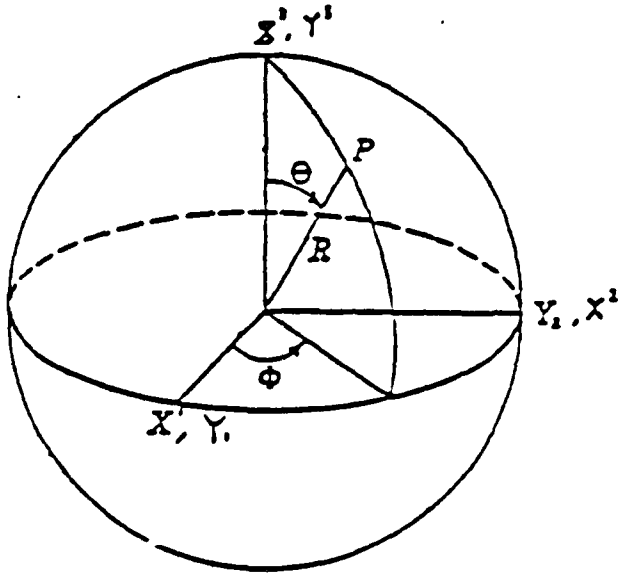

Fig.27 Expansion of a sphere

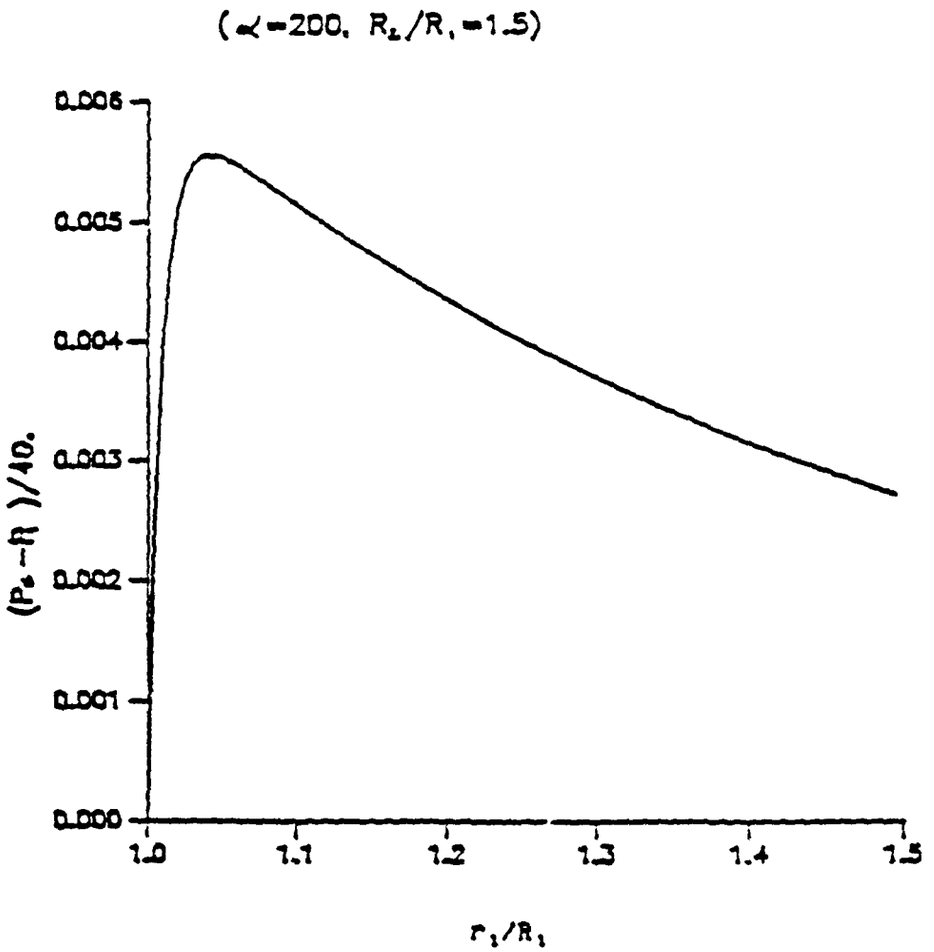

Fig.28 The variation of (P_2-P_1) with respect to r_1/R_1 .

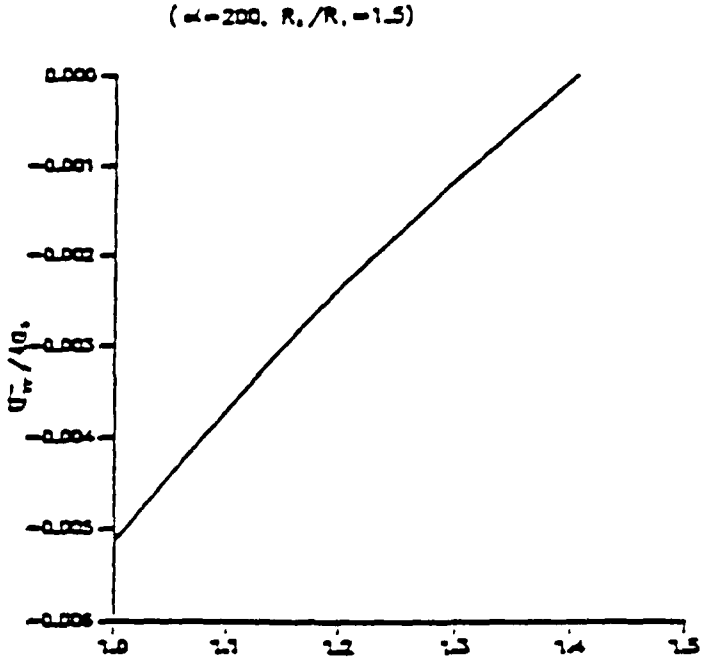

Fig.29 The distribution of the stress σ_{rr} along radial direction for $P_1/4G_0=0.0051$, $P_2=0$.

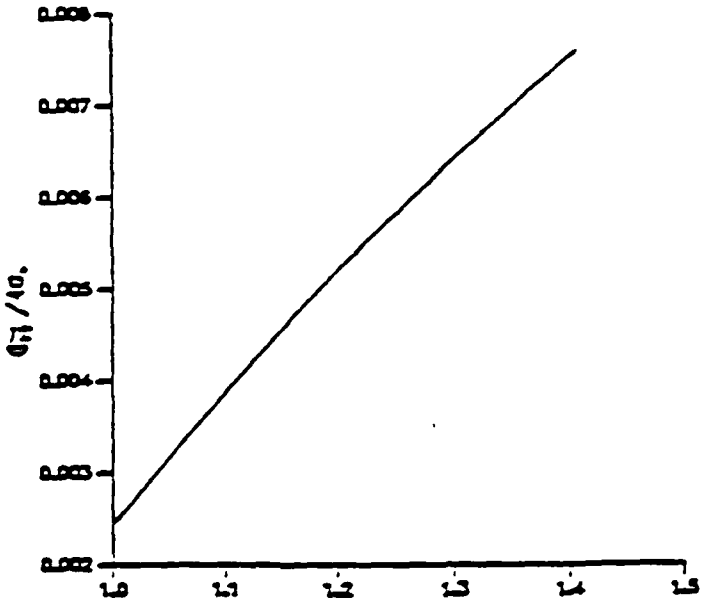

Fig.30 The distribution of the stress $\sigma_{\theta\theta}(\sigma_{\theta\theta})$ along radial direction for $P_1/4G_0=0.0051$, $P_2=0$.

CHAPTER 4 - ENDOCHRONIC CONSTITUTIVE RELATION OF COMPRESSIBLE PLASTICITY WITH FINITE DEFORMATION

The assumption of plastic incompressibility, which is pivotal in the development of the classical theory of plasticity, is an approximation and simplification to the real situation. For some rubber-like materials this assumption may be a good approximation, but it is not a universal rule. In reference [57] the assumption was evaluated through a series of simple tension tests on some very important materials such as aluminum, copper and low carbon steel. The experimental results showed that those materials are plastically compressible and that the compressibility increases with straining in the plastic region. Hence developing a theory for compressible plasticity is very important task. In this chapter, the plastic compressibility will be introduced into the endochronic constitutive equation. To do this the free energy density in the thermodynamic formulation will be first modified. Then the method used for developing the constitutive relation for incompressible plasticity in the Chapter 2 will be used to get the constitutive equation in the presence of compressible plastic deformation.

4.1 Development of the Constitutive Equation

In chapter 2 a constant term Ψ_0 in the free energy form was assumed. It is noticed that this assumption led to the constitutive equation of

incompressible plasticity. Now the constant term is replaced by a function of I_3, the third invariant of the Cauchy-Green deformation tensor. Hence, the free energy density becomes

$$\Psi = \Psi_o(I_3) + A^{(r)} q_{ii}^{(r)} + 1/2 C^{(r)} q_{ij}^{(r)} q_{ij}^{(r)} \quad . \qquad (4.1.1)$$

Along the line of the development of the constitutive relation for the incompressible material, it can be seen that with this modification to the free energy density the covariant components of q_r in the material frame remain of the form

$$q_{\alpha\beta}^{(r)} = -\frac{A^{(r)}}{C^{(r)}} C_{\alpha\beta} + \frac{A^{(r)}}{C^{(r)}} \int_0^z e^{-\alpha_r (z-z')} \hat{C}_{\alpha\beta}(z')\, dz' \quad , \qquad (4.1.2)$$

where $\alpha_r = \frac{C^{(r)}}{b^{(r)}}$.

For the constitutive relation now the contravariant components of the stress, upon use of eq.(2.1.8) in conjunction with eq.(4.1.1), are

$$T^{\alpha\beta} = \frac{\rho}{\rho_o} [2I_3 \frac{\partial \Psi_o}{\partial I_3} C^{\alpha\beta} - 2(A^{(r)} q_{(r)}^{\alpha\beta} + C^{(r)} q^{(r)\alpha}_{\beta'} q^{(r)\beta'}_{\beta})] \qquad (4.1.3)$$

or the covariant components of the stress

$$T_{\alpha\beta} = \frac{\rho}{\rho_o} [2I_3 \frac{\partial \Psi_o}{\partial I_3} C_{\alpha\beta} - 2(A^{(r)} q_{\alpha\beta}^{(r)} + C^{(r)} q_{\alpha\beta'}^{(r)} q^{(r)\beta'}_{\beta})] \quad . \qquad (4.1.4)$$

Substitution q.(4.1.2) into eq.(4.1.4) gives the following relation for the covariant components of the stress

$$T_{\alpha\beta} = \frac{\rho}{\rho_o}\left[2I_3 \frac{\partial \Psi_o}{\partial I_3} C_{\alpha\beta} + \int_0^z G(z-z')\hat{C}_{\alpha\beta}(z')\, dz' - \right.$$

$$\left. -C^{\mu\nu}\int_0^z\int_0^z G(2z-z_1-z_2)\frac{dC_{\alpha\mu}}{dz_1}\frac{dC_{\beta\nu}}{dz_2}\, dz_1 dz_2\right] \quad . \qquad (4.1.5)$$

Once again ignore the small quantity of the double integral in eq.(4.1.5) and get the constitutive equation as

$$T_{\alpha\beta} = \frac{\rho}{\rho_o}\left[2I_3 \frac{\partial \Psi_o}{\partial I_3} C_{\alpha\beta} + \int_0^z G(z-z')\hat{C}_{\alpha\beta}(z')\, dz'\right] \quad . \qquad (4.1.6)$$

In the matrix form

$$[T] = \frac{\rho}{\rho_o}\left\{2I_3 \frac{\partial \Psi_o}{\partial I_3}[C] + \int_0^z G(z-z')[\hat{C}(z')]\, dz'\right\} \qquad (4.1.6a)$$

with

$$G(z) = 2\sum_r \frac{A^{(r)}}{C^{(r)}} e^{-\alpha_r z} \qquad (4.1.6b)$$

When the condition of incompressibility is imposed, $|C_{\alpha\beta}|=1$, the term $\partial\Psi_o/\partial I_3$ is indefinite. If the term is set to be -P (the factor $2I_3$ is also absorbed), eq.(2.1.25) is again derived, which is the constitutive relation for incompressible plasticity,

$$T_{\alpha\beta} = -P\, C_{\alpha\beta} + \int_0^z G(z-z')\hat{C}_{\alpha\beta}(z')\, dz' \quad . \qquad (2.1.25)$$

For intrinsic time scale, d_{ii} is no longer vanishing under a compressible plastic deformation, thus

$$\left(\frac{d\zeta}{dt}\right)^2 = p_1 d_{ii} d_{jj} + p_2 d_{ij} d_{ij} \quad . \qquad (2.1.15)$$

Eq.(2.1.15), after using eq.(2.2.16), becomes

$$\left(\frac{d\zeta}{dt}\right)^2 = p_1/4\,(C^{-1}_{\alpha\beta}\,\dot{C}_{\alpha\beta})^2 + p_2/4\,C^{-1}_{\gamma\alpha}\,\dot{C}_{\alpha\beta}\,C^{-1}_{\beta\eta}\,\dot{C}_{\eta\gamma} \qquad (4.1.7)$$

or

$$d\zeta^2 = p_1/4\,(C^{-1}_{\alpha\beta}\,dC_{\alpha\beta})^2 + p_2/4\,C^{-1}_{\gamma\alpha}\,dC_{\alpha\beta}\,C^{-1}_{\beta\eta}\,dC_{\eta\gamma} \quad . \qquad (4.1.8)$$

In matrix form

$$d\zeta^2 = p_1/4\,\{tr[B]\}^2 + p_2/4tr[D] \quad , \qquad (4.1.9)$$

where

$$[D] = [C]^{-1}d[C][C]^{-1}d[C] \qquad (4.1.9a)$$

and

$$[B] = [C]^{-1}d[C] \qquad (4.1.9b)$$

An intrinsic time scale z is still defined to account for the hardening or softening character of a material,

$$z = \int_0^{\zeta} \frac{d\zeta'}{f(\zeta')} \qquad (4.1.10)$$

where $f(\zeta)$ is a positive function of ζ. If no hardening (softening) takes place $f(\zeta)=1$.

In the curvilinear system as described in section 2 of Chapter 2, the curvilinear components of the Cauchy-Green deformation tensor were given by

$$\tilde{C}_{\mu\nu} = g_{kl}\,\frac{\partial\theta_k}{\partial\phi^{\mu}}\,\frac{\partial\theta_l}{\partial\phi^{\nu}} \qquad (2.2.8)$$

and the curvilinear components of stress $T_{\alpha\beta}$ by

$$\tau_{\mu\nu} = T_{\alpha\beta}\,\frac{\partial\phi^{\alpha}}{\partial X^{\mu}}\,\frac{\partial\phi^{\beta}}{\partial X^{\nu}} \quad . \qquad (2.2.23)$$

Upon use of eq.(2.2.8) an alternative form of the intrinsic time can be derived,

$$(d\zeta)^2 = p_1/4 \, (\bar{C}^{-1}_{\alpha\beta} \, d\bar{C}_{\alpha\beta})^2 + P_2 /4 \, \bar{C}^{-1}_{\gamma\alpha} \, d\bar{C}_{\alpha\beta} \, \bar{C}^{-1}_{\beta\eta} \, d\bar{C}_{\eta\gamma} \qquad (4.1.11)$$

or, in matrix form,

$$(d\zeta)^2 = p_1/4 \, \{tr[\bar{B}]\}^2 + p_2/4 \, tr[\bar{D}] \qquad (4.1.12)$$

where

$$[\bar{D}] = [\bar{C}]^{-1} d[\bar{C}] \, [\bar{C}]^{-1} d[\bar{C}] \qquad (4.1.12a)$$

and

$$[\bar{B}] = [\bar{C}]^{-1} d[\bar{C}] \qquad (4.1.12b)$$

The constitutive eq.(4.1.6), by use of eq.(2.2.23), becomes

$$\tau_{\mu\nu} = \frac{\rho}{\rho_o} [2I_3 \frac{\partial \Psi_o}{\partial I_3} \bar{C}_{\mu\nu} + \int_0^z G(z-z') \hat{\bar{C}}_{\mu\nu}(z') \, dz'] \qquad (4.1.13)$$

or

$$[\tau] = \frac{\rho}{\rho_o} \{2I_3 \frac{\partial \Psi_o}{\partial I_3} [\bar{C}] + \int_0^z G(z-z') [\hat{\bar{C}}(z')] \, dz'\} \quad . \qquad (4.1.13a)$$

4.2 Discussion of the Function Ψ_o

In last section the function Ψ_o appears as a functional form in the constitutive equation. How to choose the function so that it can describe the compressible behavior of a material well needs much effort. In this paper a particular form of Ψ_o given by eq.(4.2.1) is taken to demonstrate the application of the constitutive equation:

$$\Psi_o = (\lambda/8)[\ln(I_3)]^2 \quad , \qquad (4.2.1)$$

where λ is a material constant.

It is now shown that the constitutive equation with the assumed Ψ_0 is consistent with elasticity theory under infinitesimal deformation. Substituting eq.(4.2.1) into the constitutive equation (4.1.6),

$$T_{\alpha\beta} = \rho/\rho_0\{\lambda \ln(J) C_{\alpha\beta} + \int_0^z G(z-z')\hat{C}_{\alpha\beta}(z')dz'\} \qquad (4.2.2)$$

where J is the Jacobian defined as

$$J = I_3^{1/2} = |\partial Y_i/\partial X^\alpha| \quad . \qquad (4.2.3)$$

When a deformation is very small, $\rho/\rho_0 = 1$, $C_{\alpha\beta} = \delta_{\alpha\beta}$, and without lose any generality

$$J = \lambda_1\lambda_2\lambda_3 = (1+\varepsilon_{11})(1+\varepsilon_{22})(1+\varepsilon_{33})$$

$$= 1+(\varepsilon_{11}+\varepsilon_{22}+\varepsilon_{33})+O(\varepsilon^2) \approx 1+\varepsilon_{ii} \quad , \qquad (4.2.4)$$

where λ_i and ε_{ii} (i=1,2,3) are principal values of the deformation gradient matrix and the strain tensor, respectively. Hence,

$$\ln(J) \approx \ln(1+\varepsilon_{ii}) \approx \varepsilon_{ii}+O(\varepsilon_{ii}^2) \approx \varepsilon_{ii} \quad . \qquad (4.2.5)$$

Eq.(4.2.5) represents the dilation of a material for infinitesimal deformation. With the help of eq.(4.2.5), the Hooke's law is got,

$$T_{\alpha\beta} = \lambda\varepsilon_{ii}\delta_{\alpha\beta} + 2G(0)\varepsilon_{\alpha\beta} \qquad (4.2.6)$$

where λ is a Lame constant and G(0) the shear modulus.

In next chapter the constitutive relation given in eq.(4.2.2) will be used to analyze the problems by means of the finite element technique.

CHAPTER 5 - NUMERICAL SOLUTION

A numerical algorithm based on the finite element method of analysis of the boundary value problem is developed in this chapter. The formulation of the finite element equations is referred to the material system, namely, the Lagrangian formulation. The finite element formulations for both compressible and incompressible material are developed. A computer code is established to solve a plane strain boundary value problem under a compressible-plastic deformation by use of the linear triangular element. Finally, the solutions of upsetting of a block (a forging process) are presented.

5.1 Fundamental Equation (the Principle of Virtual Work)

Equations of equilibrium, when body forces are absent, in rectangular coordinates of a material system can be shown to be

$$(JT^{\alpha}_{i})_{,\alpha} = 0 \qquad (5.1.1)$$

where (JT^{α}_{i}) is the stress per unit undeformed area. The mixed stress T^{α}_{i}, which is the projection of the force T^{α} along i-direction in spatial system, is defined as

$$T^{\alpha}_{i} = \sigma_{ij}\, x^{\alpha}_{j} \quad , \quad \sigma_{ij} = T^{\alpha}_{i} y_{j,\alpha} \qquad (5.1.2)$$

where $x^{\alpha}_{j} = \partial x^{\alpha}/\partial y_{j}$, σ_{ij} is the Cauchy stress, $(\ )_{,\alpha}$ represents $\partial(\ )/\partial x^{\alpha}$.

After defining U to be the displacement and u_i the components of the displacement and δu_i the components of the virtual displacement, Multiplication of δu_i to the equilibrium equation (5.1.1) and then integration of the resultant equation over the undeformed volume give the following

$$\int_{V_o} (JT^{\alpha}_{\ i})_{,\alpha}\, \delta u_i dV_o = 0 \quad . \qquad (5.1.3)$$

The application of Green's theorem to (5.1.3) yields the equation of the principle of virtual work under large deformation as

$$\int_{V_o} (JT^{\alpha}_{\ i}) \delta u_{i,\alpha} dV_o = \int_{S_o} (JT^{\alpha}_{\ i}) u_i d\bar{S}_o \quad , \qquad (5.1.4)$$

where the surface integration of the right side of (5.1.4) is over the undeformed surface. Equation (5.1.4) will be the basis of the finite element formulation.

5.2 Incremental Form of the Endochronic Constitutive Equation

In Chapter 4 the endochronic constitutive equation for compressible material was derived as

$$JT_{\alpha\beta} = \lambda \log(J) C_{\alpha\beta} + \int_0^z G(z-z') \hat{C}_{\alpha\beta}(z')\, dz' \quad . \qquad (4.2.4)$$

The incremental form, with respect to the intrinsic time scale, can be obtained from the intrinsic time derivative of (4.2.4) as

$$d(JT_{\alpha\beta})/dz = (\lambda/J) \dot{J} C_{\alpha\beta} + \bar{G}\, \hat{C}_{\alpha\beta} + dQ_{\alpha\beta} \qquad (5.2.1)$$

or

$$d(JT_{\alpha\beta}) = (\lambda/J)\, dJ\, C_{\alpha\beta} + \bar{G}\, dC_{\alpha\beta} + dQ_{\alpha\beta}dz \quad , \qquad (5.2.2)$$

where

$$\bar{G} = \lambda \log(J) + G(0)$$

and

$$dQ_{\alpha\beta} = \int_0^z \frac{dG(z-z')}{dz} \frac{dC_{\alpha\beta}}{dz'}\, dz' \quad . \qquad (5.2.3)$$

For an incompressible material,

$$d(JT_{\alpha\beta}) = -(dP)C_{\alpha\beta} + \bar{G}\,(dC_{\alpha\beta}) + dQ_{\alpha\beta}dz \qquad (5.2.4)$$

where $\bar{G} = G(0) - P$ and $dQ_{\alpha\beta}$ remains the same as in (5.2.3).

5.3 Formulation of the Finite Element Equations

The finite element approximation is developed from a displacement assumption within each element, which gives the displacements at any point within the element as a linear combination of the displacements at a finite number of nodes of the element, the coefficients being constants or functions of the position within the element. In this section we adopt such a displacement assumption in general form using material coordinates, i.e., a Lagrangian formulation.

Assuming the displacement within any element in the form

$$u_i = \phi_i^m(x^\alpha, \underline{x}^\alpha) q_m \quad , \qquad (5.3.1)$$

where q_m denotes the nodal displacements; ϕ is the transformation function which gives the displacements at any point within the element; $\underline{x}^{\alpha}$ are the nodal coordinates.

The following equations are some derived geometric relations which will be used in the finite element formulation.

(1) The derivative of u_i with respect to x^{α}

$$u_{i,\alpha} = \phi^{m}_{i\alpha}\, q_m \quad , \tag{5.3.2}$$

where $\phi^{m}_{i\alpha} = \partial(\phi^{m}_{i})/\partial x^{\alpha}$.

(2) The increment of u_i with respect to intrinsic time scale, since ϕ^{m}_{i} is a function of the material system,

$$\frac{du_i}{dz} = \phi^{m}_{i}\,\frac{dq_m}{dz} \qquad \text{or} \qquad du_i = \phi^{m}_{i}\, dq_m \quad . \tag{5.3.3}$$

(3) The corresponding spatial coordinates within the element

$$y_k = x^{k} + u_k \quad . \tag{5.3.4}$$

Hence

$$dy_k = du_k = \phi^{m}_{k}\, dq_m \quad , \tag{5.3.5}$$

$$y_{k,\alpha} = \delta_{k\alpha} + u_{k,\alpha} = \delta_{k\alpha} + \phi^{m}_{k\alpha}\, q_m \tag{5.3.6}$$

and

$$dy_{k,\alpha} = \phi^{m}_{k\alpha}\, dq_m \tag{5.3.7}$$

(4) Since we have the relation

$$y_{k,\alpha}\, x^{\alpha}_{j} = \delta_{kj} \tag{5.3.8}$$

then

$$x^{\alpha}_{j} = [y_{j,\alpha}]^{-1} \quad . \tag{5.3.9}$$

(5) A differentiation of both sides of eq.(5.3.8) gives

$$d(y_{k,\alpha})x^{\alpha}_{j} + y_{k,\alpha}\, d(x^{\alpha}_{j}) = 0 \quad . \tag{5.3.10}$$

Then what follows is

$$dx^{\alpha}_{k} = - x^{\alpha}_{i}\, x^{\beta}_{k}\, dy_{i,\beta} = - x^{\alpha}_{i}\, x^{\beta}_{k}\, \phi^{m}_{i\beta} dq_{m} = - x^{\alpha}_{i}\, \psi^{m}_{ik} dq_{m} \quad , \tag{5.3.11}$$

where

$$x^{\beta}_{k}\, \phi^{m}_{i\beta} = \psi^{m}_{ik} \quad \text{(defined)} \quad . \tag{5.3.12}$$

(6) The Cauchy-Green deformation tensor and its incremental form are

$$C_{\alpha\beta} = y_{k,\alpha}\, y_{k,\beta}$$

and

$$dC_{\alpha\beta} = (\phi^{m}_{k\alpha} y_{k,\beta} + \phi^{m}_{k\beta} y_{k,\alpha}) dq_{m} = 2\psi^{m}_{(ik)} y_{k,\alpha} y_{i,\beta} dq_{m} \quad , \tag{5.3.13}$$

where

$$\psi^{m}_{(ik)} = 1/2(\psi^{m}_{ik} + \psi^{m}_{ki}) \quad \text{(defined)} \quad . \tag{5.3.14}$$

(7) The Jacobian and its incremental form are

$$J = |y_{i,\alpha}|$$

and

$$dJ = Jx_i^{\alpha}\,\phi_{i\alpha}^{m}dq_m = J\psi_{ii}^{m}dq_m \quad . \tag{5.3.15}$$

Having the assumed displacement, we get the equilibrium equation for an element by direct substitution of (5.3.1) and (5.3.2) into the equation of the principle of virtual work (5.1.4)

$$\int_{V_o}(JT^{\alpha}{}_i)\phi_{i\alpha}^{m}\delta q_m dV_o = \int_{S_o}(JT^{\alpha}{}_i)\phi_i^{m}\delta q_m n_{\alpha}dS_o \tag{5.3.16}$$

Since the virtual displacement δq_m (m=1,2.....) are independent of each other, the following m equations are obtained

$$\int_{V_o}(JT^{\alpha}{}_i)\phi_{i\alpha}^{m}dV_o = f_m \quad , \tag{5.3.17}$$

where

$$f_m = \int_{S_o}(JT^{\alpha}{}_i)\phi_i^{m}n_{\alpha}dS_o \quad . \tag{5.3.18}$$

The incremental form of (5.3.17) can be written as

$$\int_{V_o} d(JT^{\alpha}{}_i)\,\phi_{i\alpha}^{m}dV_o = d(f_m)_{ex} \tag{5.3.19}$$

wnere

$$d(f_m)_{ex} = \int_{S_o} d(JT^{\alpha}{}_i)\,\phi_i^{m}n_{\alpha}dS_o \quad . \tag{5.3.20}$$

From the tensor transformation

$$\sigma_{ki} = x_k^{\alpha}\,x_i^{\beta}\,T_{\alpha\beta} \tag{5.3.21}$$

and

$$T^{\alpha}_{\ i} = x^{\alpha}_{k}\, x^{\gamma}_{k}\, x^{\beta}_{i}\, T_{\gamma\beta} \qquad (5.3.22)$$

then

$$d(JT^{\alpha}_{\ i}) = d(x^{\alpha}_{k}\, x^{\gamma}_{k}\, x^{\beta}_{i}\, JT_{\gamma\beta}) \quad . \qquad (5.3.23)$$

Applying the chain rule of differentiation to (5.3.23) and having recourse to (5.3.11) and (5.3.21), it is obtained

$$\begin{aligned} d(JT^{\alpha}_{\ i}) &= d(x^{\alpha}_{k})\, x^{\gamma}_{k}\, x^{\beta}_{i}\, JT_{\gamma\beta} + x^{\alpha}_{k}\, d(x^{\gamma}_{k})\, x^{\beta}_{i}\, JT_{\gamma\beta} \\ &\quad + x^{\alpha}_{k}\, x^{\gamma}_{k}\, d(x^{\beta}_{i})\, JT_{\gamma\beta} + x^{\alpha}_{k}\, x^{\gamma}_{k}\, x^{\beta}_{i}\, d(JT_{\gamma\beta}) \\ &= -[x^{\alpha}_{s}\psi^{m}_{sk}(J\sigma_{ki}) + x^{\alpha}_{k}\psi^{m}_{sk}(J\sigma_{si}) + x^{\alpha}_{k}\psi^{m}_{si}(J\sigma_{ks})]dq_{m} + x^{\alpha}_{k}\, x^{\gamma}_{k}\, x^{\beta}_{i}\, d(JT_{\gamma\beta}) \\ &= -x^{\alpha}_{k}\,\{2\psi^{m}_{(ks)}(J\sigma_{si}) + \psi^{m}_{si}(J\sigma_{ks})\}dq_{m} + x^{\alpha}_{k}\, x^{\gamma}_{k}\, x^{\beta}_{i}\, d(JT_{\gamma\beta}) \quad . \qquad (5.3.24) \end{aligned}$$

Substitution of eq.(5.2.2) into the last term in eq.(5.3.24) and then eq.(5.3.12) into the resultant equation gives

$$\begin{aligned} x^{\alpha}_{k}\, x^{\gamma}_{k}\, x^{\beta}_{i}\, d(JT_{\gamma\beta}) &= x^{\alpha}_{k}\, x^{\gamma}_{k}\, x^{\beta}_{i}\, [(\lambda/J)(dJ)C_{\gamma\beta} + \bar{G}d(C_{\gamma\beta}) + dQ_{\gamma\beta}dz] \\ &= x^{\alpha}_{k}\,\{[\lambda\psi^{m}_{nn}\delta_{ki} + 2\bar{G}\psi^{m}_{(ik)}]dq_{m} + dQ_{ki}dz\} \quad , \qquad (5.3.25) \end{aligned}$$

where

$$dQ_{ki} = x^{\gamma}_{k}\, x^{\beta}_{i}\, dQ_{\gamma\beta} \quad . \qquad (5.3.26)$$

Substitution of (5.3.25) back into (5.3.24) yields

$$d(JT^{\alpha}_{\ i}) = x^{\alpha}_{k}\{[\lambda\psi^{m}_{nn}\delta_{ki} + 2\bar{G}\psi^{m}_{(ik)} - 2\psi^{m}_{(ks)}(J\sigma_{si}) - \psi^{m}_{si}(J\sigma_{ks})]dq_{m} + dQ_{ki}dz\} \quad . \qquad (5.3.27)$$

Finally, (5.3.19) in conjunction with (5.3.27) results in the following, a set of j linear equations in dq_m ,

$$\int_{V_o}[\lambda\psi^m_{nn}\psi^j_{kk}+ 2\bar{G}\psi^m_{(ik)}\psi^j_{ik}-2\psi^m_{(ks)}\psi^j_{ik}(J\sigma_{si})-\psi^m_{si}\psi^j_{ik}(J\sigma_{ks})]dV_o\ dq_m$$

$$= d(f_j)_{ex}- \int_{V_o}\psi^j_{ik}dQ_{ki}dzdV_o \quad . \qquad (5.3.28)$$

Alternatively, (5.3.28) can be written in matrix form as

$$[k_{jm}]\ dq_m = d(f_j)_{ex} + d(f_j)_p = d(f_j^{(t)}) \quad , \qquad (5.3.29)$$

where the element stiffness matrix k_{jm} is

$$k_{jm}= \int_{V_o}[\lambda\psi^m_{nn}\psi^j_{kk}+ 2\bar{G}\psi^m_{(ik)}\psi^j_{ik}-2\psi^m_{(ks)}\psi^j_{ik}(J\sigma_{si})-\psi^m_{si}\psi^j_{ik}(J\sigma_{ks})]dV_o$$

and the incremental pseudo-force vector

$$d(f_j)_p = - \int_{V_o}\psi^j_{ik}dQ_{ki}dzdV_o \quad , \qquad (5.3.30)$$

where the integration is performed over the undeformed area of an element.

Considering the equilibrium of the entire structure, we obtain the structure stiffness matrix in the form

$$[K]\ \{dq\} = \{dF\} \qquad (5.3.31)$$

where [K] is global stiffness matrix, {dq} the total incremental nodal displacements, {dF} the total incremental nodal force which consists of applied force and the incremental plastic pseudo-force calculated using the second equation of (5.3.30).

To complete this section, the formulation for incompressible materials is derived through the mixed finite element method as follows. The

displacement and the pressure are taken as the primary variables. The displacement within any element remains in the form of (5.3.1),

$$u_i = \phi_i^m(x_\cdot^\alpha, \underline{x}^\alpha)q_m \qquad (5.3.1)$$

and the pressure within the element is approximated as

$$P = \rho^n(x^\alpha, \underline{x}^\alpha)p_n \quad , \qquad (5.3.32)$$

where p_n is the nodal pressure. The degree of the interpolation function ρ^n for the pressure should be one order less than the degree of the function ϕ for the displacements in order to have consistency of approximation for the displacements and the pressure. This will be seen clearly from the following derivation because P is one order less differentiable than u_i. The incremental form of P is

$$dP = \rho^n(x^\alpha, \underline{x}^\alpha)dp_n \quad . \qquad (5.3.33)$$

When the incremental form of constitutive equation for incompressible material (5.2.4) is used in the last term of eq.(5.3.24) with J=1 (hereafter in this section),

$$x_k^\alpha\, x_k^\gamma\, x_i^\beta\, d(T_{\gamma\beta}) = x_k^\alpha\, x_k^\gamma\, x_i^\beta\, [-dP\, C_{\gamma\beta} + \bar{G}\, d(C_{\gamma\beta}) + dQ_{\gamma\beta}dz]$$

$$= x_k^\alpha\, [-\rho^n\delta_{ki}dp_n + 2\bar{G}\psi^m_{(ik)}dq_m + dQ_{ki}dz] \quad . \qquad (5.3.34)$$

Substituting (5.3.34) into (5.3.24),

$$d(T^{\alpha}_{i}) = x^{\alpha}_{k}\{[2\bar{G}\psi^{m}_{(ik)} - 2\psi^{m}_{(ks)}(\sigma_{si}) - \psi^{m}_{si}(\sigma_{ks})]dq_{m} - \rho^{n}\delta_{ki}dp_{n} + dQ_{ki}dz\} \quad . \quad (5.3.35)$$

Finally, (5.3.19) in conjunction with (5.3.35) results in the following

$$\int_{V_o}[2\bar{G}\psi^{m}_{(ik)}\psi^{j}_{ik} - 2\psi^{m}_{(ks)}\psi^{j}_{ik}(J\sigma_{si}) - \psi^{m}_{si}\psi^{j}_{ik}(J\sigma_{ks})]dV_o dq_m - \int_{V_o}\rho^{n}\psi^{j}_{ii}dV_o dp_n$$

$$= d(f_j)_{ex} - \int_{V_o}\psi^{j}_{ik}dQ_{ki}dzdV_o \quad . \quad (5.3.36)$$

In matrix form eq.(5.3.26) becomes

$$[k_{jm}]dq_m + [L_{jn}]dp_n = d(f_j)_{ex} + d(f_j)_p = d(f_j^{(t)}) \quad . \quad (5.3.37)$$

where the element stiffness matrix k_{jm} is

$$k_{jm} = \int_{V_o}[2\bar{G}\psi^{m}_{(ik)}\psi^{j}_{ik} - 2\psi^{m}_{(ks)}\psi^{j}_{ik}(J\sigma_{si}) - \psi^{m}_{si}\psi^{j}_{ik}(J\sigma_{ks})]dV_o \ ,$$

$$L_{jn} = -\int_{V_o}\rho^{n}\psi^{j}_{ii}dV_o \quad (5.3.38)$$

and

$$d(f_j)_p = -\int_{V_o}\psi^{j}_{ik}dQ_{ki}dzdV_o \quad .$$

Now we have m equations but m+n unknowns (m for displacement and n for pressure). The constraints of incompressibility, i.e., J=1 or $\dot{J}$=0 must considered. From equation (5.3.15),

$$J\psi^{m}_{ii}dq_m = 0 \quad . \quad (5.3.39)$$

If we multiply ρ^n to both sides of eq.(5.3.39) and then integrate the resultant equation over the undeformed element, we can obtain n additional equations given by eq.(5.3.40)

$$\int_{V_o} \rho^n \psi_{ii}^m dV_o \, dq_m = 0 \quad . \tag{5.3.40}$$

In the matrix form, (5.3.40) becomes

$$[L_{nm}]dq_m = 0 \quad . \tag{5.3.41}$$

The simultaneous equations of q's and p's can be written as

$$\begin{bmatrix} K_{jm} & L_{jn} \\ L_{nm} & 0 \end{bmatrix} \begin{Bmatrix} dq_m \\ dp_n \end{Bmatrix} = \begin{Bmatrix} df_j^{(t)} \\ 0 \end{Bmatrix} \quad . \tag{5.3.42}$$

For an entire structure we have the equation in the following form,

$$\begin{bmatrix} K_{NN} & L_{NM} \\ L_{MN} & 0 \end{bmatrix} \begin{Bmatrix} dq_M \\ dp_N \end{Bmatrix} = \begin{Bmatrix} dF_N^{(t)} \\ 0 \end{Bmatrix} \quad . \tag{5.3.43}$$

where N and M are the total degrees of freedom for displacement and pressure in the entire structure.

In general, the integrands of (5.3.30) and (5.3.38) are functions of the material coordinates x^α. It becomes very complicated when high order of shape function is used. Therefore the numerical integration technique must be adopted in the calculation. However, when the linear triangular element

is used, ψ's, J, and σ's are constants within each element at each incremental intrinsic time. This simplifies the calculation a great deal. On the other hand when a relatively fine mesh is used, the linear triangular elements can provide the convergent results. The linear triangular elements are still used by many researchers. Hence it will be used in this work. The formulation of triangular element for plane strain problem will be discussed in detail in next section.

5.4 Formulation of Linear Triangular Element for Plane Strain

The plane strain is considered as a material deformation occurring in a plane while the deformation in direction normal to the plane vanishes. Such a deformation can be described as

$$y_i = y_i(x^\alpha, t) \qquad (i,\alpha = 1,2) \ ,$$

$$y_3 = x^3 \qquad (5.4.1)$$

The Cauchy-Green deformation tensor and its inverse and its incremental form can be calculated as follows

$$[C_{\alpha\beta}] = \begin{bmatrix} C_{\mu\nu} & 0 \\ 0 & 1 \end{bmatrix} \quad , \quad [C_{\alpha\beta}]^{-1} = \begin{bmatrix} C^{-1}_{\mu\nu} & 0 \\ 0 & 1 \end{bmatrix}$$

and

$$[\hat{C}_{\alpha\beta}] = \begin{bmatrix} \hat{C}_{\mu\nu} & 0 \\ 0 & 0 \end{bmatrix} \qquad (\mu,\nu = 1,2) \qquad (5.4.2)$$

where $C_{\mu\nu}$, $C^{-1}_{\mu\nu}$, and $\hat{C}_{\mu\nu}$ are functions of x^1 and x^2 only. The stresses

related to the x^3 direction from (5.2.1) are the following

$$T_{13} = \sigma_{13} = 0 \quad ,$$

$$T_{23} = \sigma_{23} = 0 \qquad (5.4.3)$$

and

$$T_{33} = \sigma_{33} = \lambda \log(J)/J$$

where $J = |C_{\alpha\beta}|^{1/2} = |C_{\mu\nu}|^{1/2}$ remains the same for both cases. Hence we need only deal with the quantities related to the x^1 and x^2 directions.

In the linear triangular element, the deformation can be written explicitly as

$$y_i = x^i + u_i = x^i + \phi^m_{i\alpha} x^\alpha q_m \quad (i=1,2;\ \alpha=0,1,2;\ m=1,2,\ldots 6) \ ,$$

$$y_3 = x^3 \qquad (u_3=0) \qquad (5.4.4)$$

where the ϕ's comprise a set of constants related to the nodal coordinates. For a typical triangular element shown in Fig.31, we denote the nodal deformation as

$$q_m = (q_1, q_2, q_3, q_4, q_5, q_6)^T$$

$$= (u_1, v_1, u_2, v_2, u_3, v_3)^T \qquad (5.4.5)$$

where u's are the displacement in x^1 direction and v's in x^2 direction, respectively. The symbol $(\cdot)^T$ denotes the transpose of a vector.

Then, we can write the displacement in eq.(5.4.4) more explicitly as following

$$u = [1\ x^1\ x^2] \begin{bmatrix} a_1 & 0 & a_2 & 0 & a_3 & 0 \\ b_1 & 0 & b_2 & 0 & b_3 & 0 \\ c_1 & 0 & c_2 & 0 & c_3 & 0 \end{bmatrix} \{q_m\}$$

and

$$v = [1\ x^1\ x^2] \begin{bmatrix} 0 & a_1 & 0 & a_2 & 0 & a_3 \\ 0 & b_1 & 0 & b_2 & 0 & b_3 \\ 0 & c_1 & 0 & c_2 & 0 & c_3 \end{bmatrix} \{q_m\} \quad , \tag{5.4.6}$$

where

$$\begin{aligned} a_1 &= (x^1_{(2)}x^2_{(3)} - x^1_{(3)}\, x^2_{(2)})/(2\Delta) \\ b_1 &= (x^2_{(2)} - x^2_{(3)})/(2\Delta) \\ c_1 &= (x^1_{(3)} - x^1_{(2)})/(2\Delta) \end{aligned} \tag{5.4.7}$$

and other a's, b's and c's can be obtained by the subscripts (1), (2), and (3) permuting in a natural order. Δ is the area of the triangle,

$$\Delta = \begin{bmatrix} 1 & x^1_{(1)} & x^2_{(1)} \\ 1 & x^1_{(2)} & x^2_{(2)} \\ 1 & x^1_{(3)} & x^2_{(3)} \end{bmatrix} \tag{5.4.8}$$

The derivatives of displacements with respect to the material system

$$u_{i,\alpha} = \phi^{m}_{i\alpha} q_m \qquad (\alpha=1,2;\ i=1,2;\ m=1,6) \quad , \qquad (5.4.9)$$

where the constants ϕ's, in matrix form, can be written as

$$[\phi_{i\alpha}]^m = \begin{bmatrix} b_n & c_n \\ 0 & 0 \end{bmatrix} \qquad \text{for } m=(2n-1)$$

and $\qquad n = 1,2\ 3 \qquad (5.4.10)$

$$[\phi_{i\alpha}]^m = \begin{bmatrix} 0 & 0 \\ b_n & c_n \end{bmatrix} \qquad \text{for } m = 2n$$

Since ϕ's as well as ψ's, J, and σ's are constants at each intrinsic time step, the element stiffness (5.3.29) and (5.3.30) become, in the case of linear triangular element as

$$[k_{jm}]\, dq_m = d(f_j)_{ex} + d(f_j)_p = df_j^{(t)} \quad , \qquad (5.4.11)$$

where the element stiffness matrix k_{jm} is

$$k_{jm} = \Delta\, [\lambda \psi^m_{nn} \psi^j_{kk} + 2\bar{G} \psi^m_{(ik)} \psi^j_{ik} - 2\psi^m_{(ks)} \psi^j_{ik} (J\sigma_{si}) - \psi^m_{si} \psi^j_{ik} (J\sigma_{ks})]$$

and the incremental force vector

$$d(f_j)_p = -\psi^j_{ik} dQ_{ki} \Delta\, dz \quad . \qquad (5.4.12)$$

At this moment, the degenerate cases of (5.4.10) and (5.4.12), namely the case under the small deformation, are given bellow. In eq.(5.4.12) if σ's = 0 , and ψ's = ϕ's, the equations represent the small deformation of plasticity [55],

$$[k_{jm}]\, dq_m = d(f_j)_{ex} + d(f_j)_p = df_j^{(t)} \quad , \tag{5.4.13}$$

where

$$k_{jm} = \Delta\, [\lambda \phi^m_{nn} \phi^j_{kk} + 2G(0) \phi^m_{(ik)} \phi^j_{ik}] \quad ,$$

$$d(f_j)_p = -\psi^j_{ik} dQ_{ki} \Delta\, dz \tag{5.4.14}$$

Furthermore, if $f_p = 0$, the equations represent the small deformation of the elasticity [57],

$$[k_{jm}] q_m = (f_j)_{ex} \quad , \tag{5.4.15}$$

where the element stiffness matrix k_{jm} is

$$k_{jm} = \Delta\, [\lambda \phi^m_{nn} \phi^j_{kk} + 2G \phi^m_{(ik)} \phi^j_{ik}] \tag{5.4.16}$$

and $(f_j)_{ex}$ is an external force vector.

5.5 Brief Discussion of the Calculation of Q's

It has been seen that the effect of plasticity is represented by the pseudo-force df_p in (5.5.12). In the calculation of this force, $dQ_{\alpha\beta}$ plays a very important role. Recall $dQ_{\alpha\beta}$ in (5.2.3)

$$dQ_{\alpha\beta}(z) = \int_0^z \frac{dG(z-z')}{dz} \frac{dC_{\alpha\beta}}{dz'}\, dz' \tag{5.2.3}$$

At each incremental step, $dC_{\alpha\beta}$ needs to integrate from 0 to z, the current intrinsic time scale. To calculate $dC_{\alpha\beta}$ numerically, the equation for $dC_{\alpha\beta}$

at $z_{i+1} = z_i + \Delta z$ after knowing the value of $C_{\alpha\beta}$ at z_i is now derived. Eq.(5.2.3) at z_{i+1} can be written as follows

$$dQ_{\alpha\beta}(z_{i+1}) = \int_0^{z_{i+1}} \frac{dG(z-z')}{dz} \frac{dC_{\alpha\beta}}{dz'} dz'$$

$$= \int_0^{z_i} \frac{dG(z-z')}{dz} \frac{dC_{\alpha\beta}}{dz'} dz' + \int_{z_i}^{z_i+\Delta z} \frac{dG(z-z')}{dz} \frac{dC_{\alpha\beta}}{dz'} dz' \quad . \qquad (5.5.1)$$

From the mean value theorem and the smoothness of $C_{\alpha\beta}$, the last term in eq.(5.5.1) can be written, as a good approximation,

$$\int_{z_i}^{z_i+\Delta z} \frac{dG(z-z')}{dz} \frac{dC_{\alpha\beta}}{dz'} dz' \approx \left.\frac{dC_{\alpha\beta}}{dz}\right|_{z=z_{i+1}} \int_{z_i}^{z_i+\Delta z_i} \frac{dG(z-z')}{dz} \Big|_i dz' \quad . \qquad (5.5.2)$$

Substitution of $G(z) = \sum G_r e^{-\alpha_r z}$ into (5.5.1) gives

$$dQ_{\alpha\beta}(z_{i+1}) = \sum_r \{Q^{(r)}_{\alpha\beta}(z_i) e^{-\alpha_r \Delta z_i} + \left.\frac{dC_{\alpha\beta}}{dz}\right|_{z_i+1} G_r(e^{-\alpha_r \Delta z_i} - 1)\} \quad i=0,1,\ldots$$

where $Q_{\alpha\beta}(0)=0$. (5.5.3)

Eq.(5.5.3) tells that the history dependence of the material response [through $dC_{\alpha\beta}(z_{i+1})$] at the intrinsic time z_{i+1} will be determined by $Q_{\alpha\beta}(z_i)$ plus the effect caused only by the new incremental step through $\left.\frac{dC_{\alpha\beta}}{dz}\right|_{z_i+1}$ and Δz_{i+1} .

For r=1, i.e., $G(z) = G_0 e^{-\alpha z}$,

$$dQ_{\alpha\beta}(z_{i+1}) = Q_{\alpha\beta}(z_i) e^{-\alpha \Delta z_i} + \left.\frac{dC_{\alpha\beta}}{dz}\right|_{z_i+1} G_0(e^{-\alpha \Delta z_i} - 1) \quad . \qquad (5.5.4)$$

5.6 The Iterative Process and Programming Steps

After defining the problem, giving the dimension and tolerance of the intrinsic time, meshing the domain, and calculating the values of ϕ's and the area of each element, the incremental load step starts. For each incremental step the values of ψ's are updated and then the stiffness matrix is calculated. An initial value Δz^0 is assigned to the increment of intrinsic time at every step. The plastic pseudo-forces corresponding to the dz^0 are then evaluated. Now the linear simultaneous equations of incremental nodal displacements are set. After imposing the boundary conditions, this set of equations is solved. Upon use of the incremental displacements, incremental strains, stresses, and Cauchy-Green deformation tensor etc. are obtained. The incremental intrinsic time dz_1 is calculated. Knowing the new incremental intrinsic time, the new pseudo-force are again obtained. The simultaneous linear equations with the same stiffness matrix are solved and new incremental nodal displacements are obtained. The new dz follows to the new displacements. The iteration process is continued until the difference in dz between any two consecutive iterations is less than some defined tolerance. Then the next new incremental step is repeated. Above iteration procedure is described in the flow chart as shown in Fig.32.

On the basis of the formulae in section 5.4 and the flow chart in Fig.32, a computer program with Fortran language called FELP is developed to analyze the plane strain of finite plastic deformation problems. The computer program consists of five parts.

Part one

In this part the dimensioning of the program variables is first set up and the main control parameters (such as the total number of elements, nodes, the number of degree of freedom for each node, etc.) and the material constants (G_0, α, and λ) are input. The informations of mesh, namely the coordinates for every node and the nodes for each element are then input. The nodes of elements are stored in an array NOD(N,I) in which N denotes the number of element and I the number of node. The array plays a very important role in the connection of elements and whole structure. The node and element data are defined by two ways in the program, which are automatic mesh forming in the compute program and the data inputing from read statement. Former way is efficient for relatively regular domains while the later way is for irregular ones. The necessary boundary conditions are read in. Finally all input and calculated data are printed out for checking and recording.

Part two

The quantities related to the material system are calculated in this part, which include the area of the elements and ϕ's, i.e., a's, b's, and c,s defined in eq.(5.4.7). These quantities also are primary variables to the stiffness matrix. To save storage the stiffness matrix is stored in the half bandwidth. So the width of the half band is obtained in this part. The arrays are initialized and get ready for following main calculation.

Part three

We start outer do-loop for the incremental steps of load or deformation. The values of incremental forces or deformations at each step are applied through the boundary conditions. For each step the values of Ψ's are updated. Then the stiffness matrix for each element is obtained upon use of eq.(5.4.12) and summed to the half banded global stiffness matrix. This is accomplished by a subroutine called STIFF. What follows next is imposing the displacement boundary condition in the equation to get the modified global stiffness matrix and the modified force vector through a subroutine BNAR. The initial force boundary condition, i.e., node forces are added to force vector directly. It has been seen from eq.(5.4.11) that to complete force vector needs to add the pseudo-plastic force. We will describe this in inner do-loop in part 5.

Part four

The inner do-loop is designed for the iteration process. At each incremental step, an initial values of intrinsic time dz° is given. The pseudo-plastic forces are calculated upon use of the eq.(5.4.12) and the subroutine PF. Then they are added to the appropriate positions in total force vector. Now the linear simultaneous equations for the nodal displacements are set. The equations are solved by use of the Gauss-Jordan method. After obtaining the displacement increments, new intrinsic time dz can be obtained by calling a subroutine DZ. The iteration process continues until the value $(dz^{\circ}-dz)/dz$ less than the tolerance.

Part five

When inner do-loop stops the converge displacement increments are obtained at the incremental step. Then the necessary quantities such as stains, stresses, and other related parameters through a subroutine called RES can be calculated. If the results for incremental values are interested, they are printed out. Otherwise they are added to the total values and the next step starts. The program consists of the main program and 10 subroutines. It will listed in Appendix A.

5.7 Numerical Example

Previous analysis is now applied to study a problem of metal forging --- upsetting process of a block shown in Fig.33. A similar problem "The upsetting of a cylindrical block " was taken up by a Joint Examination Program of the Validity of Various Numerical Methods for the Analysis of Metal Forming Processes and discussed around table by fourteen groups in the IUTAM SYMPOSIUM TUTZING/GERMANY [58]. The collected results showed considerable discrepancies. However, what agreed in discussion was two important factors responsible for the discrepancies, which are the selections of the elements and the deformation increments. What was suggested was to use finer element and smaller deformation increment up to 0.25%. To explore the computational capability of the theory in our research, following data will be taken in the calculation.

The dimension of original block are set to be 2 unit in width, 3 in height, and 1 unit in third direction since the plane stain is concerned. Sticking, i.e., no slip condition, is assumed along the tool-work interface.

The material constants G_0, λ, and α are set to be 1., 1., and 200. The geometrical dimension and the material constant are taken in such a way so that all quantities in the problem are normalized. $G_0=\lambda$ in elastic case represents $\nu=0.25$. Due to the symmetry of the problem, a quarter part of the block is analysed by using the mesh division depicted in Fig.34 in which we have 143 nodes and 252 elements. The increment per each reduction (in hight) step is set to be 0.001.

Fig.35 shows the deformation profiles for different reduction levels. When reduction reaches 0.7, i.e., about 50%, the folding was observed. Fig.36 shows the distorted grid vs. the original grid. The relatively rigid part has been seen in the up-left of the domain, i.e., the up-middle of the block. Fig.37 gives the bulge ratio, w_{max}/w_0, at the different stages of reduction in height. At large reduction, the material gets softer in the x^1-direction. The variation of intrinsic time z respect to the reduction is shown in Fig.38.

Fig 39 illustrates the computed results of upsetting load as a function of the reduction in hight. The variations of stresses with respect to the reduction and the intrinsic time at elements No.251 and No.231 are shown in Fig.40-43. Fig.40 and 42 give the variation of stresses at element No.251 in x^2-direction with respect to the reduction in height. The results show the stress in this element reaches the maximum at a critical value of the reduction and continues to decrease so that the sign of the stress is changed. However the variation of stress at element No.231 which is located

inner of the domain does not show the same phenomenon. The phenomenon occurred at element No.251 is due to the dramatic distortion of the structure. In Fig. 44-45 we show the distribution of stresses in y_1 and y_2 direction along with the width of the upset block.

The convergence in this calculation in this problem is excellent. Under the current chosen incremental reduction, the average number iteration for each increment step is two. This is a beauty of the endochronic theory in finite element method. because we control dz, the intrinsic time, in the iteration which plays the crucial rule in the endochronic theory.

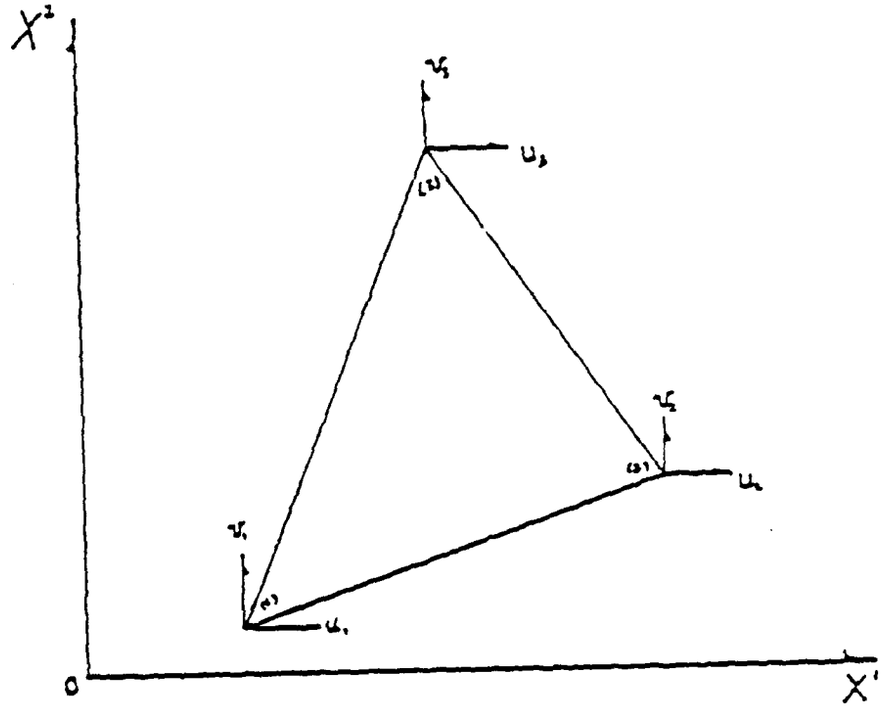

Fig.31 A triangle element

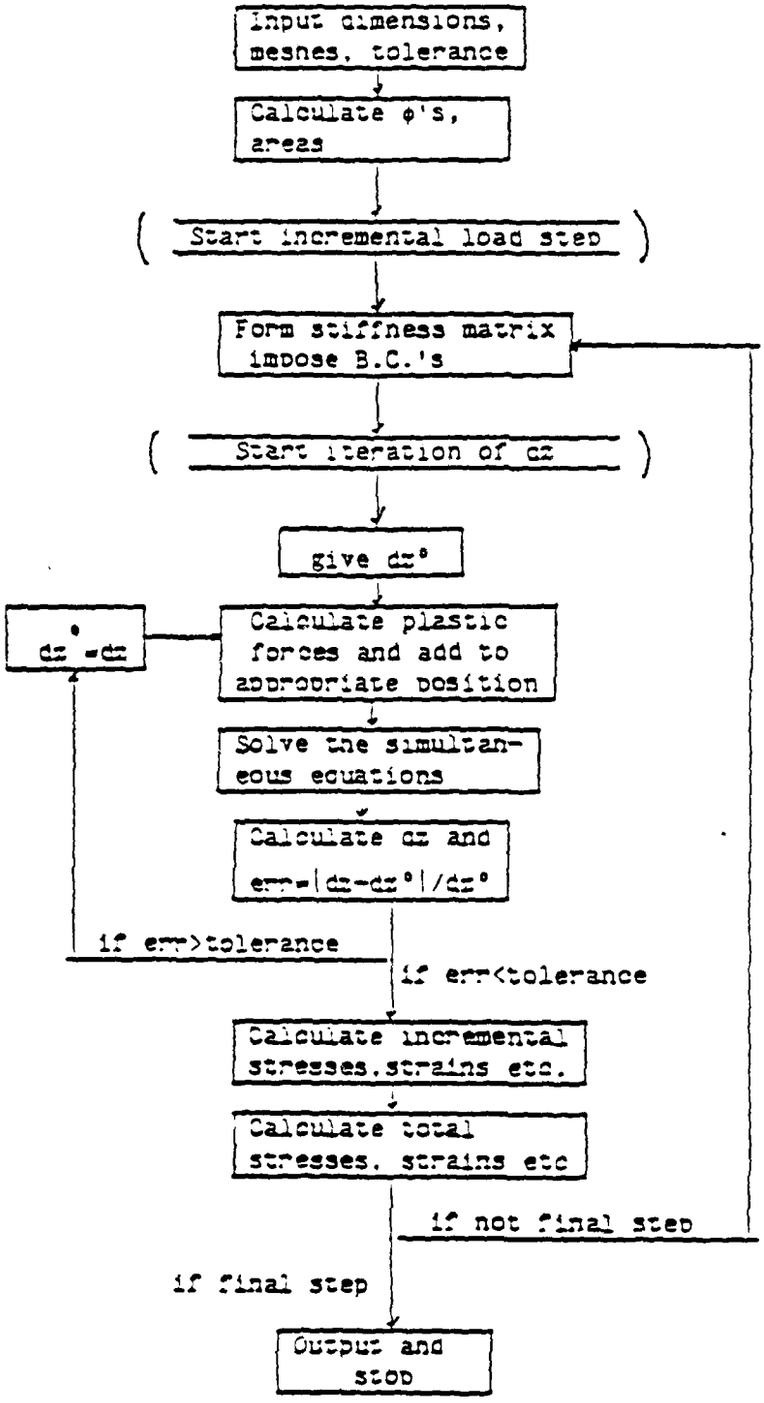

Fig.32 Flow chart

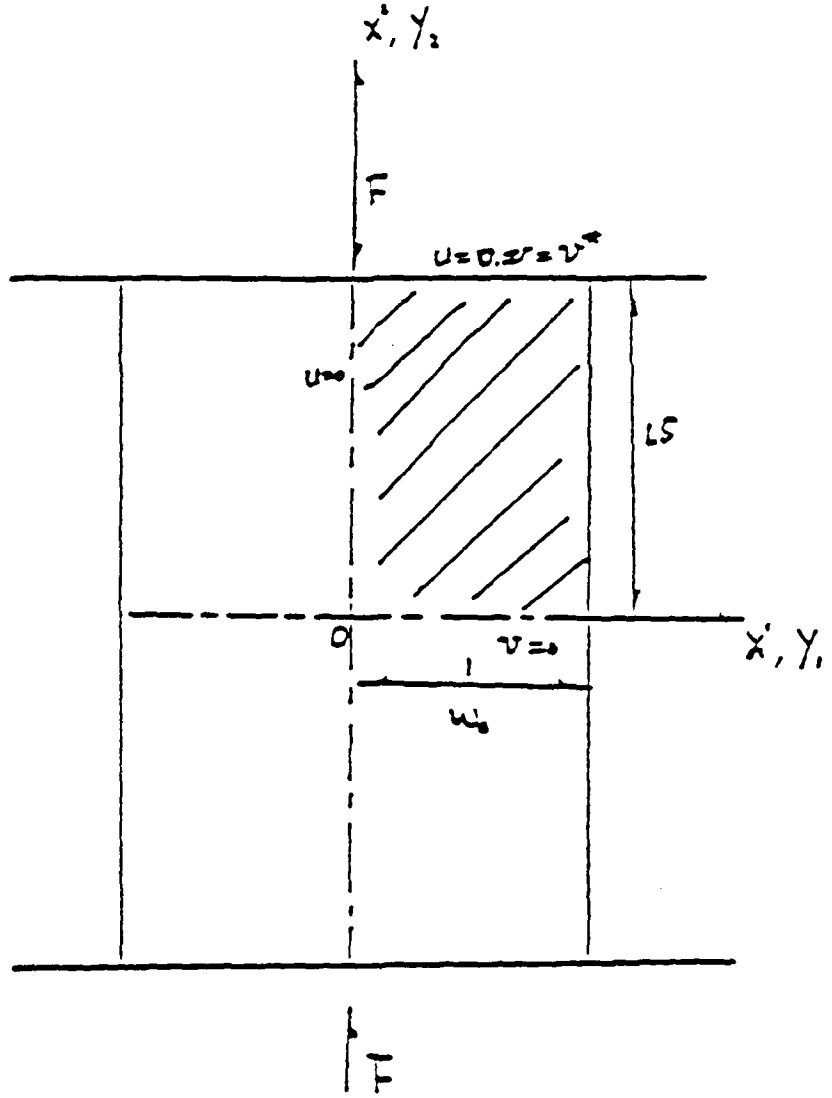

Fig.33 Upsetting of a block

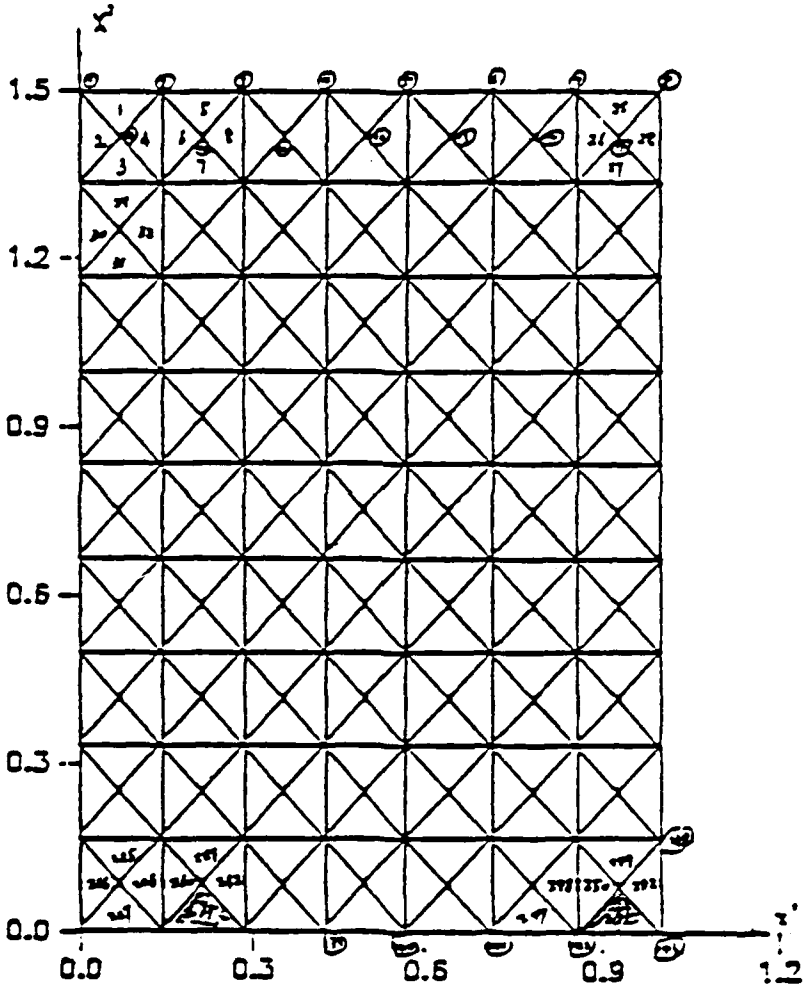

Fig.34 Division of mesh

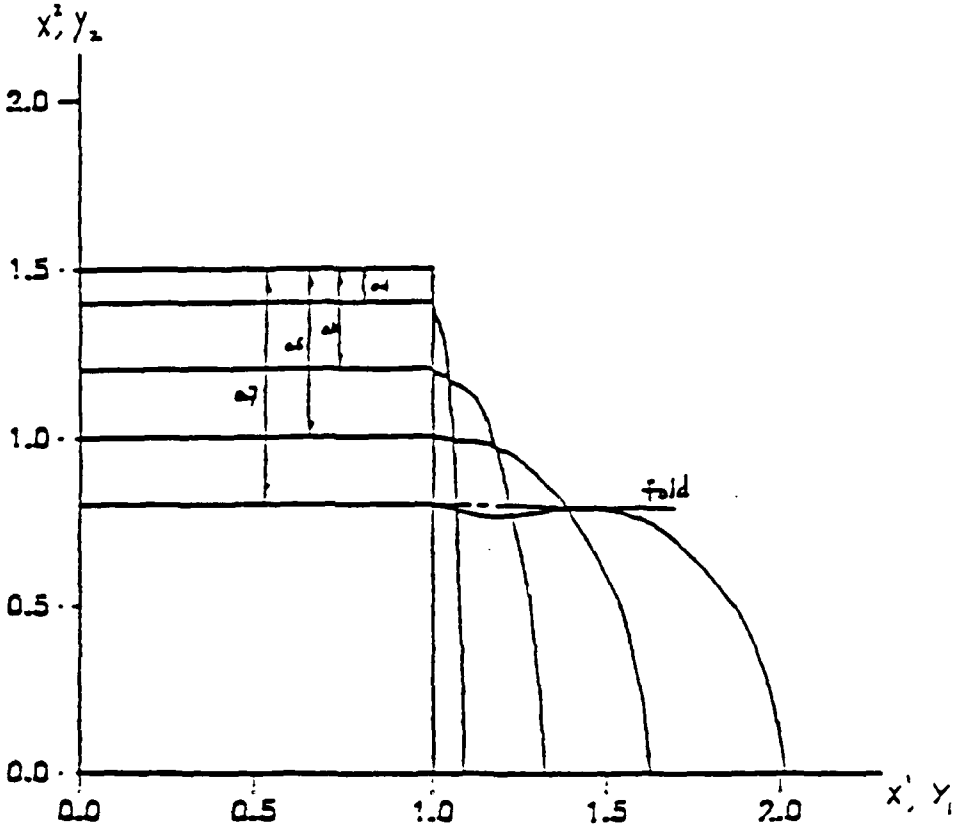

Fig. 35 Deformation profiles for different reduction level

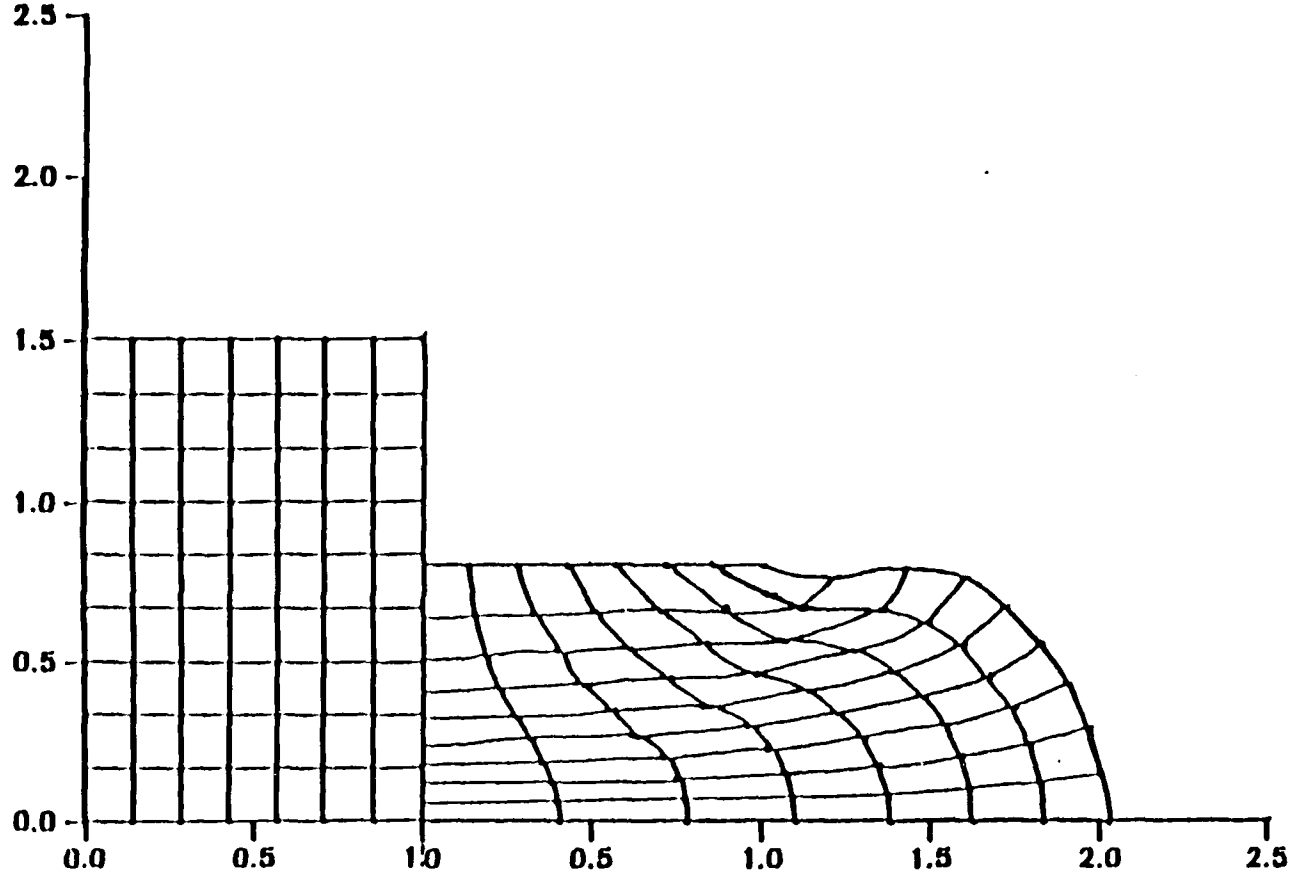

Fig.36 Distorted grid vs. the original grid

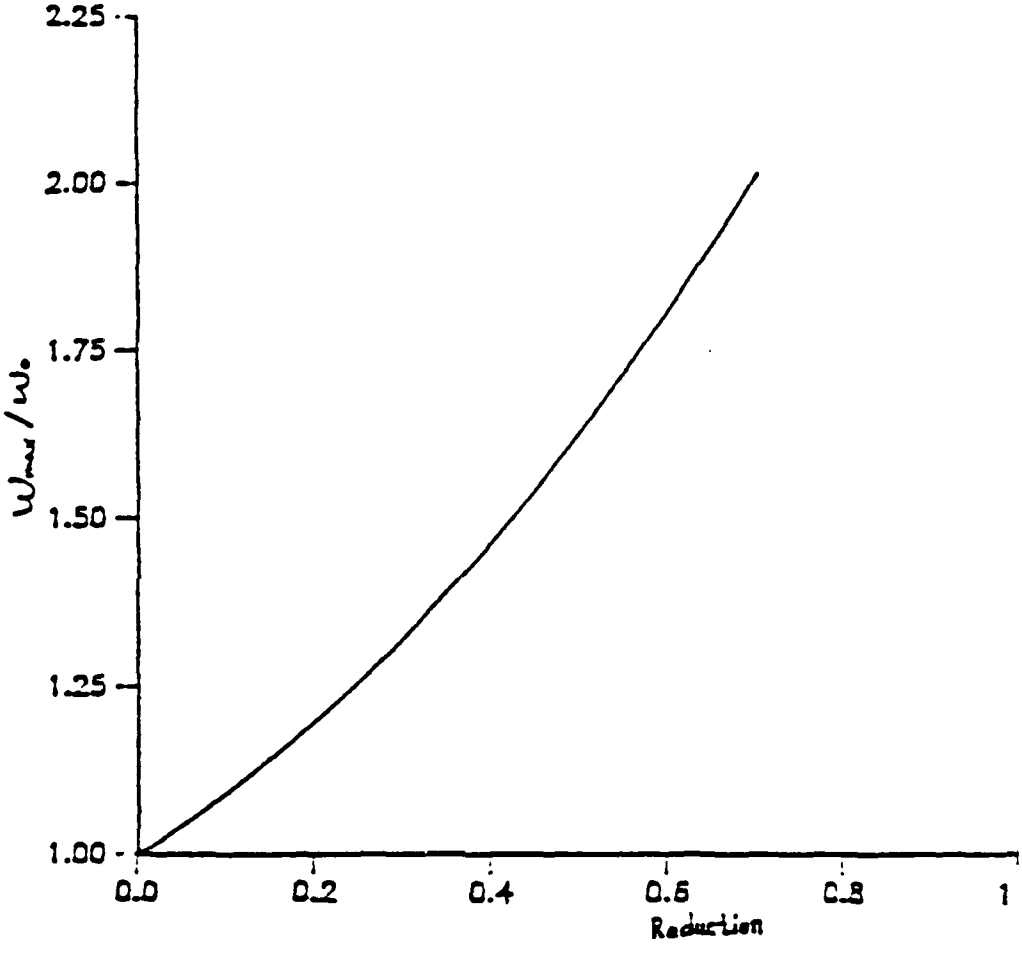

Fig. 37 The bulge ratio w_{max}/w_o vs.

the reduction in height

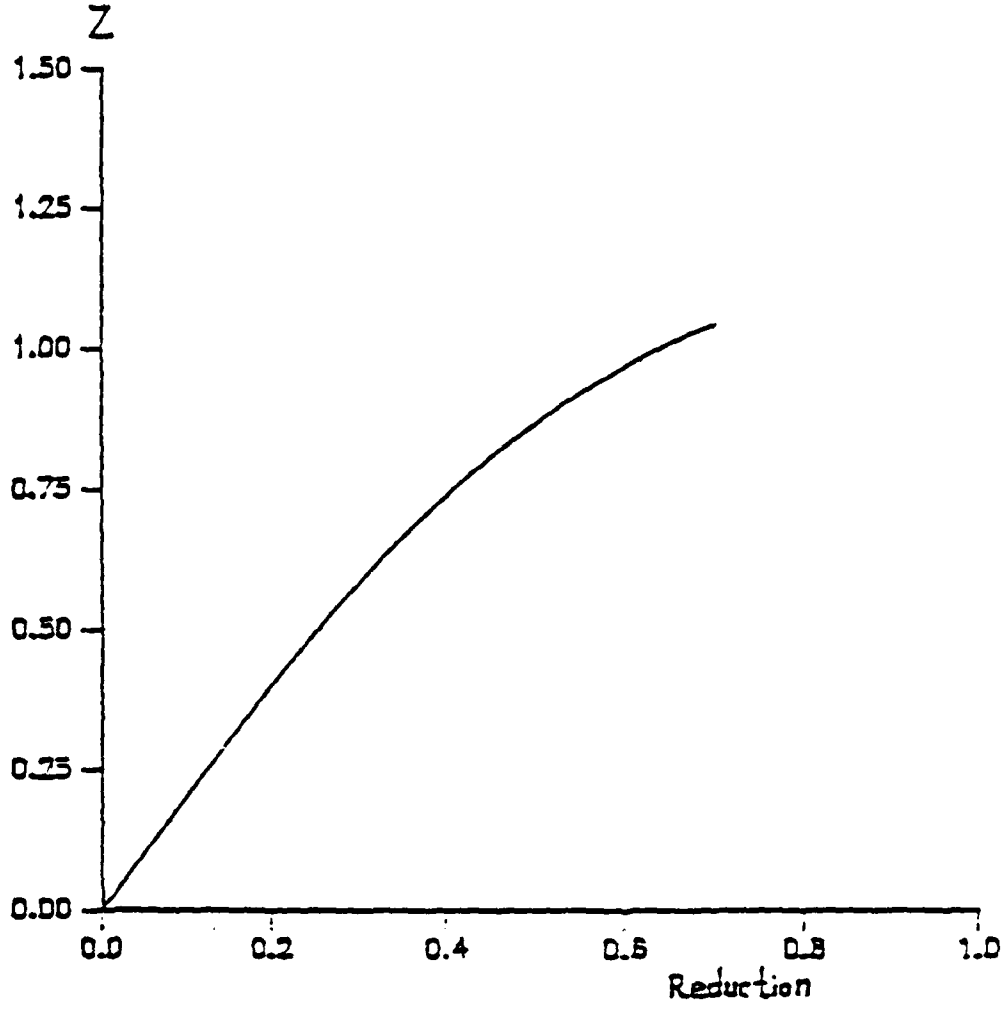

Fig.38 The variation of intrinsic time with respect to reduction in height

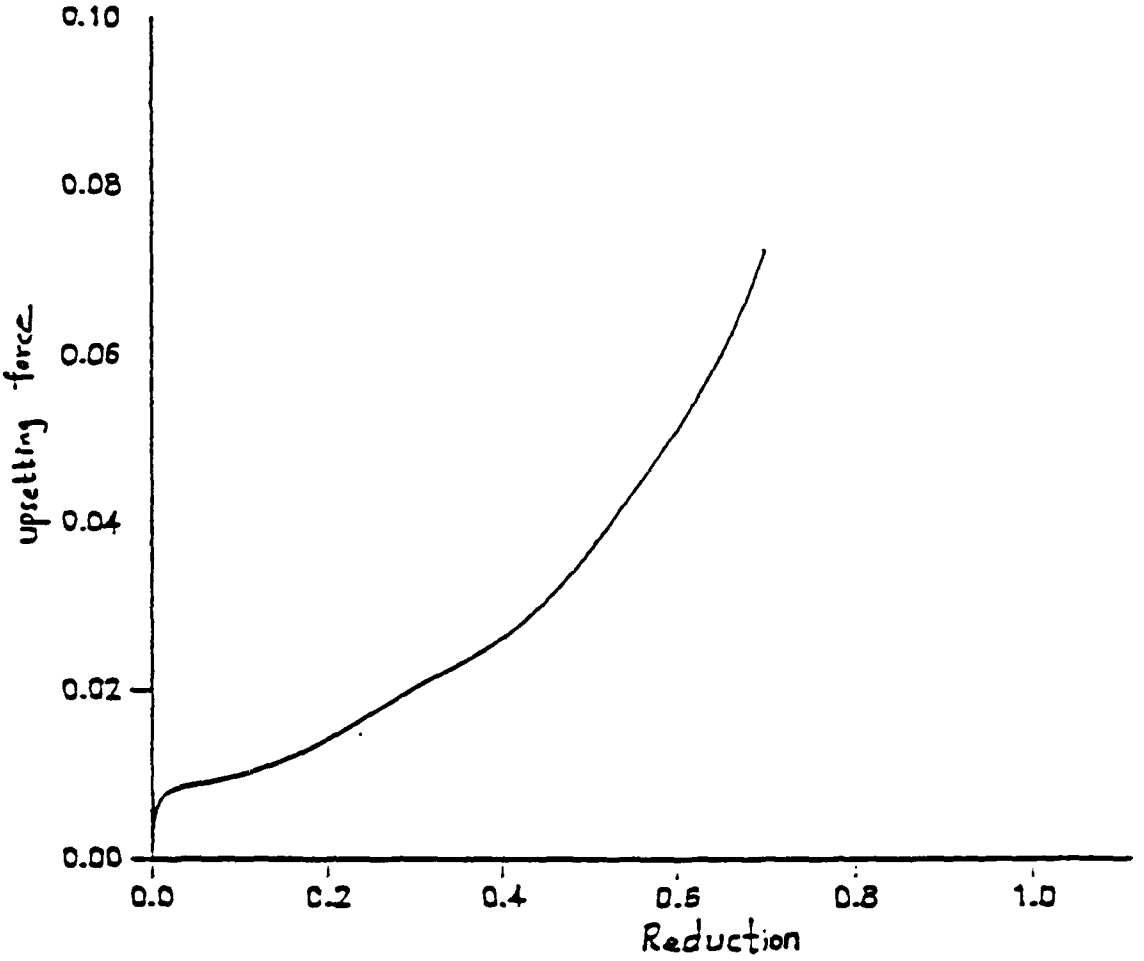

Fig.39 The variation of the upsetting load with respect to reduction in height

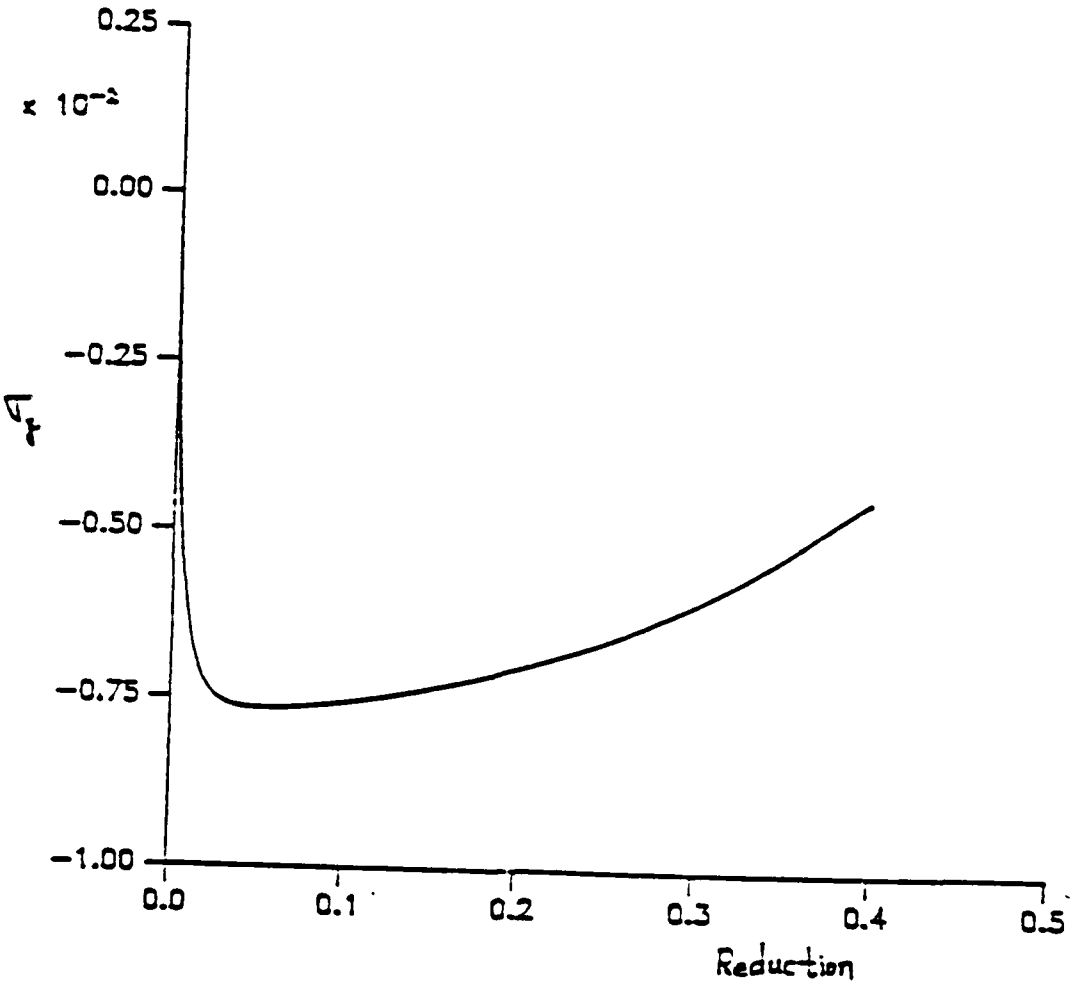

Fig.40 The variation of stress (y_2 direction)

with respect to the reduction in

height in element 251

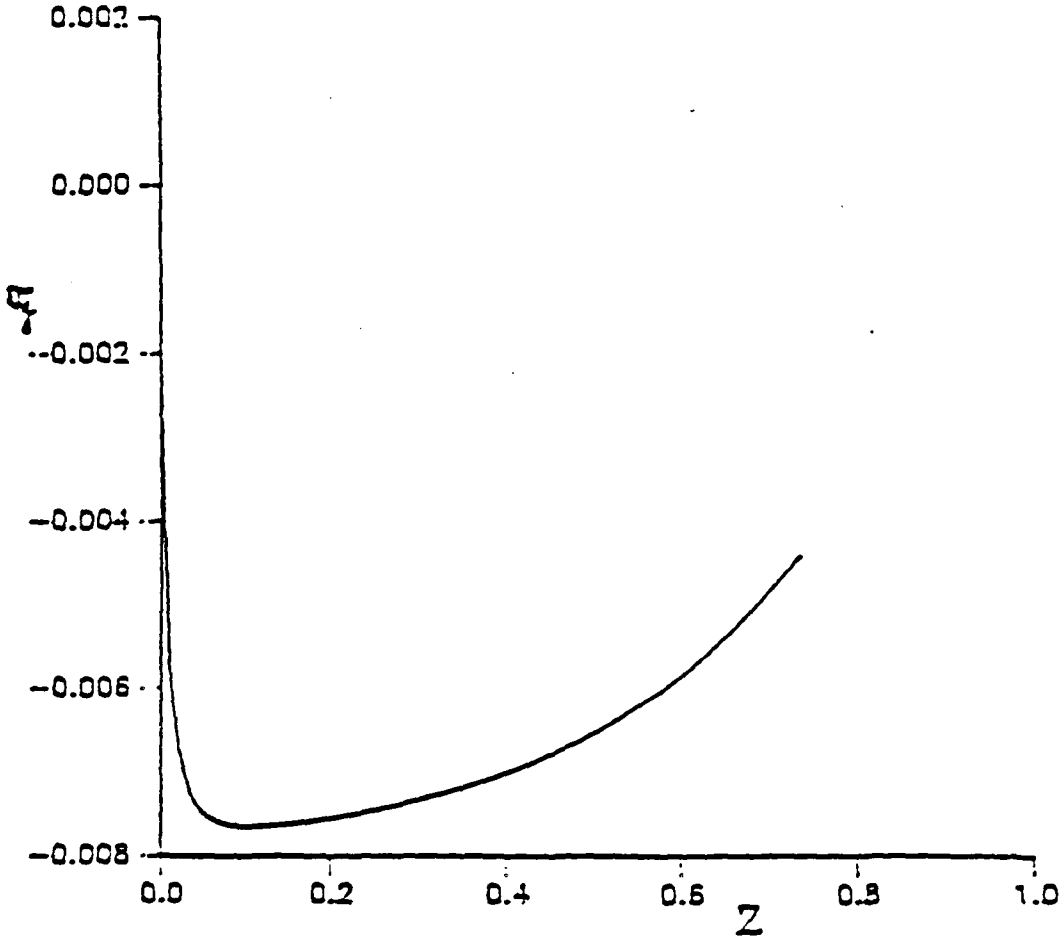

Fig.41 The variation of stress (y_2 direction)

with respect to the intrinsic time

z in element 251

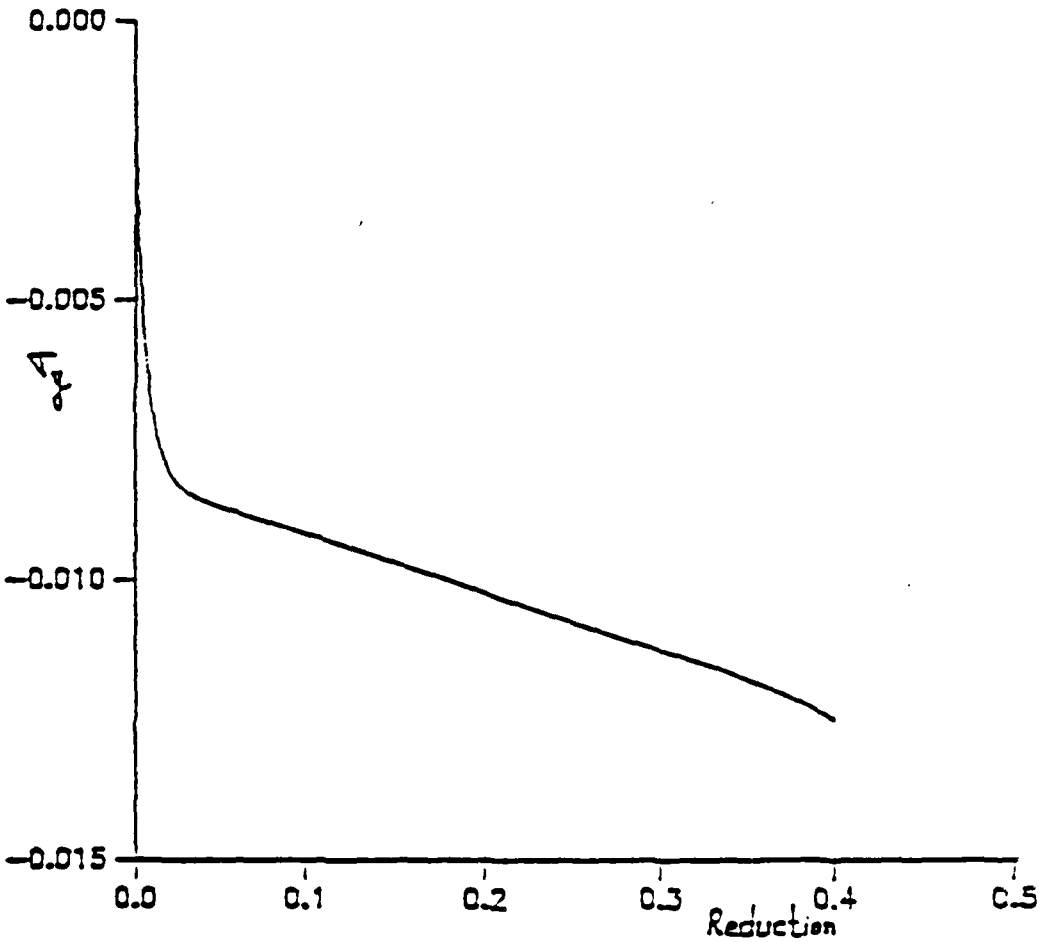

Fig.42 The variation of stress (y_2 direction) with respect to the reduction in height in element 231

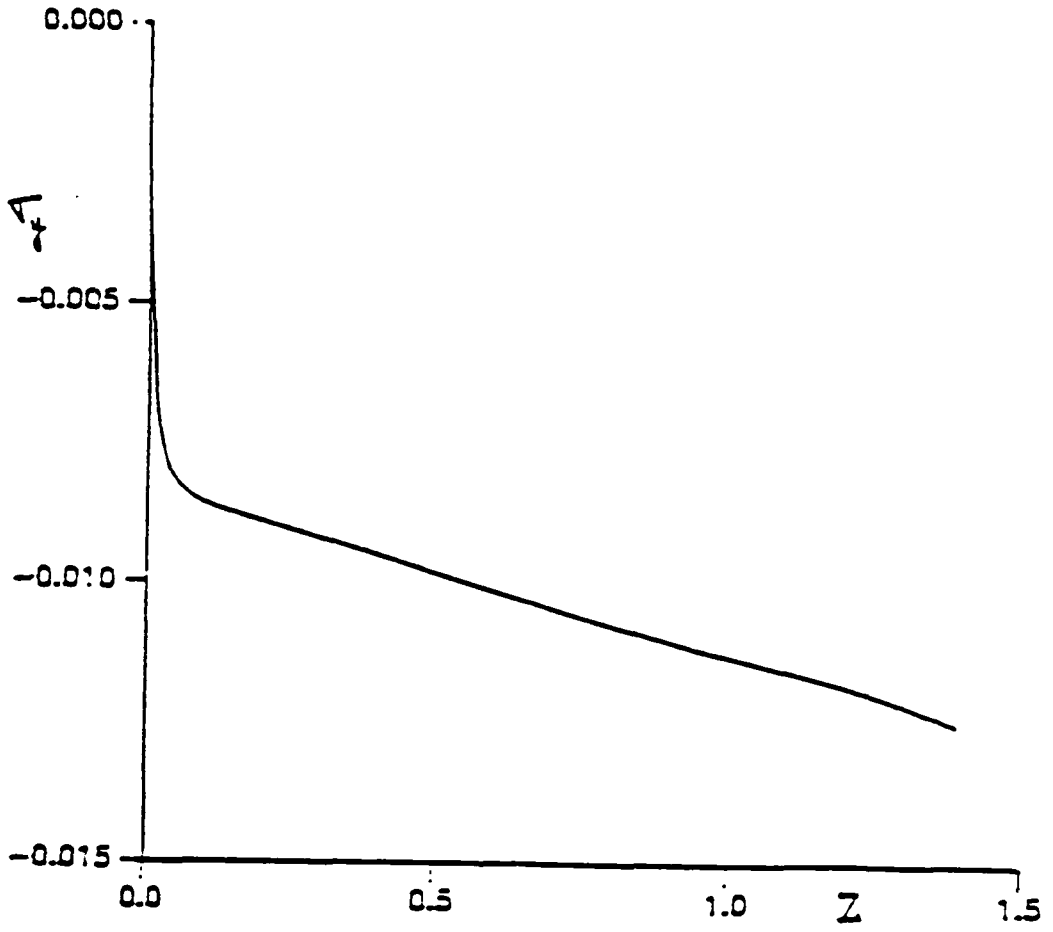

Fig.43 The variation of stress (y_2 direction)

with respect to the intrinsic time

in element 231

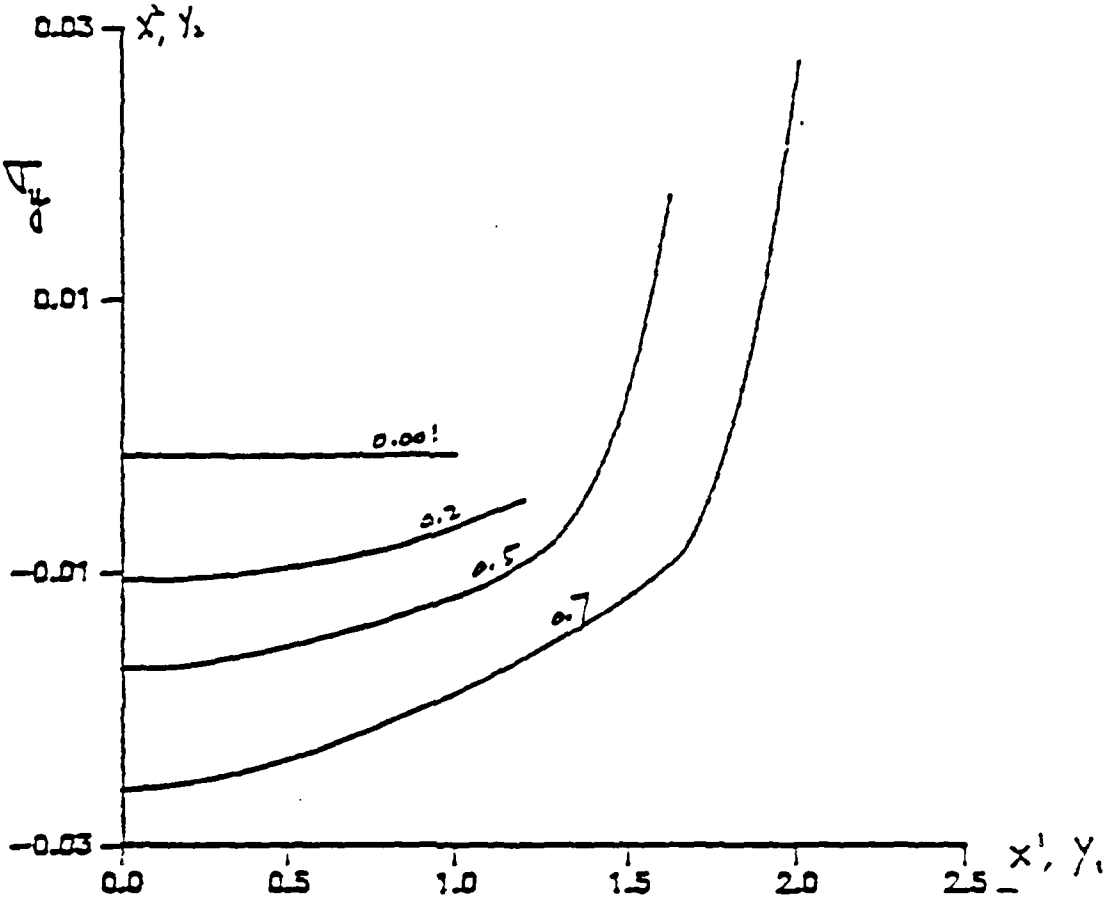

Fig.44 The distribution of stress σ_y along the width of the upset block

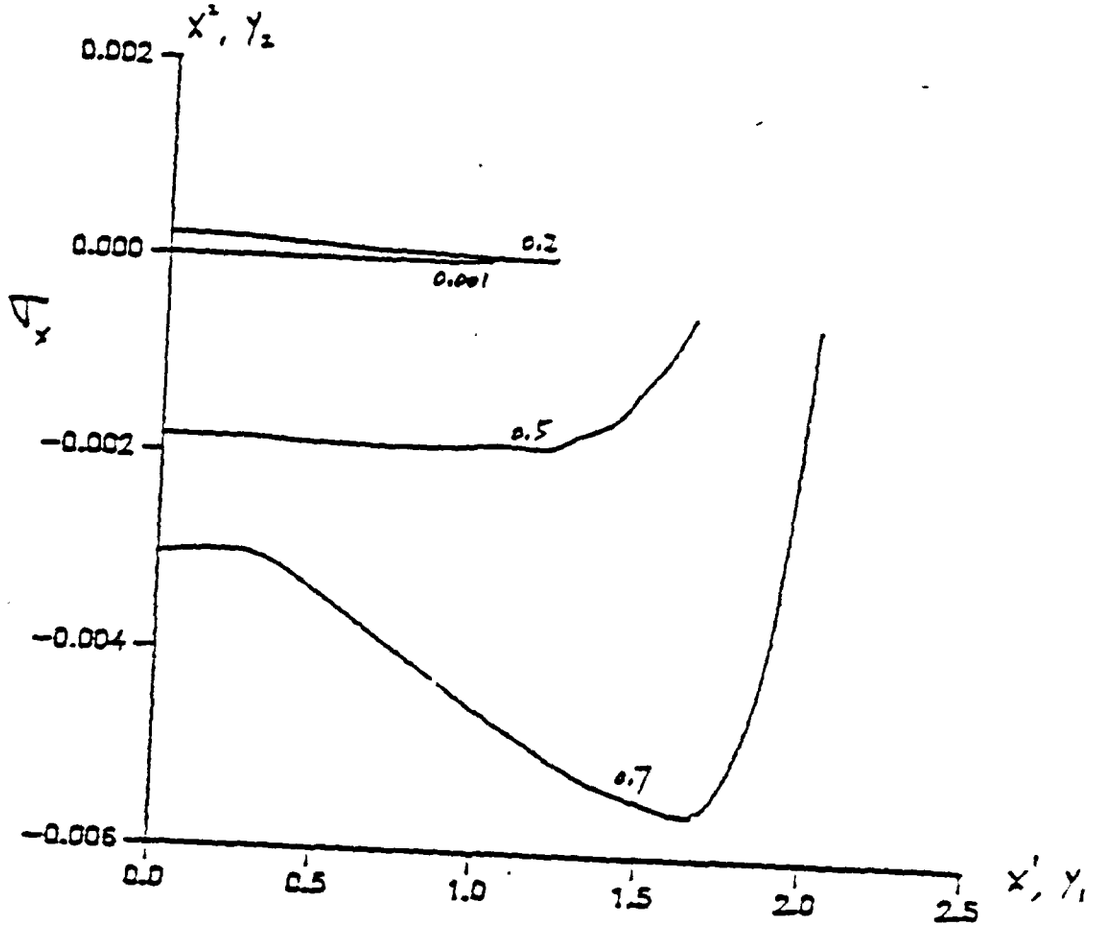

Fig.45 The distribution of stress σ_x along the width of the upset block

CONCLUSIONS AND RECOMMENDATIONS

Finite plasticity has very significant applications in engineering problems. With the rapid progress of the modern technology, developing a sophisticated theory and applying it to solve engineering problem are the tasks of the science and engineer.

Endochronic theory of plasticity has come to a fully developed stage after about 15 years' development since 1970's. Its predictive power of the behavior of materials, computational capability, application to the practical problems have been seen and proved through analysis and experiments. In this research we have studied extensively the endochronic theory of plasticity and its practical applications under large deformation.Again we show the contribution of endochronic theory to the plasticity regime.

The endochronic theory of incompressible plasticity was reviewed and applied to the analysis of a set of special problems which have significance in the theory as well as the practice of metal forming processes and pressure vessel structures. To our knowledge, this is the first time in the field that this set of problems are solved in closed form solutions.

The theory was also extended to model compressibility of plastic deformation. Incompressibility is an idealization and simplification of the reality and is the key point of the development of the classical plasticity. We added a term, representing the volume change, to the free energy and developed a constitutive equation of compressible plasticity with a functional term which reflects the compressibility of materials. Then with a

special form of the function, we developed a numerical scheme with a finite element technique and a computer program code for plane strain problems. Finally, an example of metal forming of forging process (upsetting a block), was analyzed and solved by the developed computer program. The solution obtained by this method is very resonable. The application of endochronic theory to the large plastic deformation has a great potential for application to more complicated engineering problems.

The numerical algorithm could be extended to cover axial symmetry and three-dimensional problems. Carefully controlled experiments are needed for further verification of the validity of the theory.

REFERENCES

1. Valanis, K.C., 'A theory of viscoplasticity without a yield surface, Part 1. General theory,' Archives of Mechanics, 23, 517-533, 1971.

2. Valanis, K.C., 'A theory of viscoplasticity without a yield surface, Part 2. Application to mechanical behavior of metals,' Archives of Mechanics, 23, 535-551, 1971.

3. Tresca, H., 'Sur l'ecoulement des corps solids soumis a de fortes pression,' Compt. Rend., 59, 1864, p. 754.

4. Levy, M., 'Memoire sur les equations generales des mouvements interieurs des corps solides ductiles au dela des limites ou l'elasticite pourrait les ramener a leur premier etat,' Comp. Rend., 70, 1970. pp.1323-1325.

5. Von Mises, R., 'Mechanik der festen koerper im plastisch deformablen zustant, Goettinger Nachr.,' Math.-Phys. Kl., 1913, pp. 582-592.

7. Hencky, H., 'Zur Theorie plastischer deformationen und der hierdurch im material hervorgerufenen neben-spannungen,' Proceedings of the ist International Congress on Applied Mechanics, Delft, Technische Boekhandel en Druckerij, J. Waltman, Jr., 1925, pp. 312-317.

8. Prandtl, L., 'Spannungsverteilung in plastische koerpern,' Proceedings of the ist International Congress on Applied Mechanics, Delft, 1924, pp. 43-54.

9. Lode, W., 'Versuch uber den einfluss der mittleren hauptspannung auf das fliessen der metalle eisen, kupfer, und nickel,' Z. Phys., 36, 913, 1926.

10. Taylor, G.I. and Quinney, H., 'The plastic distortion of metals,' Phil. Trans. R. Soc. A 230, 323, 1931.

11. Von Karman, T., 'Beitrag zur theorie des Walzvorganges,' Z. Angew, Math. Mech., 7, 235, 1927.

12. Sieble, E., 'The plastic forming of metals (translated by J.H. Hitchcock),' Steel, Oct. 16, 1933 to May 7, 1934.

13. Sachs, G., ;Beitrag zur theorie des ziehvorganges,' Z. Angew. Math. Mech., 5, 130, 1925.

14. Drucker, D.C., 'Some implications of work-hardening and ideal plasticity,' Quarterly of Applied Mathematics, v.7, N. 4, Jan. 1950, pp. 411-418.

15. Ilyushin, A.A., 'On the relation between stresses and small deformation in the mechanics of continuous media,' Drill. Mat. I. Mekh, 18, p. 641, 1954.

16. Hill, R., 'The mathematical theory of plasticity,' Oxford, 1950.

17. Hodge, Jr., P.G., 'The theory of piecewise linear isotropic plasticity,' IUTAM Colloquium Madred 1955, Deformation and Flow of Solids,' Berlin, 1956.

18. Prager, W., 'The theory of plasticity: A survey of recent achievements,' Proc. Inst. Mech. Engrs. 169, 41, 1955.

19. Ziegler, H., 'A modification of Prager's hardening rule,' Quart. Appl. Math., 17, pp. 55-65, 1959.

20. Mroz, Z., 'An attempt to Describe the behavior of metals under cyclic loads using a more general work hardening model,' Acta Mechanics 7, pp. 199-212, 1969.

21. Mendelson, A., 'Plasticity: Theory and Application,' The MacMillan Company, 1968.

22. Odgvist, F.K., 'Non-linear mechanics, past, present and future,' Applied Mechanics Reviews, Vol.21, N. 12, pp. 1213-1222, 1968.

23. Hill, R., 'On the classical constitutive laws for elastic-plastic solids,' Recent Progress in Applied Mechanics, F.k.g. Odgvist volume, Wiley, New York, 1967.

24. Hill, R., 'On constitutive macro-variables for heterogeneous solids at finite strain,' Proc. R. Soc. Lond., Ser. A 326, pp. 131-147, 1972.

25. Rice, J.R., 'Inelastic constitutive relations for solids: an internal variable theory and its application to metal plasticity,' J. Mech. Phys. Solids 19, pp. 433-455, 1971.

26. Rice, J.R., 'Continuum plasticity in relation to microscale deformation mechanisms,' Metallurgical Effects at High Strain Rates (Eds R.W. Rohde, B.M. Butcher, J.R. Holland and C.H. Karners), Plenum Press, New York, pp. 93-106, 1973.

27. Mandel, J., 'plasticite et viscoplasticite,' CISM Lecture Notes N.97, Udine, Springer Wien, 1971.

28. Mandel, J., 'Equations constitutives et directeurs dans les millieux plastiques et viscoplastiques,' Int. J. Solids Struct. 9, pp. 725-740, 1973.

29. Lee, E.H., 'Elastic-plastic deformation at finite strains,' J. Appl. Mech., 36, pp. 1-6, 1969.

30. Lee, E.H., 'Some comments on elastic-plastic analysis,' Int. J. Solids Struct., 17, pp. 859-872, 1981.

31. Green, A.E. and P.M. Naghdi, 'A general theory of an elastic-plastic continuum,' Arch. Rat. Mech. Anal., 18, pp. 251-281, 1965.

32. Rice, J.R., 'The localization of plastic deformation,' Theoretical and Applied Mechanics(Edited by W. T. Koiter), 207-220. North-Holland, Amsterdam, 1977.

33. Hutchinson, J.W., 'Survey of some recent work on the mechanics of necking,' Proc. 8th U.S. Nat. Conge. Appl. Mech. (Edited by R. E. Kelly), PP. 87-98. Western Periodicals, 1979.

34. Nagtegaal J.C. and J.E. de Jong, 'Some aspects of non-isotropic work hardening in finite plasticity,' Plasticity of Metals at Finite Strain: Theory, Computation, and Experiment (Edited by E. H. Lee and R.L. Mallett), 65-102, 1982.

35. Neale K.W. and S.C. Shrivastava, `Finite elastic-plastic torsion of a circular bar,' Engr. Fracture Mech., vol. 21, No. 4, pp. 747-754, 1985.

36. Valanis, K.C., 'The viscoelastic potential and its thermodynamic foundations,' J. of Math. and Phy., 47, 262, 1968.

37. Valanis, K.C., 'Effect of prior deformation on cyclic responses of metals,' J. Appl. Mech., 41, pp. 441-447, 1974.

38. Wu, H.C. and H.C. Lin,'Combined plastic waves in a thin walled tube,' Int.' J. Solids Structures, 10, 1947, pp. 92-96.

39. Valanis, K.C. and Wu, H.C., ' Endochronic representation of cyclic creep and relaxation of Metals,' J. Appl. Mech., 1975, pp. 67-73.

40. Wu, H.C. and H.C. Lin, 'Strain-rate effect in the endochronic theory of viscoplasticity,' J. Appl. Mech., 43, 1976, pp. 92-96.

41. Bazant, Z.P., 'A new approach to inelasticity and failure of concrete, sand and rock: Endochronic theory,' Proc. Soc. of Engng. Sci. 11th Annual Meeting, ED. G.J.Dvorak, 1974, pp. 158-159.

42. Bazant, Z. P. and P. D. Bhat., 'Endochronic theory of inelasticity and failure of concrete,' J. Eng. Mech. Div., ASCE, 102, 1976, 701-722.

43. Bazant, Z. P. and R. J. Krizek, ' Endochronic constitutive law for liquefaction of sand,' J. Engng. Mech. Div., Proc. Am. Soc. Civil Eng., 102, 1976, pp. 225-238.

44. Sandler, I.S., 'On the uniqueness and stability of endochronic theories of material behavior,' J. Appl. Mech., 45 263, 1978.

45. Valanis, K. C. and H. E. Read, 'A new endocronic plasticity model for soils,' Soil Mechanics-Transient and Cyclic Loads (Ed. G. H. Pande and O. C. Zienkiewicz), John Wiley, New York, 1982.

46. Valanis, K.C., 'Fundamental consequences of a new intrinsic time measure plasticity as a limit of the endochronic theory,' Arch. Mechanics, pp.171-191, 1980.

47. Valanis, K.C., 'Endochronic theory with proper hysteresis loop closure properties,' Systems, Science and Software Report SSS-R-80-4182,1979.

48. Valanis, K. C. and C. F. Lee, 'Endocronic theory of cyclic plasticity with application,' J. appl. Mech., March, 1983.

49. Lin, H.C. and H.C. Wu, 'On the improved endochronic theory of viscoplasticity and its application to plastic-wave propagation,' Int. J. Solids Structures, Vol. 19, No. 7, pp 587-599, 1983.

50. Valanis, K.C., and J. Fan, 'Endochronic analysis of cyclic elasto-plastic strain fields in a notched plate,' J. Appl. Mechanics. 1984.

51. Pindera, M. J. and C. T. Herakovich, 'An endochronic modal for the response of unidirectional composites under off-axis tensile load,' Mech. of Composite Materials (Ed. Z. Hashin and C. t. Herakovich),1982.

52. Valanis, K. C., 'Endochronic theory of plastic fluids,' Proceedings, Symposium on Applications of Numerical Methods to Forming Processes, ED. H. Armen and R.F. Jones Jr., ASME, AMD vol. 28, pp.49, San Francisco 1978.

53. Valanis, K.C. and J.Y. Wang, 'Endochronic analysis of finite plastic bending,' to be submitted to J. Appl. Mechanics.

54. Valanis, K.C. and T. Nashiro, 'Systematic determination of material functions in the endochronic theory,' J. of Engineering Materials and Technology, 1985.

55. Fan, J. 'A comprehensive numerical study and experimental verification of endochronic plasticity,' Dissertation, Univ. of Cincinnati, 1983.

56. Householder, A.S., 'Principle of numerical analysis,' Chapter 3, pp.86, 1953.

57. Valanis, K.C., and H.C. Wu, 'Material instabilities in the experimental study of the plastic compressibility of some important metals,' Report No. M & H 1.03, AFOSR Grant Nr70-1916, August, 1971.

58. Kudo, H. and S. Matsubara, 'Joint examination project of validity of various numerical methods for the analysis of metal forming processes,' Metal Forming Plasticity, Ed. H. Lippmann, IUTAM symposium tutzing/Gremany, 1978,pp.378-403.

APPENDIX - COMPUTER PROGRAM

```
C PROGRAM NAME              FELP
C
C FUNCTION          ENDOCHRONIC ANALYSIS OF LARGE PLASTIC
C                     DEFORMATION OF PLANE STRAIN
C
C DISCRIPTION OF IMPORTANT PARAMETERS IN THE PROGRAM
C   NEM --- NUMBER OF ELEMENT
C   NNM --- NUMBER OF NODES
C   NDF --- NUMBER OF DEGREE OF FREEDOM AT A NODE
C   NPE --- NUMBER OF NODES PER ELEMENT
C   TH --- THICKNESS OF PLANE
C   GO,GAMA,CR1,AR1 --- MATERIAL CONSTANTS RELATED TO KERNEL FUNCTION
C   NRMAX,NCMAX --- MAXIMUM NUMBER OF ROW AND COLUM OF STIFFNESS MATRIX
C   MAXE,MAXD --- MAXIMUM NUMBER OF ELEMENT AND DISPLACEMENT B.C.
C   NHBW --- HALF BAND WIDTH
C   ERRO,ERR --- TOLERANCE FOR INTRINSIC TIME
C   NBDF,NBSF --- NUMBER OF NODES (DISPLACEMENT AND FORCE PRESCRIBED)
C
C DISCRIPTION OF IMPORTANT ARRAIES IN THE PROGRAM
C   GSTIFT(NRMAX,NCMAX) --- BANDED GLOBEL STIFFNESS MATRIX
C   GF,GFE,GFP(NCMAX) --- VECTORS OF TOTAL, APPLIED, AND PSEUDOFORCE, RESPECTIVELY
C   XT,YT(NNM) --- MATERIAL COORDINATES OF NODES
C   BI'S,CI'S(NEM) --- DIEEERENCE OF MATERIAL COORDINATES B'S AND C'S
C   PSIT(NEM,2,2,6) --- VALUES OF
C   DXYT,DYXT(NEM) --- DX/DY AND DY/DX
C   CX,CY,CXY(NEM) --- CAUCHY-GREEN DEFORMATION TENSOR
C   DCX,DCY,DCXY(NEM) --- INCREMENTAL OF CAUCHY-GREEN DEFORMATION TENSOR
C   TX,TY,TXY(NEM) --- STRESS
C   DZO,DZ1(NEM) --- PREVIOUS AND PRESENT INCREMENTAL INTRINSIC TIME
C   BQ'S Q'S(NEM) --- QUANTITIES RELATED TO CALCULATION OF PSEUDOFORCEO
C   UT,VT(NNM) --- DISPLACEMENT AT NODES IN X AND Y DIRECTION
C   IBDF,VBDF(NBDF) --- NODES AND VALUE VECTOR OF DISPLACEMENT B.C.
C   IBSF,VBSF(NBSF) --- NODES AND VALUE VECTOR OF FORCE B.C.
C   NOD(NEM,3) --- NODES OF ELEMENTS
C   VOT(NEM) --- VOLUM OF ELEMENTS
C
      IMPLICIT REAL*8(A-H,O-Z)
      DIMENSION GSTIFT(300,50),GF(300),GFE(300),GFP(300),GF1(300),
     1         DXY(2,2),DYX(2,2),NEDGE(50),IPRINT(30),DELT(700),
     1         BRT(700),SEL(700),FTU(700),EDZ(700), SEL1(700),
     1         EDZ1(260)
      COMMON/UNIT1/BI1(260),BI2(260),BI3(260),CI1(260),CI2(260),
     1       CI3(260)
      COMMON/UNIT2/DCX(260),DCY(260),DCXY(260),DZO(260),DZ1(260),
     1       CX(260),CY(260),CXY(260),TX(260),TXY(260),TY(260),
     1       DXYT(260,2,2),DYXT(260,2,2),QX1(260),QY1(260),QXY1(260),
     1       BQX1(260),BQY1(260),BQXY1(260),UT(150),VT(150),
     1       PSIT(260,2,2,6)
      COMMON/UNIT3/XT(150),YT(150),NOD(260,3),VOT(260)
```

```
      COMMON/UNIT4/IBDF(50),VBDF(50),IBSF(20),VBSF(20)
      COMMON/CONST/NEM,NNM,NDF,NPE
C
      DATA TH/1.0D0/
      DATA NRMAX,NCMAX,MAXE,MAXD/300,50,260,50/
      DATA G0,GAMA,CR1,AR1/1.d+0,1.0D+0,1.0D+0,200.0D+0/
C
      NDF=2
      NPE=3
C
      READ(15,*)NNP,NDZ
C NNP --- NUMBER OF INCREMENTAL STEPS
C NDZ --- NUMBER OF ITERATION FOR INTRINSIC TIME
C
      READ(15,*)NPRINT
      DO 9605 I=1,NPRINT
      READ(15,*)IPRINT(I)
 9605 CONTINUE
C NPRINT --- NUMBER OF INTERMEDIATE STEPS AT WHICH RESULTS PRINTED
C IPRINT(NPRINT) --- STEP NUMBER VECTOR
C
      READ(15,*)IMES
C IMES --- TYPE OF INPUT: IMES=0 INFORMATION FOR NODES AND ELEMENTS
C      FROM READ STATEMENT IMES=1 FROM CALCULATION FOR REGULAR DOMAIN
C
      IF(IMES.EQ.0)GO TO 9500
C
C INFORMATION FOR RECTAGULAR BLOCK IN FORGE PROCESS
C NX,NY --- NUMBER OF NODES IN X AND Y DIRECTION
C XL,YL --- LENGTH OF PLATE IM X AND Y DIRECTION
C ITYPE --- ITYPE=1 FIXD END, ITYPE=0 SHEAR FREE END
      READ(15,*)NX,NY,XL,YL,ITYPE
      CALL NODE(NX,NY,XL,YL,NEQ)
      CALL DFSF(NX,NY,ITYPE,NBDF,NBSF)
      ND=2*NX+2*NY-4
      DO 260 I=1,NX
      NEDGE(I)=I
      NEDGE(NX+NY+I-2)=NNM-I+1
  260 CONTINUE
      NEDGE(NX+1)=3*NX-1
      NEDGE(2*NX+NY-1)=(2*NX-1)*(NY-2)+1
      DO 270 I=1,NY-3
      NEDGE(NX+I+1)=NEDGE(NX+I)+2*NX-1
      NEDGE(2*NX+NY-1+I)=NEDGE(2*NX+NY-2+I)-2*NX+1
  270 CONTINUE
      GO TO 9600
C
 9500 READ(15,*)NEM,NNM
      DO 9300 I=1,NNM
      READ(15,*)XT(I),YT(I)
 9300 CONTINUE
```

```
      DO 9310 I=1,NEM
      READ(15,*)NOD(I,1),NOD(I,2),NOD(I,3)
 9310 CONTINUE
      READ(15,*)NBDF
      DO 9320 I=1,NBDF
      READ(15,*)IBDF(I),VBDF(I)
 9320 CONTINUE
      READ(15,*)NBSF
      DO 9400 I=1,NBSF
      READ(15,*)IBSF(I),VBSF(I)
 9400 CONTINUE
C
 9600 NEQ=NNM*NDF
      WRITE(16,300)
  300 FORMAT(4X,'ELEMENT',10X,'NODES'/)
      WRITE(16,301)(N,(NOD(N,I),I=1,NPE),N=1,NEM)
  301 FORMAT(2X,I5,7X,3I5)
      WRITE(16,310)
      WRITE(16,305)
  305 FORMAT(4X,'NODE',15X,'COORDINATES'/)
      WRITE(16,306)(N,XT(N),YT(N),N=1,NNM)
  306 FORMAT(1X,I5,10X,2F10.4)
      WRITE(16,310)
  310 FORMAT(///)
      WRITE(16,315)NBDF
  315 FORMAT(4X,'DISPLACSMENT B.C.',I5/)
      IF(NBDF.EQ.0) GO TO 10
      WRITE(16,314)
  314 FORMAT(7X,'POSITION      VALUE'/)
      DO 5 I=1,NBDF
      WRITE(16,*)IBDF(I),VBDF(I)
    5 CONTINUE
   10 WRITE(16,310)
      WRITE(16,316)NBSF
  316 FORMAT(4X,'FORCE B.C.',I5/)
      IF(NBSF.EQ.0) GO TO 8
      WRITE(16,314)
      DO 6 I=1,NBSF
      WRITE(16,*)IBSF(I),VBSF(I)
    6 CONTINUE
C
    8 ERRO=0.01
      WRITE(16,310)
      WRITE(16,*)'GO =',GO
      WRITE(16,*)'LAMDA =',GAMA
      NHBW=0
      DO 15 N=1,NEM
      DO 15 I=1,NPE
      DO 15 J=1,NPE
      NW=(IABS(NOD(N,I)-NOD(N,J))+1)*NDF
      IF(NHBW.LT.NW) NHBW=NW
```

```
   15 CONTINUE
      WRITE(16,310)
      WRITE(16,325) NHBW
  325 FORMAT(4X,'NHBW  =',I5)
C
      DO 20 I=1,NEQ
      GFE(I)=0.0
   20 CONTINUE
C
      DYX(1,1)=1.
      DYX(2,2)=1.
      DYX(1,2)=0.
      DYX(2,1)=0.
      DXY(1,1)=1.
      DXY(2,2)=1.
      DXY(1,2)=0.
      DXY(2,1)=0.
      DO 35 I=1,NEM
      DZ0(I)=0.
      DZ1(I)=0.
      TX(I)=0.
      TXY(I)=0.
      TY(I)=0.
      BQX1(I)=0.
      BQY1(I)=0.
      BQXY1(I)=0.
      CX(I)=1.
      CY(I)=1.
      CXY(I)=0.
      DCX(I)=0.
      DCY(I)=0.
      DCXY(I)=0.
      DO 36 I1=1,2
      DO 36 I2=1,2
      DXYT(I,I1,I2)=DXY(I1,I2)
      DYXT(I,I1,I2)=DYX(I1,I2)
   36 CONTINUE
   35 CONTINUE
      DO 38 I=1,NNM
      UT(I)=0.
      VT(I)=0.
   38 CONTINUE
C
      CALL BC(TH)
C
C****** STARTING THE LOADING STEPS ******
C
      DO 60 NP=1,NNP
      DO 45 I=1,NEQ
      GF1(I)=0.
      DO 45 J=1,NHBW
```

```
      GSTIFT(I,J)=0.
   45 CONTINUE
      IRES=0
C
      CALL STIFF(GSTIFT,NRMAX,NCMAX,GO,GAMA)
C
      IF (NBDF.EQ.0)GO TO 100
      DO 102 I=1,NBDF
      IE=IBDF(I)
      VE=VBDF(I)
      CALL BNDRY(NRMAX,NCMAX,NEQ,NHBW,GSTIFT,GF1,IE,VE)
  102 CONTINUE
  100 CONTINUE
C
      IF(NBSF.EQ.0)GO TO 105
      DO 25 I=1,NBSF
      II=IBSF(I)
      GF1(II)=GF1(II)+VBSF(I)
   25 CONTINUE
  105 CONTINUE
C
C$$$$$ STARTING THE INTERATION FOR DZ $$$$$
C
      DO 110 NZ=1,NDZ
      DO 115 I=1,NEQ
      GFP(I)=0.
  115 CONTINUE
C
      CALL PF(GFP,IBDF,NRMAX,MAXD,CR1,AR1,NBDF)
C
      DO 160 N=1,NEQ
      GF(N)=GF1(N)-GFP(N)
  160 CONTINUE
C
      CALL SOL(NRMAX,NCMAX,NEQ,NHBW,GSTIFT,GF,IRES)
      IRES=1
C
      CALL DZZ(GF,NRMAX)
C
      DO 175 N=1,NEM
      Z1=DZ1(N)
      Z0=DZ0(N)
      ERR=DABS(Z1-Z0)/Z1
      IF(ERR.GT.ERR0) GO TO 180
  175 CONTINUE
      ITER=NZ
C
      GO TO 200
  180 DO 210 N=1,NEM
      DZ0(N)=DZ1(N)
  210 CONTINUE
```

```
  110 CONTINUE
C
C$$$$$ ENDING THE INTERATION FOR DZ $$$$$
C
  200 CONTINUE
C
      CALL RES(GO,GF,NRMAX,GAMA)
C
C  QUANTITIES RELVENT TO BLOCH FORGING PROCESS
      DISMAX=XL+UT(NNM)
      DISRT=DISMAX/XL
      DELT(NP)=VT(1)
      BRT(NP)=DISRT
      SEL(NP)=TY(NEM-5)
      SEL(NP)=TY(NEM-21)
      EDZ(NP)=DZ1(NEM-5)
      EDZ1(NP)=DZ1(NEM-21)
      STY=0.
      JJJ=NX-1
      DO 254 I=1,JJJ
      STY=TY(4*I-3)+STY
  254 CONTINUE
      FTU(NP)=STY/JJJ
C
C PRINTING INTERMIDIATE RESULTS
C
      DO 2005 I=1,NPRINT
      IF(NP.EQ.IPRINT(I)) GO TO 2006
 2005 CONTINUE
      GO TO 60
 2006 WRITE(16,310)
      WRITE(16,340)
  340 FORMAT(4X,'ELEMENT                STRAIN'/)
      DO 2000 N=1,NEM
      EX=(CX(N)-1.0d+0)/2.0d+0
      EY=(CY(N)-1.0d+0)/2.0d+0
      EXY=CXY(N)/2.0d+0
      WRITE(16,2010)N,EX,EY,EXY
 2000 CONTINUE
 2010 FORMAT(2X,I5,3F20.7)
      WRITE(16,310)
      WRITE(16,600)
  600 FORMAT(4X,'ELEMENT                    STRESSES    '/)
      DO 220 N=1,NEM
      WRITE(16,605)N,TX(N),TY(N),TXY(N)
  220 CONTINUE
  605 FORMAT(4X,I5,4F15.7)
      WRITE(16,310)
      WRITE(16,410)
  410 FORMAT(4X,' NODES          DISPLACEMENTS'/)
      DO 230 N=1,NNM
```

```
      WRITE(16,415)N,UT(N),VT(N)
  230 CONTINUE
  415 FORMAT(4X,I5,4X,2F15.10)
      WRITE(16,310)
      WRITE(16,420)
  420 FORMAT(4X,'   NODES                    STRESSES'/)
      DO 250 I=1,NNM
      NCON=0
      SUMX=0.0D+0
      SUMY=0.0D+0
      SUMXY=0.0D+0
      DO 255 N=1,NEM
      DO 255 J=1,NPE
      NI=NOD(N,J)
      IF(I.NE.NI) GO TO 255
      SUMX=SUMX+TX(N)
      SUMY=SUMY+TY(N)
      SUMXY=SUMXY+TXY(N)
      NCON=NCON+1
  255 CONTINUE
      SUMX=SUMX/NCON
      SUMY=SUMY/NCON
      SUMXY=SUMXY/NCON
      WRITE(16,605)I,SUMX,SUMY,SUMXY
  250 CONTINUE
      WRITE(16,310)
      WRITE(16,610)
  610 FORMAT(4X,'EDGE'/)
      DO 275 I=1,ND
      II=NEDGE(I)
      UD=XT(II)+UT(II)
      VD=YT(II)+VT(II)
      WRITE(16,*)UD,VD
  275 CONTINUE
   60 CONTINUE
C
C****** ENDING LOADING STEPS *****
C
C PRINTING QUANTITIES RELVENT TO BLOCH FORGE PROCESS
      WRITE(16,310)
      WRITE(16,610)
      DO 280 I=1,ND
      II=NEDGE(I)
      WRITE(16,*)XT(II),YT(II)
  280 CONTINUE
      WRITE(16,310)
      WRITE(16,620)
  620 FORMAT(4X,'RATIO'/)
      DO 290 N=1,NNP
      WRITE(16,*)DELT(N),BRT(N)
  290 CONTINUE
```

```
      WRITE(16,310)
      DO 291 N=1,NNP
      WRITE(16,*)DELT(N),SEL(N)
  291 CONTINUE
      STOP
      END
C
      SUBROUTINE SOL(NRM,NCM,NEQNS,NBW,BAND,RHS,IRES)
C***SOLVING A BAND SYMMETRIC SYSTEMS OF EQNS
C***IN RESOLVING, IRES .GT. 0. LHS ELIMINATION IS SKIPPED
      IMPLICIT REAL*8(A-H,O-Z)
      DIMENSION BAND(NRM,NCM),RHS(NRM)
      MEQNS=NEQNS-1
      IF(IRES.GT.0) GO TO 40
      DO 30 NPIV=1,MEQNS
      NPIVOT=NPIV+1
      LSTSUB=NPIV+NBW-1
      IF(LSTSUB.GT.NEQNS) LSTSUB=NEQNS
      DO 20 NROW=NPIVOT,LSTSUB
C***INVERT ROWS AND COLUMNS FOR ROW FACTOR
      NCOL=NROW-NPIV+1
      FACTOR=BAND(NPIV,NCOL)/BAND(NPIV,1)
      DO 10 NCOL=NROW,LSTSUB
      ICOL=NCOL-NROW+1
      JCOL=NCOL-NPIV+1
   10 BAND(NROW,ICOL)=BAND(NROW,ICOL)-FACTOR*BAND(NPIV,JCOL)
   20 RHS(NROW)=RHS(NROW)-FACTOR*RHS(NPIV)
   30 CONTINUE
      GO TO 70
   40 DO 60 NPIV=1,MEQNS
      NPIVOT=NPIV+1
      LSTSUB=NPIV+NBW-1
      IF(LSTSUB.GT.NEQNS) LSTSUB=NEQNS
      DO 50 NROW=NPIVOT,LSTSUB
      NCOL=NROW-NPIV+1
      FACTOR=BAND(NPIV,NCOL)/BAND(NPIV,1)
   50 RHS(NROW)=RHS(NROW)-FACTOR*RHS(NPIV)
   60 CONTINUE
C***BACK SUBSTITUTION
   70 DO 90 IJK=2,NEQNS
      NPIV=NEQNS+IJK+2
      RHS(NPIV)=RHS(NPIV)/BAND(NPIV,1)
      LSTSUB=NPIV-NBW+1
      IF(LSTSUB.LT.1) LSTSUB=1
      NPIVOT=NPIV-1
      DO 80 JKI=LSTSUB,NPIVOT
      NROW=NPIVOT-JKI+LSTSUB
      NCOL=NPIV-NROW+1
      FACTOR=BAND(NROW,NCOL)
   80 RHS(NROW)=RHS(NROW)-FACTOR*RHS(NPIV)
   90 CONTINUE
```

AD-A194 167 AN ENDOCHRONIC RATE-SENSITIVE CONSTITUTIVE EQUATION FOR METALS APPLICATIO..(U) CINCINNATI UNIV OH K C VALANIS 01 MAR 88 ARO-21663.2-EG DAAG29-85-K-0017 3/3

UNCLASSIFIED F/G 11/6.1 NL

[redacted]

END
DATE FILMED
8 88
DTIC

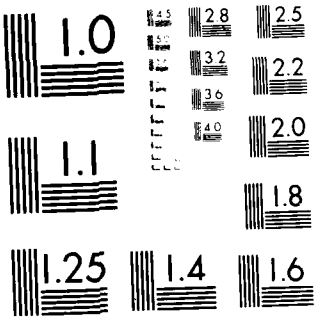

```
      RHS(1)=RHS(1)/BAND(1,1)
      RETURN
      END
C
      SUBROUTINE BNDRY(NRMAX,NCMAX,NEQ,NHBW,S,SL,IE,SVAL)
C***THIS PROGRAM IMPOSES THE PRESCRIBED B. C. ON
C***THE SYSTEM MATRIX(BANDED SYMMETRIC MATRIX)
C***S IS THE STIFFNESS MATRIX
C***SL IS THE LOAD VECTOR
C***IE IS THE LABEL OF THE VARIABLE THAT IS PERSCRIBED
C***SVAL IS THE VALUE OF PRESCRIBED VARIABLE
      IMPLICIT REAL*8(A-H,O-Z)
      DIMENSION S(NRMAX,NCMAX),SL(NRMAX)
      IT=NHBW-1
      I=IE-NHBW
      DO 10 II=1,IT
      I=I+1
      IF(I.LT.1) GO TO 10
      J=IE-I+1
      SL(I)=SL(I)-S(I,J)*SVAL
      S(I,J)=0.0
   10 CONTINUE
      S(IE,1)=1.0
      SL(IE)=SVAL
      I=IE
      DO 20 II=2,NHBW
      I=I+1
      IF(I.GT.NEQ) GO TO 20
      SL(I)=SL(I)-S(IE,II)*SVAL
      S(IE,II)=0.0
   20 CONTINUE
      RETURN
      END
C
      SUBROUTINE MV(N,A,MAXE)
C***THE INVERSE OF MATRIX A(DIMENSION IS N)
      IMPLICIT REAL*8(A-H,O-Z)
      DIMENSION A(MAXE,MAXE),B(200),C(200)
      A(1,1)=1.0/A(1,1)
      NN=N-1
      DO 360 M=1,NN
      K=M+1
      DO 300 I=1,M
      C(I)=0.0
      B(I)=0.0
      DO 300 J=1,M
      B(I)=B(I)+A(I,J)*A(J,K)
  300 CONTINUE
      D=0.0
      DO 310 I=1,M
      D=D+A(K,I)*B(I)
```

```
  310 CONTINUE
      D=A(K,K)-D
      A(K,K)=1.0/D
      DO 320 I=1,M
      A(I,K)=-B(I)/D
  320 CONTINUE
      DO 330 J=1,M
      DO 330 I=1,M
  330 C(J)=C(J)+A(K,I)*A(I,J)
      DO 340 J=1,M
      A(K,J)=-C(J)/D
  340 CONTINUE
      DO 350 I=1,M
      DO 350 J=1,M
  350 A(I,J)=A(I,J)-B(I)*A(K,J)
  360 CONTINUE
      RETURN
      END
C
      SUBROUTINE DXDY(N,DYX,DXY,EUV)
C***TO CALCULATE DX/DY AND DY/DX
      IMPLICIT REAL*8(A-H,O-Z)
      COMMON/UNIT1/BI1(260),BI2(260),BI3(260),CI1(260),CI2(260),
     1     CI3(260)
      DIMENSION BE(3),CE(3),EUV(6),DYX(2,2),DXY(2,2)
      BE(1)=BI1(N)
      BE(2)=BI2(N)
      BE(3)=BI3(N)
      CE(1)=CI1(N)
      CE(2)=CI2(N)
      CE(3)=CI3(N)
      DO 50 I=1,2
      DYX(I,1)=0.
      DYX(I,2)=0.
      DO 50 J=1,3
      IF(I.EQ.1) K=2*J-1
      IF(I.EQ.2) K=2*J
      DYX(I,1)=DYX(I,1)+BE(J)*EUV(K)
      DYX(I,2)=DYX(I,2)+CE(J)*EUV(K)
   50 CONTINUE
      DYX(1,1)=DYX(1,1)+1.
      DYX(2,2)=DYX(2,2)+1.
      D=DYX(1,1)*DYX(2,2)-DYX(1,2)*DYX(2,1)
      DXY(1,1)=DYX(2,2)/D
      DXY(2,2)=DYX(1,1)/D
      DXY(1,2)=-DYX(1,2)/D
      DXY(2,1)=-DYX(2,1)/D
      RETURN
      END
C
      SUBROUTINE NODE(NX,NY,XL,YL,NEQ)
```

```
C***TO GENERIZE THE NODES OF THE ELEMENTS AND THE COORDINATES OF THE NODES.
      IMPLICIT REAL*8(A-H,O-Z)
      COMMON/UNIT1/BI1(260),BI2(260),BI3(260),CI1(260),CI2(260),
     1     CI3(260)
      COMMON/UNIT3/XT(150),YT(150),NOD(260,3),VOT(260)
      COMMON/CONST/NEM,NNM,NDF,NPE
      NX1=NX-1
      NY1=NY-1
      NEM=NX1*NY1*4
      NNM=(2*NX-1)*NY1+NX
      NEQ=NNM*NDF
      NOD(1,1)=NX+1
      NOD(1,2)=2
      NOD(1,3)=1
      NOD(2,1)=NOD(1,1)
      NOD(2,2)=NOD(1,3)
      NOD(2,3)=2*NX
      NOD(3,1)=NOD(1,1)
      NOD(3,2)=NOD(2,3)
      NOD(3,3)=2*NX+1
      NOD(4,1)=NOD(1,1)
      NOD(4,2)=NOD(3,3)
      NOD(4,3)=NOD(1,2)
      DO 50 I=1,NX-2
      DO 50 J=1,4
      DO 50 K=1,3
      II=I*4+J
      NOD(II,K)=NOD((I-1)*4+J,K)+1
   50 CONTINUE
      DO 100 I=1,NY-2
      DO 100 J=1,NX1*4
      DO 100 K=1,3
      II=I*NX1*4+J
      NOD(II,K)=NOD((I-1)*NX1*4+J,K)+2*NX-1
  100 CONTINUE
      DX=XL/NX1
      DY=YL/NY1
      DO 150 N=1,NY
      DO 150 I=1,NX
      NI=(N-1)*(2*NX-1)+I
      XT(NI)=(I-1)*DX
      YT(NI)=YL-(N-1)*DY
  150 CONTINUE
      DO 160 N=1,NY1
      DO 160 I=1,NX1
      NI=(N-1)*(2*NX-1)+NX+I
      XT(NI)=DX*(2*I-1)/2
      YT(NI)=YL-DY*(2*N-1)/2
  160 CONTINUE
      RETURN
      END
```

```
C
      SUBROUTINE STIFF(GSTIFT,NRMAX,NCMAX,GO,GAMA)
C***TO FORM THE STIFFNESS MATRIX
      IMPLICIT REAL*8(A-H,O-Z)
      DIMENSION GSTIFT(NRMAX,NCMAX),PSI(2,2,6),BE(3),CE(3),
     1    PSI1(2,2,6),PSI2(2,2,6),ELSTIF(6,6),DXY(2,2),T(2,2)
     1    ,BC(6)
      COMMON/UNIT1/BI1(260),BI2(260),BI3(260),CI1(260),CI2(260),
     1     CI3(260)
      COMMON/UNIT2/DCX(260),DCY(260),DCXY(260),DZ0(260),DZ1(260),
     1     CX(260),CY(260),CXY(260),TX(260),TXY(260),TY(260),
     1     DXYT(260,2,2),DYXT(260,2,2),QX1(260),QY1(260),QXY1(260),
     1     BQX1(260),BQY1(260),BQXY1(260),UT(150),VT(150),
     1     PSIT(260,2,2,6)
      COMMON/UNIT3/XT(150),YT(150),NOD(260,3),VOT(260)
      COMMON/CONST/NEM,NNM,NDF,NPE
      DO 45 N=1,NEM
      VOL=VOT(N)
      BE(1)=BI1(N)
      BE(2)=BI2(N)
      BE(3)=BI3(N)
      CE(1)=CI1(N)
      CE(2)=CI2(N)
      CE(3)=CI3(N)
      DO 50 I=1,2
      DO 50 J=1,2
      DXY(I,J)=DXYT(N,I,J)
   50 CONTINUE
      S1=1.
      S2=0.
      DO 65 IS=1,2
      DO 70 IK=1,2
      DO 70 IM=1,3
      M1=2*IM-1
      M2=2*IM
      PSI(IS,IK,M1)=(DXY(1,IK)*BE(IM)+DXY(2,IK)*CE(IM))*S1
      PSI(IS,IK,M2)=(DXY(1,IK)*BE(IM)+DXY(2,IK)*CE(IM))*S2
      PSIT(N,IS,IK,M1)=PSI(IS,IK,M1)
      PSIT(N,IS,IK,M2)=PSI(IS,IK,M2)
   70 CONTINUE
      S1=0.
      S2=1.
   65 CONTINUE
      GJ=DYXT(N,1,1)*DYXT(N,2,2)-DYXT(N,1,2)*DYXT(N,2,1)
      GG=GAMA*DLOG(GJ)+GO
      T(1,1)=TX(N)*GJ
      T(2,2)=TY(N)*GJ
      T(1,2)=TXY(N)*GJ
      T(2,1)=T(1,2)
      DO 80 M=1,6
      DO 80 K=1,2
```

```
      DO 80 I=1,2
      PSI1(K,I,M)=0.
      PSI2(K,I,M)=0.
      DO 80 IS=1,2
      PSI1(K,I,M)=PSI1(K,I,M)+PSI(K,IS,M)*T(IS,I)
     1  +PSI(IS,I,M)*T(K,IS)
      PSI2(K,I,M)=PSI2(K,I,M)+PSI(IS,I,M)*T(K,IS)
   80 CONTINUE
      DO 85 J=1,6
      DO 85 M=1,6
      ELSTIF(J,M)=0.
      DO 90 K=1,2
      DO 90 I=1,2
      S=PSI(I,K,J)*(PSI1(K,I,M)+PSI2(I,K,M))
      S1=PSI(I,K,J)*(PSI(I,K,M)+PSI(K,I,M))
      ELSTIF(J,M)=ELSTIF(J,M)-S+GG*S1
   90 CONTINUE
      ELSTIF(J,M)=ELSTIF(J,M)*VOL
   85 CONTINUE
      DO 150 I=1,6
      DO 150 J=1,6
      ELSTIF(I,J)=ELSTIF(I,J)+(PSI(1,1,I)+PSI(2,2,I))*
     1            (PSI(1,1,J)+PSI(2,2,J))*GAMA*VOL
  150 CONTINUE
C
      DO 92 I=1,NPE
      NR=(NOD(N,I)-1)*NDF
      DO 92 II=1,NDF
      NR=NR+1
      L=(I-1)*NDF+II
      DO 94 J=1,NPE
      NCL=(NOD(N,J)-1)*NDF
      DO 95 JJ=1,NDF
      M=(J-1)*NDF+JJ
      NC=NCL+JJ+1-NR
      IF(NC) 95,95,96
   96 GSTIFT(NR,NC)=GSTIFT(NR,NC)+ELSTIF(L,M)
   95 CONTINUE
   94 CONTINUE
   92 CONTINUE
   45 CONTINUE
      RETURN
      END
C
      SUBROUTINE DZZ(GF,NRMAX)
C***TO CALCULATE DZ
      IMPLICIT REAL*8(A-H,O-Z)
      DIMENSION DYX(2,2),GF(NRMAX),DUV(6),PSI(2,2,6),
     1    PSI1(2,2,6),PSI2(2,2,6),PSI3(2,2,6),DC(2,2)
      COMMON/UNIT2/DCX(260),DCY(260),DCXY(260),DZ0(260),DZ1(260),
     1     CX(260),CY(260),CXY(260),TX(260),TXY(260),TY(260),
```

```
     1      DXYT(260,2,2),DYXT(260,2,2),QX1(260),QY1(260),QXY1(260),
     1      BQX1(260),BQY1(260),BQXY1(260),UT(150),VT(150),
     1      PSIT(260,2,2,6)
      COMMON/UNIT3/XT(150),YT(150),NOD(260,3),VOT(260)
      COMMON/CONST/NEM,NNM,NDF,NPE
      DO 150 N=1,NEM
      DO 155 I=1,NPE
      NI=NOD(N,I)
      DO 155 J=1,NDF
      DUV((I-1)*2+J)=GF((NI-1)*2+J)
  155 CONTINUE
      DO 160 I=1,2
      DO 160 K=1,2
      DYX(I,K)=DYXT(N,I,K)
      DO 160 M=1,6
      PSI(I,K,M)=PSIT(N,I,K,M)
  160 CONTINUE
      C1=CX(N)
      C2=CY(N)
      C12=CXY(N)
      DD=C1*C2-C12*C12
      VC1=C2/DD
      VC2=C1/DD
      VC12=-C12/DD
      DO 165 M=1,6
      DO 166 I=1,2
      DO 166 IA=1,2
      PSI1(I,IA,M)=0.0
      DO 166 K=1,2
      PSI1(I,IA,M)=PSI1(I,IA,M)+PSI(I,K,M)*DYX(K,IA)
  166 CONTINUE
      DO 167 IA=1,2
      DO 167 IB=1,2
      PSI2(IA,IB,M)=0.0
      DO 167 I=1,2
      PSI2(IA,IB,M)=PSI2(IA,IB,M)+PSI1(I,IA,M)*DYX(I,IB)
  167 CONTINUE
      DO 168 IA=1,2
      DO 168 IB=1,2
      PSI3(IA,IB,M)=PSI2(IA,IB,M)+PSI2(IB,IA,M)
  168 CONTINUE
  165 CONTINUE
      DO 170 IA=1,2
      DO 170 IB=1,2
      DC(IA,IB)=0.
      DO 170 M=1,6
      DC(IA,IB)=DC(IA,IB)+PSI3(IA,IB,M)*DUV(M)
  170 CONTINUE
      DU1=VC1*DC(1,1)+VC12*DC(1,2)
      DU2=VC12*DC(1,2)+VC2*DC(2,2)
      DU12=VC1*DC(1,2)+VC12*DC(2,2)
```

```
      DU21=VC12*DC(1,1)+VC2*DC(1,2)
      DZ=DU1*DU1+2.*DU12*DU21+DU2*DU2
      DZ=DSQRT(DZ)
      DZ1(N)=DZ
      DCX(N)=DC(1,1)
      DCY(N)=DC(2,2)
      DCXY(N)=DC(1,2)
  150 CONTINUE
      RETURN
      END
C
      SUBROUTINE RES(GO,GF,NRMAX,GAMA)
      IMPLICIT REAL*8(A-H,O-Z)
C***THE RESULTS OF DISPLACEMENT AND STRESSES FOR EACH STEP
      COMMON/UNIT1/BI1(260),BI2(260),BI3(260),CI1(260),CI2(260),
     1     CI3(260)
      COMMON/UNIT2/DCX(260),DCY(260),DCXY(260),DZ0(260),DZ1(260),
     1     CX(260),CY(260),CXY(260),TX(260),TXY(260),TY(260),
     1     DXYT(260,2,2),DYXT(260,2,2),QX1(260),QY1(260),QXY1(260),
     1     BQX1(260),BQY1(260),BQXY1(260),UT(150),VT(150),
     1     PSIT(260,2,2,6)
      COMMON/UNIT3/XT(150),YT(150),NOD(260,3),VOT(260)
      COMMON/CONST/NEM,NNM,NDF,NPE
      DIMENSION DXY(2,2),DYX(2,2),EUV(6),GF(NRMAX),DUV(6)
      DO 100 N=1,NNM
      UT(N)=UT(N)+GF(2*N-1)
      VT(N)=VT(N)+GF(2*N)
  100 CONTINUE
      DO 110 N=1,NEM
      DO 120 I=1,NPE
      NI=NOD(N,I)
      EUV(2*I-1)=UT(NI)
      EUV(2*I)=VT(NI)
      DUV(2*I-1)=GF(2*NI-1)
      DUV(2*I)=GF(NI*2)
  120 CONTINUE
      DO 130 I=1,2
      DO 130 J=1,2
      DXY(I,J)=DXYT(N,I,J)
      DYX(I,J)=DYXT(N,I,J)
  130 CONTINUE
      GJ=DYX(1,1)*DYX(2,2)-DYX(1,2)*DYX(2,1)
      DJJ=0.0D+0
      DO 135 M=1,6
      DJJ=DJJ+(PSIT(N,1,1,M)+PSIT(N,2,2,M))*DUV(M)
  135 CONTINUE
      G=GAMA*DLOG(GJ)+GO
      TA=QX1(N)+G*DCX(N)+GAMA*CX(N)*DJJ
      TB=QY1(N)+G*DCY(N)+GAMA*CY(N)*DJJ
      TAB=QXY1(N)+G*DCXY(N)+GAMA*CXY(N)*DJJ
      T1J=TX(N)*GJ
```

```
      T2J=TY(N)*GJ
      T12J=TXY(N)*GJ
      D1=DXY(1,1)
      D2=DXY(2,2)
      D12=DXY(1,2)
      D21=DXY(2,1)
      T1=D1*D1*TA+2.*D1*D21*TAB+D21*D21*TB
      T2=D12*D12*TA+2.*D12*D2*TAB+D2*D2*TB
      T12=D12*D1*TA+D12*D21*TAB+D2*D1*TAB+D2*D21*TB
      F1=0.0D0
      F2=0.0D0
      F12=0.0D0
      F21=0.0D0
      DO 140 M=1,6
      F1=F1+PSIT(N,1,1,M)*DUV(M)
      F2=F2+PSIT(N,2,2,M)*DUV(M)
      F12=F12+PSIT(N,1,2,M)*DUV(M)
      F21=F21+PSIT(N,2,1,M)*DUV(M)
  140 CONTINUE
      H1=T1J*F1+T12J*F21
      H12=T1J*F12+T12J*F2
      H21=T12J*F1+T2J*F21
      H2=T12J*F12+T2J*F2
      TXJ=T1J+T1-(H1+H1)
      TYJ=T2J+T2-(H2+H2)
      TXYJ=T12J+T12-(H12+H21)
      CALL DXDY(N,DYX,DXY,EUV)
      GJ1=DYX(1,1)*DYX(2,2)-DYX(1,2)*DYX(2,1)
C
      TX(N)=TXJ/GJ1
      TY(N)=TYJ/GJ1
      TXY(N)=TXYJ/GJ1
      DO 145 I=1,2
      DO 145 J=1,2
      DXYT(N,I,J)=DXY(I,J)
      DYXT(N,I,J)=DYX(I,J)
  145 CONTINUE
      CX(N)=DYX(1,1)*DYX(1,1)+DYX(2,1)*DYX(2,1)
      CY(N)=DYX(1,2)*DYX(1,2)+DYX(2,2)*DYX(2,2)
      CXY(N)=DYX(1,1)*DYX(1,2)+DYX(2,1)*DYX(2,2)
      BQX1(N)=QX1(N)
      BQY1(N)=QY1(N)
      BQXY1(N)=QXY1(N)
  110 CONTINUE
      RETURN
      END
C
      SUBROUTINE PF(GFP,IBDF,NRMAX,MAXD,CR1,AR1,NBDF)
      IMPLICIT REAL*8(A-H,O-Z)
C***TO CALCULATE PLASTIC FORCES
      COMMON/UNIT2/DCX(260),DCY(260),DCXY(260),DZ0(260),DZ1(260),
```

```
     1      CX(260),CY(260),CXY(260),TX(260),TXY(260),TY(260),
     1      DXYT(260,2,2),DYXT(260,2,2),QX1(260),QY1(260),QXY1(260),
     1      BQX1(260),BQY1(260),BQXY1(260),UT(150),VT(150),
     1      PSIT(260,2,2,6)
      COMMON/UNIT3/XT(150),YT(150),NOD(260,3),VOT(260)
      COMMON/CONST/NEM,NNM,NDF,NPE
      DIMENSION ELQT(2,2),ELGFP(6),IBDF(MAXD),GFP(NRMAX)
      DO 115 N=1,NEM
      VOL=VOT(N)
      ELDZ=DZ0(N)
      D1=DXYT(N,1,1)
      D2=DXYT(N,2,2)
      D12=DXYT(N,1,2)
      D21=DXYT(N,2,1)
      S=DEXP(-AR1*ELDZ)
      S1=CR1*(S-1.)
      QX=BQX1(N)*S+DCX(N)*S1
      QY=BQY1(N)*S+DCY(N)*S1
      QXY=BQXY1(N)*S+DCXY(N)*S1
      QX1(N)=QX
      QY1(N)=QY
      QXY1(N)=QXY
      ELQT(1,1)=D1*D1*QX+2.*D21*QXY*D1+D21*D21*QY
      ELQT(1,2)=D1*D12*QX+D12*D21*QXY+D1*D2*QXY+D21*D2*QY
      ELQT(2,2)=D12*D12*QX+2.*D2*D12*QXY+D2*D2*QY
      ELQT(2,1)=ELQT(1,2)
      DO 120 J=1,6
      ELGFP(J)=0.
      DO 120 I=1,2
      DO 120 K=1,2
      ELGFP(J)=ELGFP(J)+PSIT(N,I,K,J)*ELQT(K,I)*VOL
  120 CONTINUE
      DO 125 I=1,NPE
      NI=NOD(N,I)
      DO 130 K=1,NDF
      NII=(NI-1)*2+K
      DO 135 J=1,NBDF
      NJ=IBDF(J)
      IF (NII.EQ.NJ) GO TO 130
  135 CONTINUE
      GFP(NII)=ELGFP((I-1)*2+K)+GFP(NII)
  130 CONTINUE
  125 CONTINUE
  115 CONTINUE
      RETURN
      END
C
      SUBROUTINE BC(TH)
C***TO CALCULATE BI,CI,AND AREAS
      IMPLICIT REAL*8(A-H,O-Z)
      COMMON/UNIT1/BI1(260),BI2(260),BI3(260),CI1(260),CI2(260),
```

```
     1     CI3(260)
      COMMON/UNIT3/XT(150),YT(150),NOD(260,3),VOT(260)
      COMMON/CONST/NEM,NNM,NDF,NPE
      DIMENSION BE(3),CE(3),X(3),Y(3)
      DO 30 N=1,NEM
      DO 32 I=1,NPE
      NI=NOD(N,I)
      X(I)=XT(NI)
      Y(I)=YT(NI)
   32 CONTINUE
      AREA=X(1)*(Y(2)-Y(3))+X(2)*(Y(3)-Y(1))+X(3)*(Y(1)-Y(2))
      DO 31 I=1,NPE
      J=I+1
      IF(J.GT.NPE)J=J-NPE
      K=J+1
      IF(K.GT.NPE)K=K-NPE
      BE(I)=(Y(J)-Y(K))/AREA
      CE(I)=(X(K)-X(J))/AREA
   31 CONTINUE
      BI1(N)=BE(1)
      BI2(N)=BE(2)
      BI3(N)=BE(3)
      CI1(N)=CE(1)
      CI2(N)=CE(2)
      CI3(N)=CE(3)
      VOT(N)=AREA/2.*TH
   30 CONTINUE
      RETURN
      END
C
      SUBROUTINE DFSF(NX,NY,ITYPE,NBDF,NBSF)
      IMPLICIT REAL*8(A-H,O-Z)
      COMMON/UNIT4/IBDF(30),VBDF(30),IBSF(20),VBSF(20)
      IF(ITYPE.EQ.0)GO TO 3000
      NBDF=2*NX+NY-1+NX
      NBSF=0
      DO 3010 I=1,NX
      IBDF(2*I-1)=I*2-1
      VBDF(2*I-1)=0.D+00
      IBDF(2*I)=I*2
      VBDF(2*I)=-1.0D-03
 3010 CONTINUE
      DO 3020 I=1,NY-1
      IBDF(2*NX+I)=(2*NX-1)*I*2+1
      VBDF(2*NX+I)=0.D+00
 3020 CONTINUE
      DO 3030 I=1,NX
      IBDF(2*NX+NY-1+I)=(2*NX-1)*(NY-1)*2+2*I
      VBDF(2*NX+NY-1+I)=0.D+00
 3030 CONTINUE
      GO TO 4000
```

```
3000 NBDF=NX+NY
     NBSF=NX
     DO 4010 I=1,NX
     IBSF(I)=2*I
     VBSF(I)=1.0D-03
4010 CONTINUE
     VBSF(1)=5.0D-04
     VBSF(NX)=5.0D-04
     DO 4020 I=1,NY
     IBDF(I)=2*NX*(I-1)+1
     VBDF(I)=0.D+00
4020 CONTINUE
     DO 4030 I=1,NX
     IBDF(NY+I)=(NX*(NY-1)+I)*2
     VBDF(NY+I)=0.D+00
4030 CONTINUE
4000 CONTINUE
     RETURN
     END
```